UNCLASSIFIED

AD NUMBER

AD858457

NEW LIMITATION CHANGE

TO
Approved for public release, distribution unlimited

FROM
Distribution authorized to U.S. Gov't. agencies and their contractors; Administrative/Operational use; June 1969. Other requests shall be referred to Air Force Aero Propulation Laboratory, APIP-2, Wright-Patterson Air Force Base, 45433.

AUTHORITY

AFAPL ltr, 12 Apr 1972

THIS PAGE IS UNCLASSIFIED

AFAPL-TR-69-17

AD858457

RADIATION DEGRADATION AND ANGULAR RESPONSE OF EXPERIMENTAL SOLAR CELLS IN A 2000 NAUTICAL MILE POLAR ORBIT

G. M. KEVERN

L. D. MASSIE

TECHNICAL REPORT AFAPL-TR-69-17

JUNE 1969

AIR FORCE AERO PROPULSION LABORATORY
AIR FORCE SYSTEMS COMMAND
PATTERSON AIR FORCE BASE, OHIO 45433

This document contains
blank pages that were
not filmed

RADIATION DEGRADATION AND ANGULAR RESPONSE OF EXPERIMENTAL SOLAR CELLS IN A 2000 NAUTICAL MILE POLAR ORBIT

G. M. KEVERN

L. D. MASSIE

FOREWORD

This report was submitted by the authors February 1969.

This technical report has been reviewed and is approved.

CURTIS KELLY
Chief, Energy Conversion Branch
Aerospace Power Division

ABSTRACT

This report describes an experimental effort to determine solar cell degradation and angular response in a 2000 NM polar orbit. Solar cell experiments including five different types of solar cells were devised for each of two Air Force orbiting vehicles. The cell types were dendritic silicon, dendritic silicon drift field, cadmium telluride thin film, cadmium sulfide thin film, and ion implanted silicon. The cells were tested in a module configuration consisting of eight, 1 x 2 centimeter cells of each type in electrical series.

The short circuit current and open circuit voltage parameters were monitored over a one year period. The measured degradation was compared with predicted degradation based upon the Van Allen inner belt proton/electron model and results of accelerator produced 1 Mev electron radiation. The total proton/electron environment in the 2000 NM polar orbit corresponded to an equivalent 1 Mev electron fluence of 7.3×10^{15} e/cm^2 per year which produced a predicted power degradation of 38 percent in non-drift field silicon cell types and 31 percent in silicon drift field types. Measured quantities were found to substantiate the validity of the 1 Mev electron method for predicting silicon solar cell damage. Thin film solar cells (in the configuration described in the report) failed in earth orbit for reasons other than radiation damage. Thermal effects and mechanical delamination are believed to be the most likely reasons for their failure.

The angular response of solar cells in space agreed with angular response measurements taken in the laboratory except for effects of stray radiation from earthshine and vehicle reflections. Angular response was also determined to be independent of radiation damage level.

TABLE OF CONTENTS

ILLUSTRATIONS

ILLUSTRATIONS (Cont'd)

ILLUSTRATIONS (Cont'd)

TABLES

SECTION 1

INTRODUCTION

1. OBJECTIVE

The Air Force Aero Propulsion Laboratory (AFAPL) has completed the analysis of data resulting from two solar cell space experiments conducted in a 2000 NM near circular polar orbit.

The objectives of these experiments were to demonstrate the space performance capability of new solar cell types, to determine their potential space environmental resistance advantages, to define operational problems for guiding future exploratory development efforts, and to define the severity of the environment with regard to solar power plant operation in this orbit over a one year period.

2. BACKGROUND

The results reported in this technical report pertain to flight tests conducted on two separate Air Force parent Agena vehicles. Each experiment was injected into the 2000 NM orbit as a tertiary flight test objective on an Atlas launch/Agena boost-orbital vehicle. The experiments were conducted as joint SAMSO (SMUME)/ AFAPL (APIP-2) efforts. The experimental solar cell (ion implanted silicon, cadmium sulfide thin film, cadmium telluride thin film, dendritic silicon and dendritic silicon drift field) modules included in the flight tests were products of AFAPL exploratory development programs in the area of solar power.

3. EXPERIMENT CONCEPT

At the time of conception of these experiments, June 1965, flight test data on solar cell performance degradation in a 2000 NM polar orbit were limited. Inclusion of the Air Force Aero Propulsion Laboratory experiments on the SAMSO vehicles afforded the opportunity to measure cell performance degradation as a function of time in orbit and to compare the measured quantities with predicted values based upon existing models of the Van Allen radiation belt.

During the on-orbit life of the experiments, short circuit current (SCC), open circuit voltage (OCV), and temperature paramenters were measured on a non-interference with primary payload basis using the command and telemetry system of the parent vehicle. Sun incidence angles were determined using sun sensor and control moment gyro rate information.

4. EXPERIMENT LIMITATIONS

Certain mission related limitations were imposed on the operation of the AFAPL solar cell experiments. Since link 5 telemetry over which solar cell experiment data transmission occurred could not be activated until Agena boost vehicle engine final shutdown, no data were obtained from the Flight 1 (FTV-1) experiment during the first 200 revolutions (23.2 days) and no data were obtained from the Flight 2 (FTV-2) experiment during the first 20 revolutions (2.32 days). Thus, on-orbit performance data upon orbit injection and radiation damage data immediately subsequent to orbit injection were not obtained.

A further restriction on the acquisition of data was that sun incidence on the experiment panels (which were rigidly mounted upon earth-oriented vehicles) had to occur in conjunction with activated link 5 telemetry and within tracking station data acquisition range. This restriction resulted in the accumulation of considerable data at very large sun incidence angles. Much of this data was discarded because of difficulties encountered in validly correcting the data over a wide range of incidence angles due to earthshine and vehicle reflections.

Regardless of the existence of dual panels on each vehicle, only a single panel was illuminated at any given time, with the periods of panel illumination/panel shadowing alternating at six month intervals, as the earth moved between conjugate points. Thus, no direct on-orbit performance comparisons between panels could be made.

SECTION II
SPACE EXPERIMENT

1. EXPERIMENTAL PANELS

Each flight vehicle carried two space experiment panels, one mounted on the -Y arm array and one mounted on the +Y arm array. Each experiment panel included one each of the following solar cell modules:

Designation	Type	Manufacturer
WN	Dendritic Silicon	Westinghouse
WD	Dendritic Silicon Drift Field	Westinghouse
GE	Cadmium Telluride Thin Film	General Electric
AR	Cadmium Sulfide Thin Film	Clevite
IP	Ion Implanted Silicon	Ion Physics

A photograph of the FTV-1 solar cell space experiment panel configuration is shown in Figure 1. The unit shown is the qualification test panel S/N 001 prior to qualification testing. The modules from the top of the photograph to the bottom are as follows: Ion Physics Corporation ion implanted silicon (IP series), Clevite Corporation cadmium sulfide thin film (AR series), General Electric Company cadmium telluride thin film (GE series), Westinghouse dendritic silicon drift field (WD series), and Westinghouse dendritic silicon (WN series). The IP, AR, GE, WD, and WN designations are used to simplify reference to the specific module types.

Each flight module consists of 8 series-connected 1 x 2 cm solar cells bonded to 10 mil thick metal substrates with RTV-41 adhesive. Silicon module substrates are Kovar. Thin film module substrates are molybdenum. Individual cell substrate dimensions are 4 cm x 12 cm which allows ample area for cell placement and edge attachment to the Lockheed Missile and Space Company (LMSC) 14 inch x 17 inch magnesium space experiment panel. The panel has 9.7 cm x 10.6 cm cutouts over which the cell modules are placed. Electrical leads from the modules are brought out through the cutouts and connected to the appropriate terminal posts on the backside. A single temperature sensor is positioned on the dendritic silicon drift field module.

3
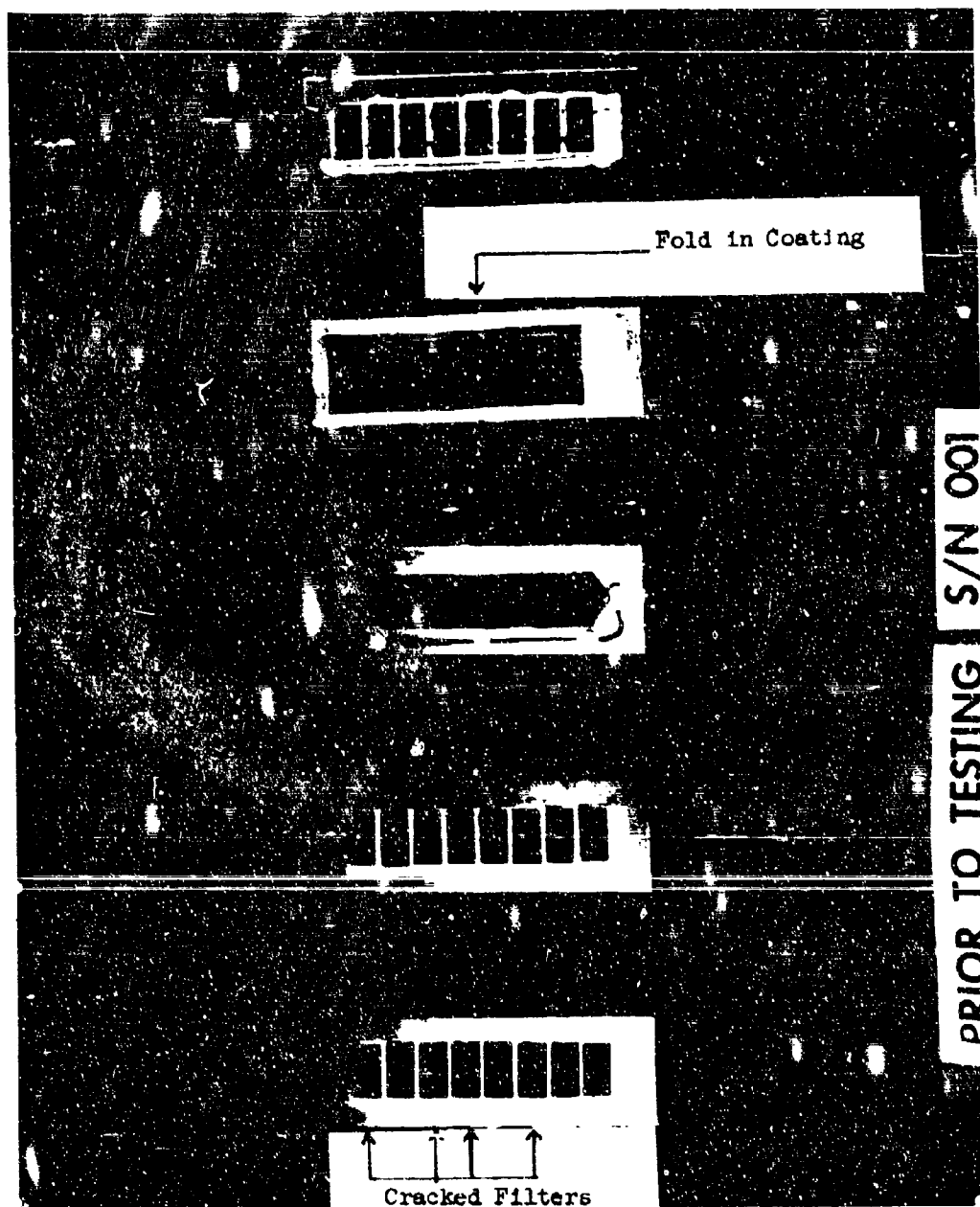
Figure 1. Photograph of AFAPL Solar Cell Space Experiment
Qualification Test Panel (Prior to Testing)

Figure 2 shows the location of the AFAPL Solar Cell Space Experiment on the vehicle forward solar arrays. One experiment panel is located on the -Y arm array and another panel on the +Y arm array. This redundant approach was taken to insure that some data would be obtained in the event one or the other experiment panels failed to survive orbit injection.

2. SOLAR CELL CHARACTERISTICS

Since the planned orbits for both Flights 1 and 2 would carry the AFAPL experiment through the magnetosphere near the center of the inner Van Allen radiation belt, it was necessary to shield the silicon cell types to prevent rapid degradation from low energy protons. Six mil thick glass shields (.04 grams/cm^2) were placed on all silicon solar cells with RTV 602 adhesive. No special shielding was provided for thin film cells other than that resulting from the nature of construction of the cells themselves. Cadmium telluride cells composing the GE modules were sprayed with a .5 mil Krylon protective overlay. Clevite cadmium sulfide cells composing the AR modules were encapsulated with 1 mil Kapton plastic as a standard construction technique.

Silicon cell types were all of the N on P type construction. The 5 - 10 ohm·cm dendritic webb silicon starting material and the ion implanted silicon starting wafers were in the 12 - 14 mil thickness range with completed cells having .3 to .5 micron junction depths and solder dipped contacts. Silicon module air mass zero efficiencies at 28°C were 7 - 8 percent for the WD (dendritic silicon drift field) modules, and 8 - 9 percent for the WN (dendritic silicon) and IP (ion implanted silicon) modules.

Thin film cell composition consisted of 1 mil N-type cadmium sulfide and cadmium telluride film on 1 mil molybdenum metal base material in the case of AR modules and GE modules respectively. Copper sulfide/cadmium sulfide and copper telluride/cadmium telluride P on N heterojunctions were formed by the cuprous ion immersion technique. In the cadmium sulfide cells, a mechanical screen grid P-layer contact was used without an intervening conductive bond in the case of Flight 1 modules and with an intervening conductive bond in the case of Flight 2 modules. Cadmium telluride cell contacting consisted of gold
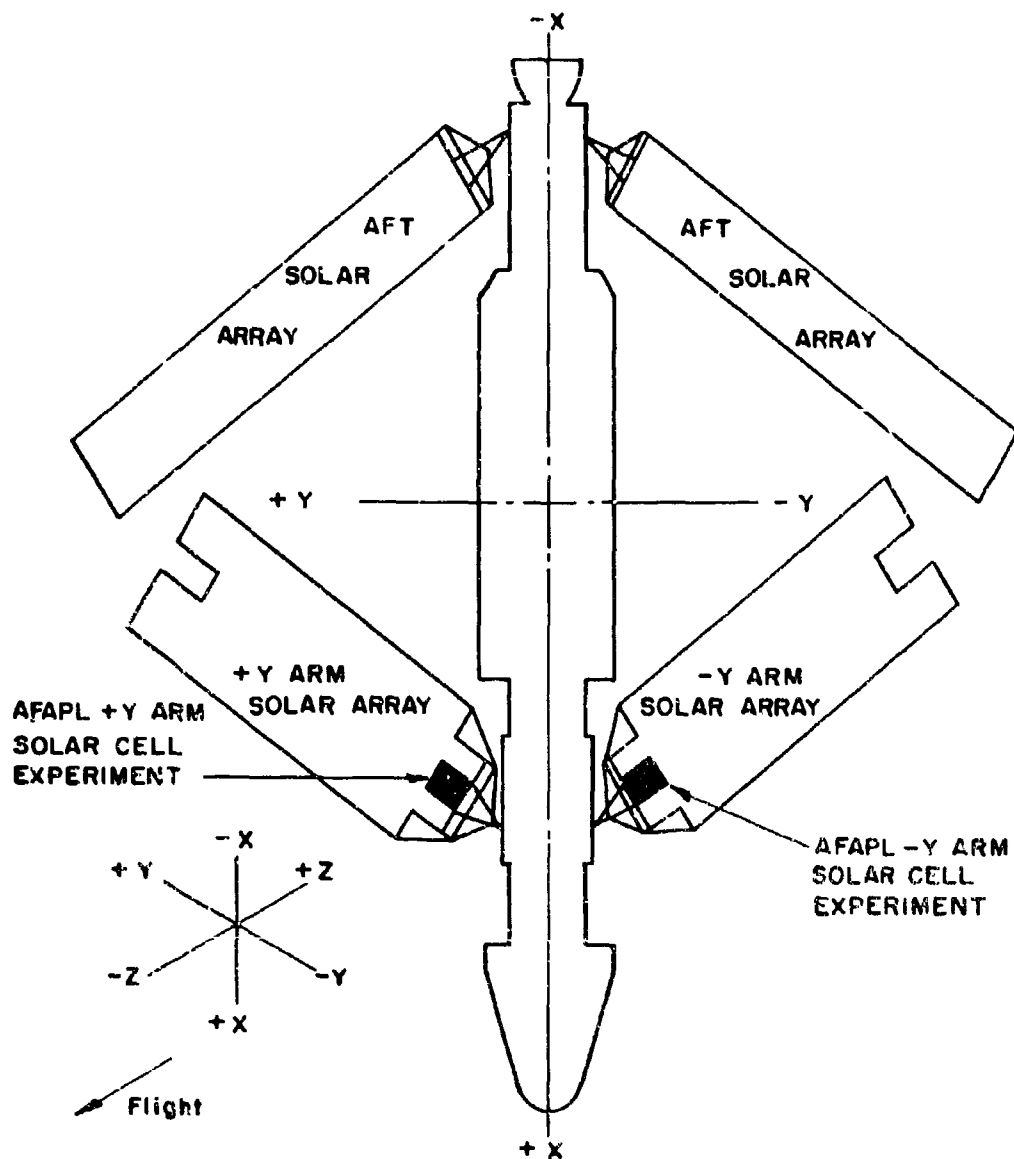
Figure 2.   Solar Cell Experiment Location on Flight Test Vehicle

fingers and bus bar formed by vacuum evaporation through a metal mask. Series connections between cadmium telluride cells were accomplished by shingling, using Epoxy Products, Inc., 3026 adhesive for the conductive bond. Thin film module air mass zero efficiencies at 28°C were 2 to 3 percent for the GE (cadmium telluride) modules and 3 to 4 percent for the AR (cadmium sulfide) modules.

3. CELL TEMPERATURE EFFECTS

Since solar cell short circuit current and open circuit voltage vary with temperature, it was recognized that all flight data would have to be corrected for temperature. Test data for the various cell types were, therefore, obtained from each manufacturer. From these data, short circuit currents and open circuit voltages relative to the 100°F values were calculated, and are plotted in Figures 3 through 6. (Preliminary analysis of flight data indicated that the most useful data were at or near 50° solar incidence, and the associated steady state temperature of approximately 100°F).

During the flight experiments, temperature was measured at only one point on the experiment panel. This point was directly behind the WD module. This one temperature measurement is considered adequate for all cell modules during steady-state conditions, but, unfortunately, steady temperatures were seldom attained, due to the frequent passage of shadows over the panel. The reported temperatures must, therefore, be regarded as approximate for all modules other than the WD module.

4. PRE-FLIGHT EVALUATION

Pre-flight module evaluation was conducted to determine the electrical performance characteristics of each flight module at normal radiation incidence, the change in characteristics as a function of varying incidence angle, and module suitability for flight through qualification testing (in the flight panel configuration) to the vehicle launch and operating environmental specifications.

Evaluation of modules for voltage-current characteristics under normally incident sunlight was accomplished at Table Mountain, California, by special
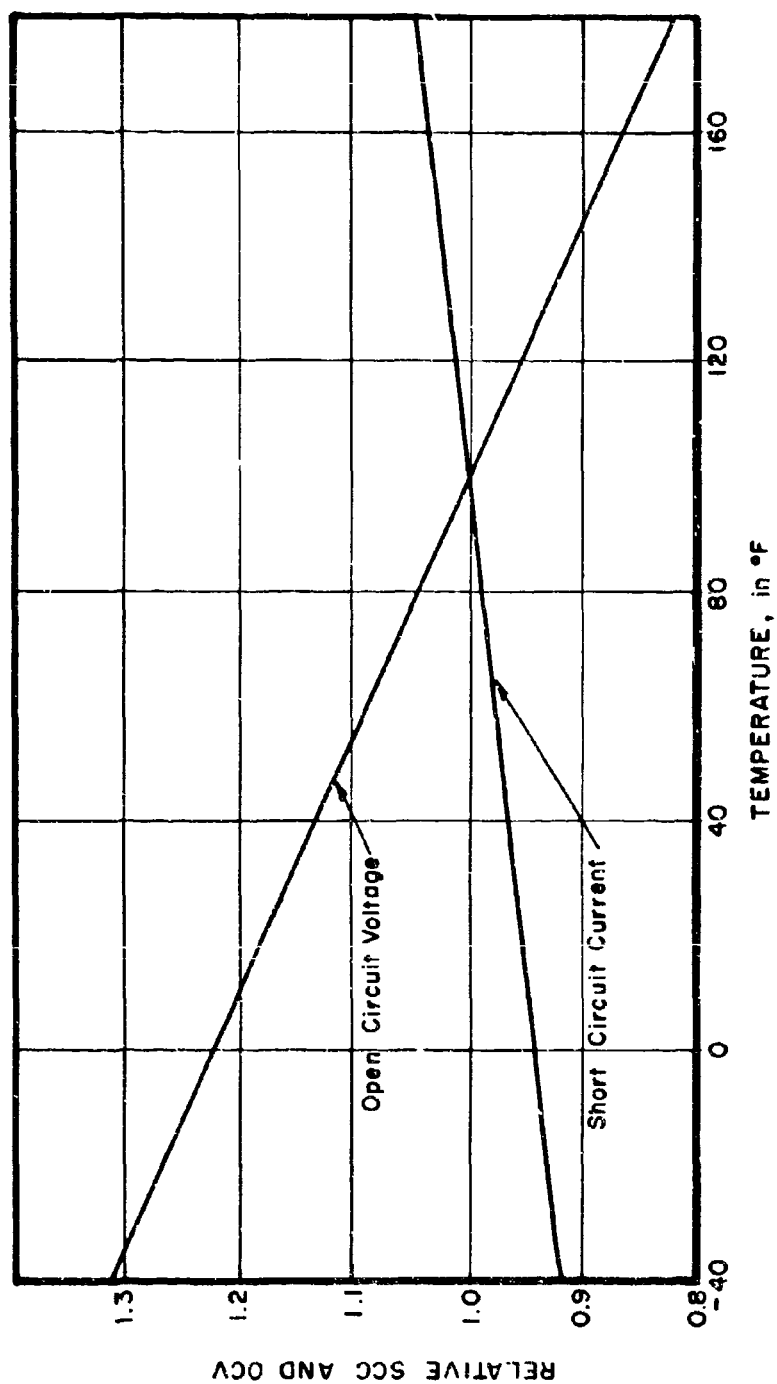
Figure 3. Silicon (WN and IP) Solar Cells, Effect of Temperature on Short Circuit Current and Open Circuit Voltage
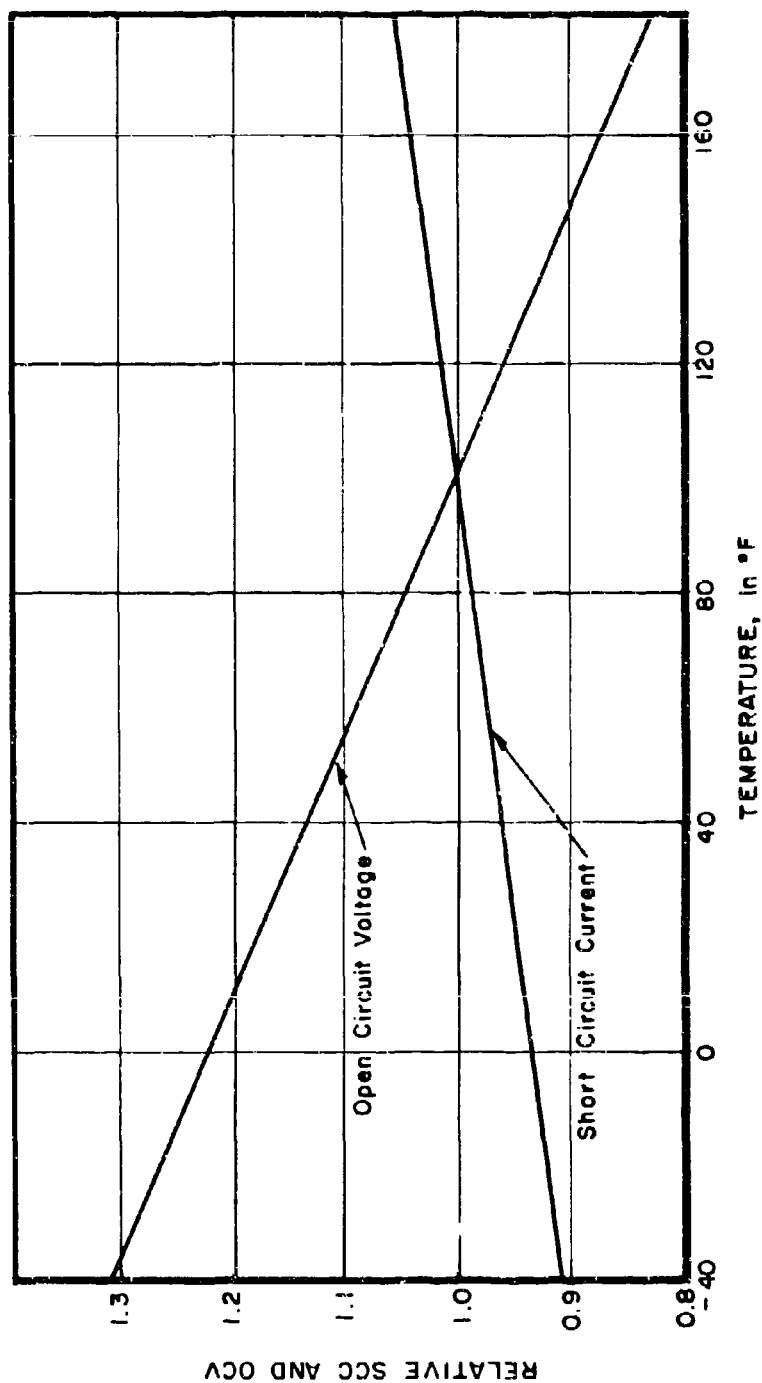
Figure 4.   Drift Field Silicon (WD) Solar Cells, Effect of Temperature on Short Circuit Current and Open Circuit Voltage
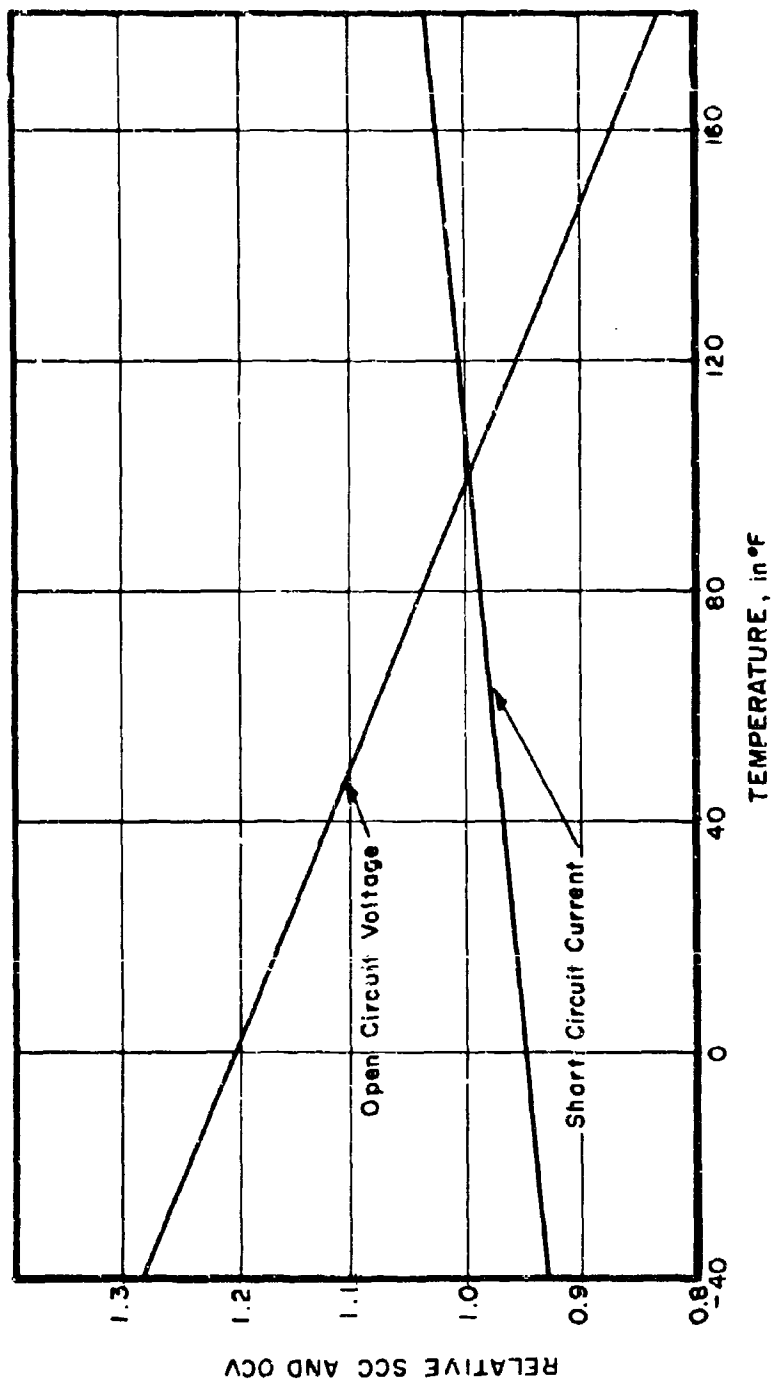
Figure 5. Cadmium Telluride (GE) Thin Film Sol-- Cells, Effect of
Temperature on Short Circuit Current and Open Circuit
Voltage

10

TEMPERATURE, in °F

RELATIVE SCC AND OCV
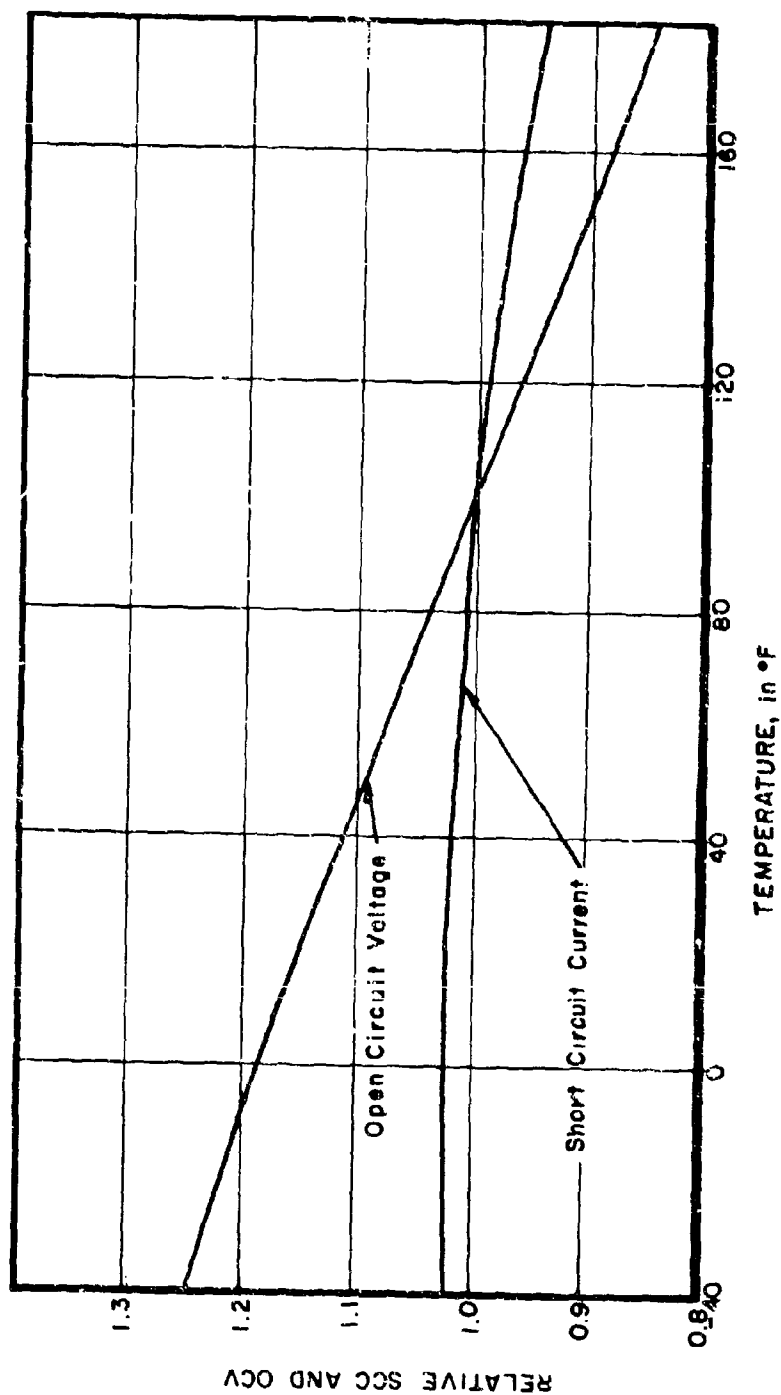
Figure 6. Cadmium Sulfide (AF, Thin Film Solar Cells, Effect of Temperature on Short Circuit Current and Open Circuit Voltage

arrangements with the Jet Propulsion Laboratory of the California Institute of Technology. A summary of performance of all modules based upon this data is shown in Table I. Similar data were also obtained at AFAPL, using a carbon arc solar simulator. Due to carbon arc fluctuations, the Table Mountain data were considered to be more accurate and are used as a basis for all flight data analysis.

Since space experiment data on flight modules would be accumulated at varying angles of incidence, it was essential to know the telemetered electrical parameters (short circuit current and open circuit voltage) as a function of incidence angle. Without knowledge of these relationships it would be impossible to correct data to normal incidence conditions. Determination of these relationships was accomplished at AFAPL using a carbon arc simulator in September 1965, and using an X-25 solar simulator from October 1967 to October 1968 (See Section III).

The vehicle contractor (LMSC) was responsible for conducting qualification tests on the S/N 001 qualification test panel as follows:

Vibration Test:

1. Random: 5 minutes of random vibration were applied at the following levels in all 3 mutually perpendicular axes.

$$14 - 400 \text{ CPS at } .07 \text{ g}^2/\text{CPS}$$
$$400 - 200 \text{ CPS at } .13 \text{ g}^2/\text{CPS}$$

2. Sinusoidal: 10 minute low level vibration sweep at approximately 1/2 g followed by a vibration sweep at a sweep rate of 3 minutes per octave at the following levels in all 3 mutually perpendicular axes.

$$5 - 14 \text{ CPS at } .5" \text{ double amplitude}$$
$$14 - 400 \text{ CPS at } 5.0 \text{ g}$$
$$400 - 2000 \text{ CPS at } 7.5 \text{ g}$$

TABLE I
PRE-FLIGHT PERFORMANCE DATA ON SOLAR CELL MODULES
TABLE MOUNTAIN SUNLIGHT
6 OCTOBER 1965

MODULE	SCC (ma)	OCV (volts)	P_{max} (mw)	AREA (cm²)	*INTENSITY (mw/cm²)	EFF %	T(°C)
WN-2	51.3	4.42	165.6	14.4	.30	8.8	28 →
WN-3	54.3	4.44	175	14.4	130	9.3	
WN-4	51.9	4.38	166	14.4	128.8	8.8	
WN-5	48.2	4.44	158.4	14.4	128.8	8.5	
WN-6	51.3	4.44	173	14.4	127.9	9.4	
WD-2	46.2	4.39	151.3	14.4	129	8.1	28 →
WD-3	44.5	4.37	145.3	14.4	129	7.8	
WD-4	43.3	4.43	146	14.4	129.7	7.8	
WD-5	47.7	4.28	152.3	14.4	129.8	8.1	
WD-6	48.0	4.24	154	14.4	129.8	8.2	
GE-2	29.9	4.0	62.2	16.0	130.2	3.0	28 →
GE-3	24.7	4.01	43.2	16.0	130	2.1	
GE-4	22	3.95	36.5	16.0	130	1.75	
GE-5	24.7	3.96	48.5	16.0	130.1	2.3	
GE-6	25.5	4.07	39.8	16.0	129.8	1.9	
AR-2	23.2	3.74	53.0	13.33	128.2	3.1	28 →
AR-3	28.2	3.68	53.9	13.33	128.9	3.14	
AR-4	25.1	3.73	57.0	13.33	129.3	3.3	
AR-5	24.2	3.73	57.0	13.33	129.2	3.3	
AR-6	24.7	3.74	55.2	13.33	129.8	3.2	
IP-2	56.5	4.33	179.9	14.4	129.0	9.65	28 →
IP-3	56.7	4.31	183.4	14.4	128.6	9.9	
IP-4	55.4	4.27	140.8	14.4	128.0	7.6	
IP-5	54.0	4.25	164.2	14.4	127.2	8.9	
IP-6	54.2	4.28	158.4	14.4	128.2	8.6	

* Space sun equivalent based upon JPL balloon flight standard 17 A.

13

Acceleration Test:

    11.0 g's - two axes

    2.5 g's - one axis   5 minute duration

Shock Test:

    Three shocks of 30 g's and 8 milliseconds uration in each of the 3 mutually perpendicular axes.

Transporation and Storage Test:

1. Ambient to +160°F in 45 minute period.
2. Maintained at 160°F for 4 hour period.
3. Reduced to -65°F over 2.5 hour period.
4. Maintained at -65°F for 8 hour period.
5. Pressure reduced to 87 Torr   maintained 10 minutes.
6. Pressure and temperature then returned to room ambient.

Humidity Test:

1. Temperature of experiment panel increased from room ambient to +140°F over a 2 hour period.

2. Maintained at +140°F and 95% relative humidity for 6 hours.

3. Temperature then reduced linearly to room ambient in a 16 hour period.

High Temperature - Low Pressure Test:

1. Experiment panel temperature was raised from room ambient to +175°F at 7.5°F per minute under subatmospheric pressure of 10^{-3} torr.

2. Temperature level of 175°F was maintained for 2 hours.

14

Low Temperature Test:

1. Experiment panel temperature was reduced to -170°F at the following rates:

> Room ambient to -60°F at 2.4°/minute
> -60°F to -140°F at 2.5°/minute
> -140°F to -170°F at 1.0°F/minute

2. Panel was maintained at -170°F for 24 hours and then returned to room temperature.

Temperature Cycling Test:

Step I - From room ambient to +110°F over a 10-minute period and maintained at +110°F for 15 minutes.

Step II - From +110°F over a 75-minute period and maintained at -140°F for 15 minutes.

Step III - From -140°F to +110°F over a 35-minute period and maintained at 110°F for 15 minutes.

Step IV - Steps II and III were repeated two times.

Step V - From +110°F to room ambient temperature over a period of 10 minutes.

Figure 7 shows the condition of the qualification test panel upon completion of the above qualification tests. As can be seen, the centrally located GE (cadmium telluride) cell strip has lifted from the molybdenum substrate with attendant electrical discontinuity. Although not apparent from the photograph, the AR (cadmium sulfide) substrate has partially separated from the magnesium experiment panel and while still responsive electrically, the open circuit voltage is only 65 percent and the short circuit current only 27 percent of the original specified values. Only minor damage was incurred by silicon modules.
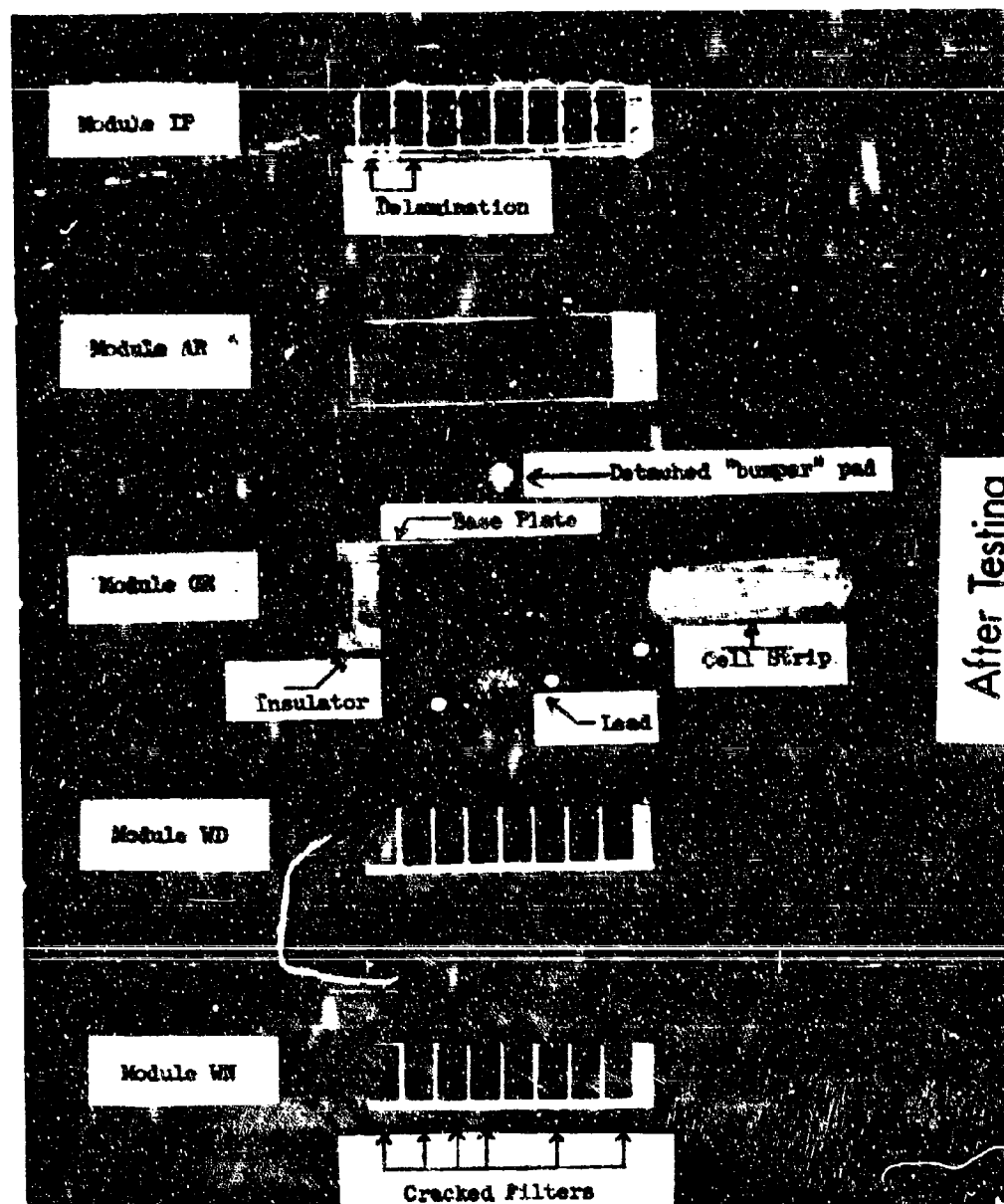
Figure 7.   Photograph of Solar Cell Experiment Panel Following
            Qualification Test

16

Tables II and III summarize the visual and electrical defects observed in the modules upon completion of each aspect of the qualification-test program. Since proper electrical operation of flight modules was not a requirement for qualification, and since no material completely left the panel during the tests, the experiment was considered to be qualified for flight on a non-interference basis.

5. SOLAR CONSTANT

Since the orbit of the earth around the sun is an ellipse with the sun at one focus, the earth-sun distance varies continuously as the earth traverses its orbital path. With respect to the calendar, the maximum earth-sun distance (94.4 million miles) occurs early in July and the minimum earth-sun distance (91.3 million miles) occurs early in January. The variations from one year to another are negligible. In general, the distance between the earth and sun is given by:

$$D = K \left[1 - \epsilon \cos \frac{2\pi t}{Y} \right]$$

Where D is the earth-sun distance

K is the mean earth-sun distance (92.9 million miles)

ϵ is the eccentricity of earth's orbit (.0167330)

t is the minimum number of days from 1 January

Y is the length of the year in days (365.2563)

Thus, the earth-sun distance can be calculated at any point in the earth's orbit.

The solar constant is defined as the radiant power delivered by the sun outside the earth's atmosphere at earth's mean distance (92.9 million miles) from the sun. The value of the solar constant is 140 mw/cm^2. This value increases as the earth approaches perihelion and diminishes as the earth approaches aphelion. The value at any point in the earth's orbit is given by the inverse square law:

$$\left[\frac{H_x}{H_o} = \frac{D_o}{D_x} \right]^2$$

17

TABLE II

DESCRIPTION OF VISUAL DEFECTS IN MODULES RESULTING FROM QUALIFICATION TESTS

Test	IP	AR	GE	WC	WN
Initial	Satisfactory appearance	Fold in outer coating	Satisfactory appearance	Satisfactory appearance	Four (4) cracked filters
Post Shock	Unchanged	Unchanged	Unchanged	Unchanged	Unchanged
Post Vibration	Unchanged	Unchanged	Unchanged*	Unchanged	Unchanged
Post Acceleration	Unchanged**	Unchanged***	Unchanged	Unchanged**	Unchanged***
Post Transportation and Storage	Unchanged	Unchanged	2 pads (wire supports) lifted free of panel. Remaining pad loose. Traces of delamination along entire strip—less than 5% of total area	Adhesive lifted at one end	Adhesive lifted at one end
Post Humidity	Unchanged	Unchanged	Both output leads detached at junction	Unchanged	Unchanged
Post High Temperature Low Pressure ***	Unchanged	Unchanged	Unchanged	Unchanged	Unchanged
Post Low Temperature	Two filter delaminations	Base plate separated from adhesive at one end	Metal base plate detached from insulator. Cell strip and thermistor detached from base plate. Approx 80% of cell area discolored. 8 filters delaminated	Unchanged	Two cracked filters
Post Temperature Cycling	Unchanged	Unchanged	Unchanged	Unchanged	Unchanged

* Lead wire broken off at terminal post folder junction
** Individual lead wire strands broken at terminal post junction
*** One bumper pad detached

18

TABLE III

EFFECTS OF QUALIFICATION TESTS ON MODULE OCV AND SCC

| | OPEN CIRCUIT VOLTAGE | | | | | SHORT CIRCUIT CURRENT | | | | | TEST CONDITIONS | | | |
| | Volts | | | | | Milliamperes | | | | | Panel Distance from Illuminator (in) | Thermistor Reading | | Thermo-couple Reading °C |
	WN	WD	GE	AR	IP	WN	WD	GE	AR	IP		Ohms	Equivalent Temp °C	
Specified Values	4.0	4.0	3.5	3.5	4.0	45	45	20	20	45	10 - nominal	1534 to 1782	30±2°	30±2°
Initial Test	4.43	4.45	3.93	3.33	4.26	49.1	35	14	16.5	45.8	7.5	1750	28.5	30(on module)
Post Shock	4.45	4.43	3.87	3.44	4.25	52.0	40.0	14.8	17.2	54.3	7.5	1775	28.2	30 "
Post Vibration	4.4	4.4	3.77	3.25	4.25	65.5	49.0	17.7	21	66.6	6	1600	30.9	30 "
Post Acceleration	4.37	4.37	3.75	3.4	4.21	49.3	37	14	16	49.8	7	1600	30.9	30 "
Post Transportation and Storage	4.45	4.43	3.88	3.28	4.27	50.1	38.0	13.0	17.0	53.7	7.5	1750	28.5	30
Post Humidity						Power Output measurements following Humidity Test were not required								
Post High Temp Low Pressure	4.22	4.40	*	2.7	4.28	48.8	36.5	*	7.0	47.6	7.5	1650	30.0	30 "
Post Low Temperature	4.4	4.4	**	2.66	4.25	47.2	36.2	**	6.5	47.8	7	***		30 "
Post Temperature Cycling	4.40	4.40	***	2.3	4.21	42.9	35.1	***	5.4	49.2	7.5	***		31 "

* No output lead wires detached from module

** Hand probed – no response

*** Thermistor detached, not employed as a temperature control

19

Where:

H_o is the value of the solar constant at known distance D_o

H_x is the unknown value (or value to be calculated) at distance D_x

Thus, the value of the solar constant can be calculated at any point in the earth's orbit corresponding to any given calendar date. Figure 8 shows the yearly variation of the solar constant relative to the value ($140 \ mw/cm^2$) at the mean earth-sun distance. As can be seen, the value varies from approximately $135 \ mw/cm^2$ at aphelion (July) to $145 \ mw/cm^2$ at perihelion (January). For purposes of solar cell space experiment data analysis, this variation in solar constant causes negligible changes in open circuit voltage, but causes proportionate changes in short circuit current. All short circuit current flight data were, therefore, corrected to $140 \ mw/cm^2$, using Figure 8.

6. FLIGHTS 1 AND 2

Flight Test Vehicle 1 (FTV-1) booster ignition occurred at 12:30 PM pacific daylight savings time on 19 August 1966. The vehicle achieved nominal orbital parameters of 2011.55 N.M apogee and 1994.89 N M perigee at an orbit plane to equatorial plane inclination of 90.15 degrees. The corresponding orbital period for FTV-1 was 167.56 minutes.

Second stage booster (SSB) shut down did not occur until 8 September 1966. Since link 5 telemetry over which solar cell experiment data transmission occurred could not be activated until SSB shut down, no data were obtained from the Flight 1 experiment during the first 200 revolutions. Link 5 telemetry activation occurred on FTV-1 revolution 196 and proper operation of the AFAPL experiment was verified. The first useful data were obtained in an active pass over the New Hampshire Tracking Station (NHS) on the 213th revolution. Additional NHS data transmissions occurred until revolution 1095 when link 5 telemetry failure occurred on 16 January 1967. The FTV-1 experiment, therefore, covered a total in-orbit time of 127.4 days. Only -Y arm data was obtained during Flight 1, as sun incidence in conjunction with activated link 5 telemetry and within tracking station data acquisition range, occurred only on the -Y arm forward solar array.
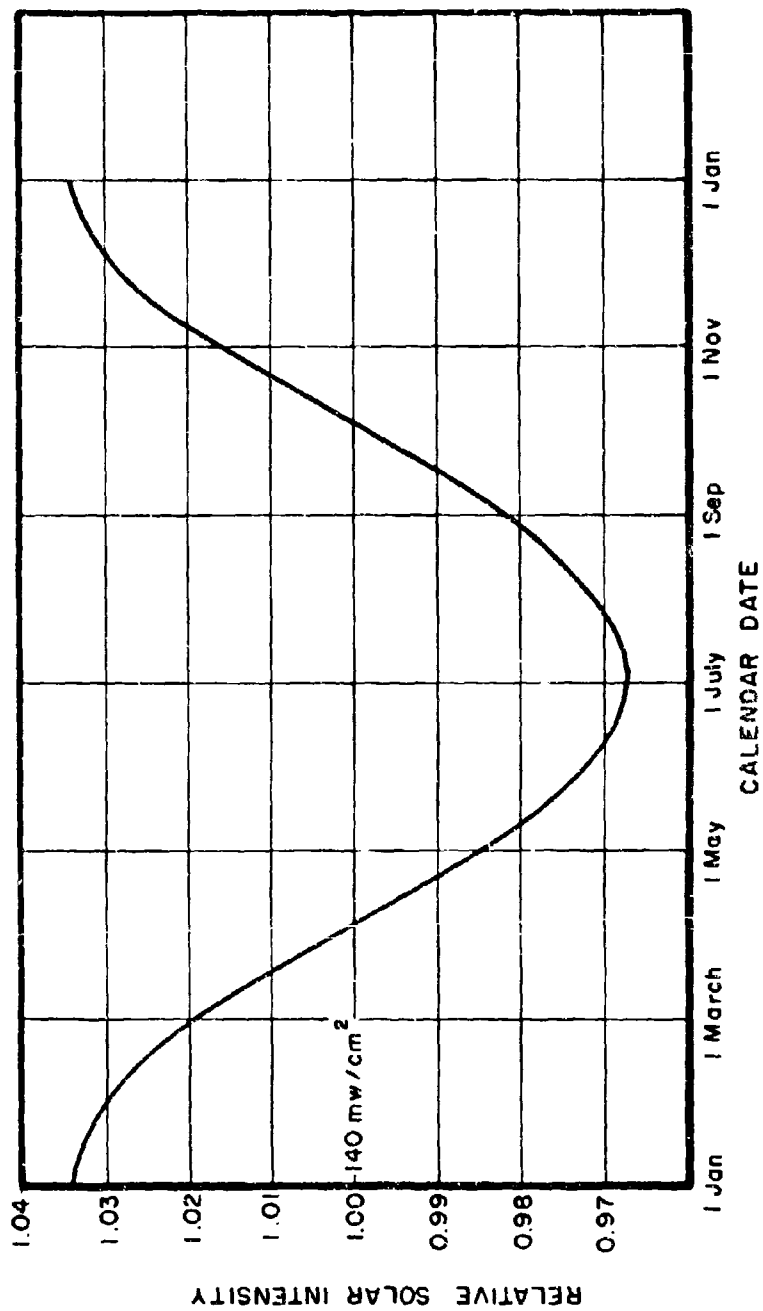
20

Figure 8. Yearly Variation of the Solar Constant

Flight Test Vehicle 2 (FTV-2) was launched on 4 October 1966. The vehicle achieved nominal orbital parameters of 2002.64 NM apogee and 1992.57 NM perigee at an orbit plane to equatorial plane inclination of 90.17 degrees. The corresponding orbital period for FTV-2 was 167.61 minutes. Useful data were obtained for the -Y arm modules from revolutions 21 to 1542, and from revolutions 1566 to 3072 for the +Y arm modules, corresponding to 358 days.

The Flight 2 experiment was terminated on 13 October 1967, when the vehicle experienced a major attitude perturbation. The condition grew progressively worse, and on 16 October 1967, the vehicle was reported to be out of control and tumbling. Ground station fixes on the vehicle telemetry transmissions could not be maintained sufficiently long to obtain further AFAPL solar cell space experiment data.

7. FLIGHT DATA ANALYSIS

Telemetry end to end transmission errors were of the order of five percent. Experiment raw data was recorded on magnetic tape during active passes over tracking stations. These recordings were subsequently shipped to Lockheed Missiles and Space Company for reduction by computer. Analysis of reduced data at AFAPL was conducted manually using the computer listings provided by Lockheed. Figure 9 shows a single page of reduced data from a 66 page listing for Flight 2 revolution number 574. This page was selected for exemplification because it shows open circuit voltage as well as short circuit current data. Since short circuit current is most affected by radiation, the experiment was geared primarily to measurement of this parameter at vehicle system time intervals of one second. The command for module open circuit voltage readout was generated at vehicle system time intervals of 200 seconds. The approximate ratio of total short circuit current readings to total open circuit voltage readings was approximately 30 to 1. The duration of experiment "on time" during active passes varied from approximately 10 to 30 minutes.

Preliminary inspection of all flight data indicated that an incidence angle of 50°, and the corresponding average temperature of 100°F, should be selected as the basis for detailed data analysis. A smaller incidence angle could not

Figure 9. Sample Telemetry Data Page, Flight 2, Revolution 574, -Y Arm

be selected, since all short circuit data exceeding 33 ma for silicon modules and 17 ma for thin film modules had to be discarded because of instrumentation/telemetry circuit saturation. All data obviously affected by shadowing of a portion of a module were also discarded.

During initial analyses, efforts were made to correct all data to 0° incidence. These efforts were abandoned because insufficient information was available to correct the error introduced by reflections from the vehicle surface and the earth's albedo. (This effect apparently varied from 0 to 30% of the short circuit current, as discussed in Section III).

Final analysis of short circuit current data was, therefore, accomplished as follows:

1. Whenever possible, for each recorded revolution, the short circuit for each module at exactly 50° incidence was extracted. Since one or two modules would usually be partially shadowed, the unshadowed data nearest to 50° incidence was selected for these modules, and corrected to 50° incidence, using the cosine law. (Data points not within 50° ± 5° were discarded.)

2. The selected current values were corrected to 100°F, using Figure 3, 4, 5 or 6, as applicable.

3. The current values were then corrected to 140 mw/cm^2, using Figure 8.

4. The above values were then converted to percent, by dividing by the corresponding preflight 50° incidence value. The 0° preflight value was obtained from Table I, and corrected to 50° incidence at 100°F, using the appropriate curves in Figures 3 through 6 and 12 through 18.

Open circuit voltage data points for final analysis were also selected and corrected in accordance with the above procedure, except that the solar constant and incidence angle corrections were found to be negligible and were omitted.

24

For purposes of data analysis it was assumed that angular response and temperature coefficients of the various modular types were independent of radiation damage level. It was also assumed that all illuminated modules were at the same temperature as the illuminated WD module with the temperature sensor. All data taken during partial or complete shading of the WD module was ignored. These simplifying assumptions should not result in large discrepancies in the results.

SECTION III

ANGULAR RESPONSE

1. OBJECTIVE

This investigation was performed to determine the angular response information required for proper analysis of the data obtained during Flights 1 and 2 of the joint AFAPL - SAMSO Solar Cell Space Experiment. This necessitated correlation of data obtained during both laboratory and space tests of the five types of solar cell modules which were included in the space experiment.

The objective of the space experiment was to determine long term (1 year) degradation in a 2000 nautical mile polar orbit, of the five types of experimental solar cells. Unfortunately, all data were obtained during continuously varying solar incidence angles, as the vehicle was earth oriented. Results of the space experiment were found to be critically dependent upon angular response so final analysis of the data from the space experiment was deferred pending completion of the angular response investigation reported herein.

In addition to many other preflight and qualification tests (see Section II) volt-ampere curves were obtained at AFAPL in September 1965 for one module of each type at 0°, 10°, 20°, 30°, 40°, 50°, 60°, and 70° angles of incidence, using a carbon arc solar simulator, an electronic load, and an X-Y plotter. Unfortunately, due primarily to stray reflections in the test area and rapid fluctuations in the carbon arc, angular response characteristics calculated from these curves were found to be of questionable value. A more detailed investigation of angular response characteristics was therefore conducted at AFAPL during the period from October 1967 to October 1968, concurrently with analysis of telemetered data from Flights 1 and 2.

2. LABORATORY ANGULAR RESPONSE TESTS

Starting in October 1967, a surplus automatically recording photometric system was modified and utilized for angular response tests. This modified system includes:

(1) A goniometer with 360° horizontal and vertical movements, accurate to ±0.1°.

26

(2) A continuous curve recording microammeter, with a 10" scale.

(3) Decade resistance boxes to provide any desired scale factor for the recorder, and any desired load for the solar cell or module under test.

(4) Electrical synchronization of goniometer, recorder paper drive, and variable speed system driving motor.

(5) Shroud and baffles to eliminate reflections and stray room light.

(6) Water-cooled, temperature-controlled mounting block for cell or module.

(7) Hollow shaft-cross hair arrangement to permit accurate alignment of module surface with goniometer axes of rotation.

The spare and qualification modules which were still operable were tested with the carbon arc simulator in an attempt to duplicate preflight test results. Because of carbon arc fluctuations, reproducible curves could not be obtained.

Curves were also obtained using readily available 28 volt, 1000 watt, PAR-64 aircraft landing lamps (General Electric #4615) connected to a regulated power source. Curves obtained while using one of these lamps as a solar simulator showed no fluctuations, and were exactly reproducible. Comparison of these curves with those obtained at a later date, using the same modules and an X-25 solar simulator showed that the difference in spectral distribution produced no noticeable change in angular response, under either short circuit or open circuit conditions.

All laboratory data utilized for this report were obtained using an X-25 simulator borrowed by AFAPL in January 1968. (Spectrolab Model X-25, Serial #112, with a 2500 watt Xenon short arc lamp.) The simulator was adjusted to provide 140 mw/cm^2 on the module surface, as measured by calibrated

standard silicon solar cells. Angular response curves similar to Figures 10 and 11 were automatically drawn for each module, under short circuit, open circuit, and load conditions, using the following procedures:

(1) Illuminate the module at 0° incidence, 140 mw/cm^2, 30-35°C.

(2) Set decade boxes to provide desired module load, and approximately 9.5" recorder deflection.

(3) Operate recorder at paper speed of 1" per minute to demonstrate that module output is stable.

(4) Set goniometer at -90° incidence, and synchronize goniometer and recorder.

(5) Rotate goniometer/recorder system at 10° per minute from -90° to 0° to +90° incidence, reverse, and rotate back to -90° incidence.

The procedure demonstrates module stability and data reproducibility and provides four data points for each incidence angle, which were then averaged to minimize systematic errors, such as the decrease in surface temperature as incidence angle is increased. The averaged values were then plotted in final angular response curves for each module as shown in Figures 12 through 16. Since all available GE and AR modules had seriously deteriorated, data were obtained for two representative individual cells in good condition, see Figures 17 and 18. It is interesting to note that the short circuit curves for the deteriorated modules GE-6 and AR-7, Figures 14 and 15, resemble the maximum power curves for good individual cells, Figures 17 and 18. The shapes of the short circuit angular response curves, therefore, indicate that Modules GE-6 and AR-7 now have high internal resistance. This is confirmed by the voltage-current characteristics of these modules. It is also evident that the shape of the angular response curve for any module or cell is determined by the sum of the internal module or cell resistance, and the external load resistance. The limiting shapes are, of course, the true short circuit and open circuit curves.

AFAPL-TR-69-17
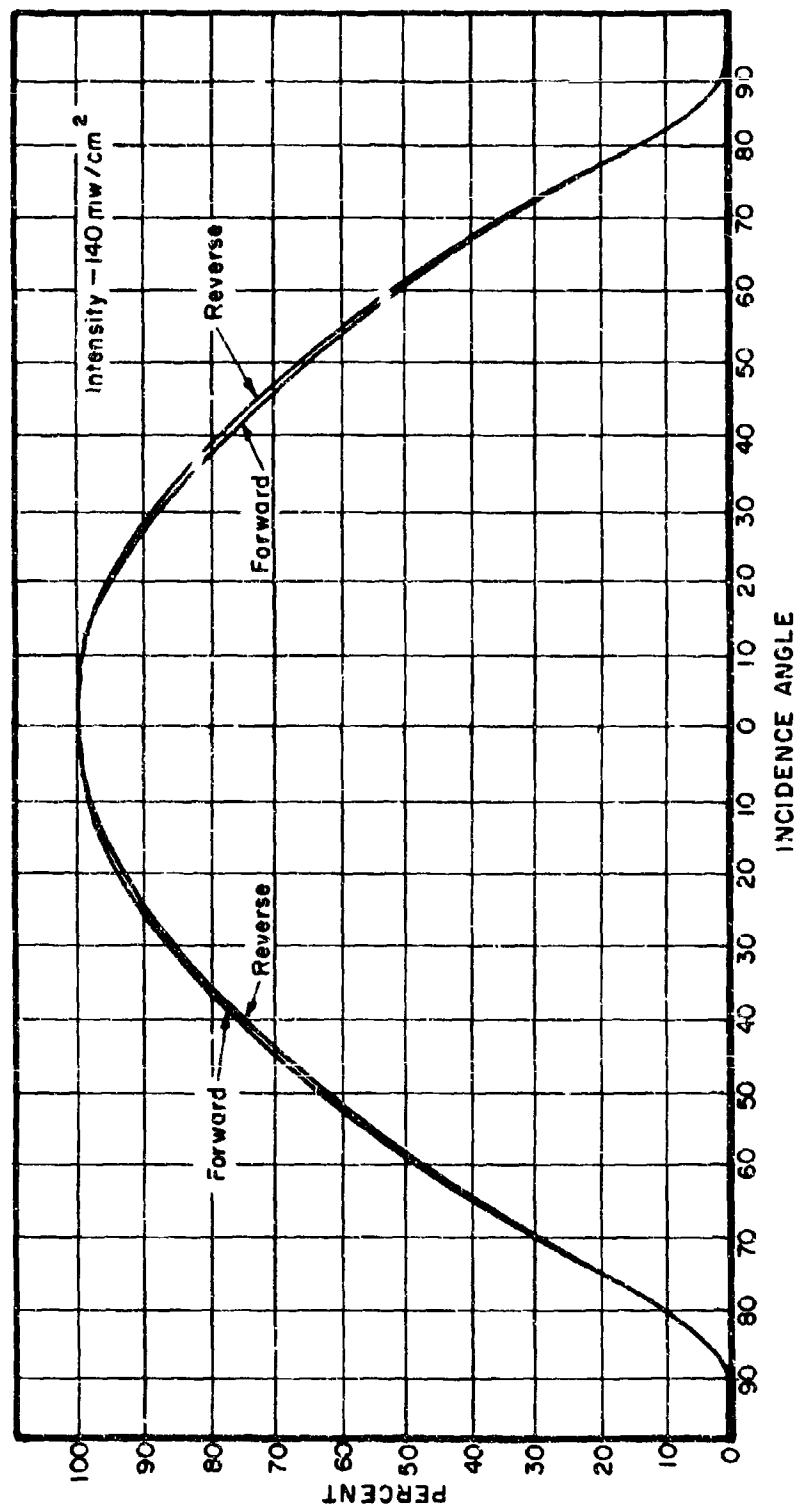
Figure 10. Sample Original Data, Angular Response, Module WD-1, Short Circuit Current With X-25 Solar Simulator

29
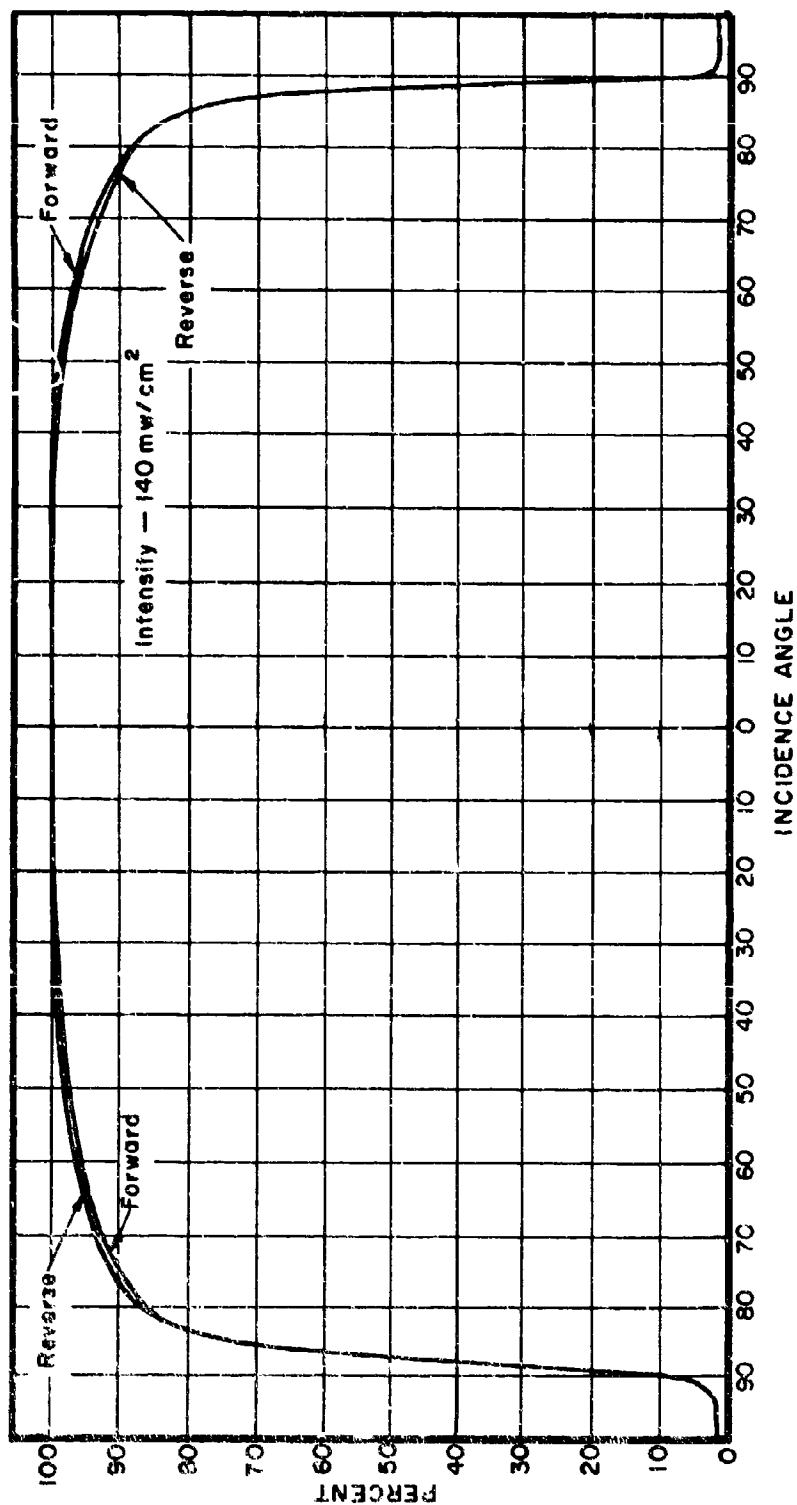
Figure 11. Sample Original Data, Angular Response, Module WD-1, Open Circuit Voltage, With X-25 Solar Simulator

AFAPL-TR-69-17
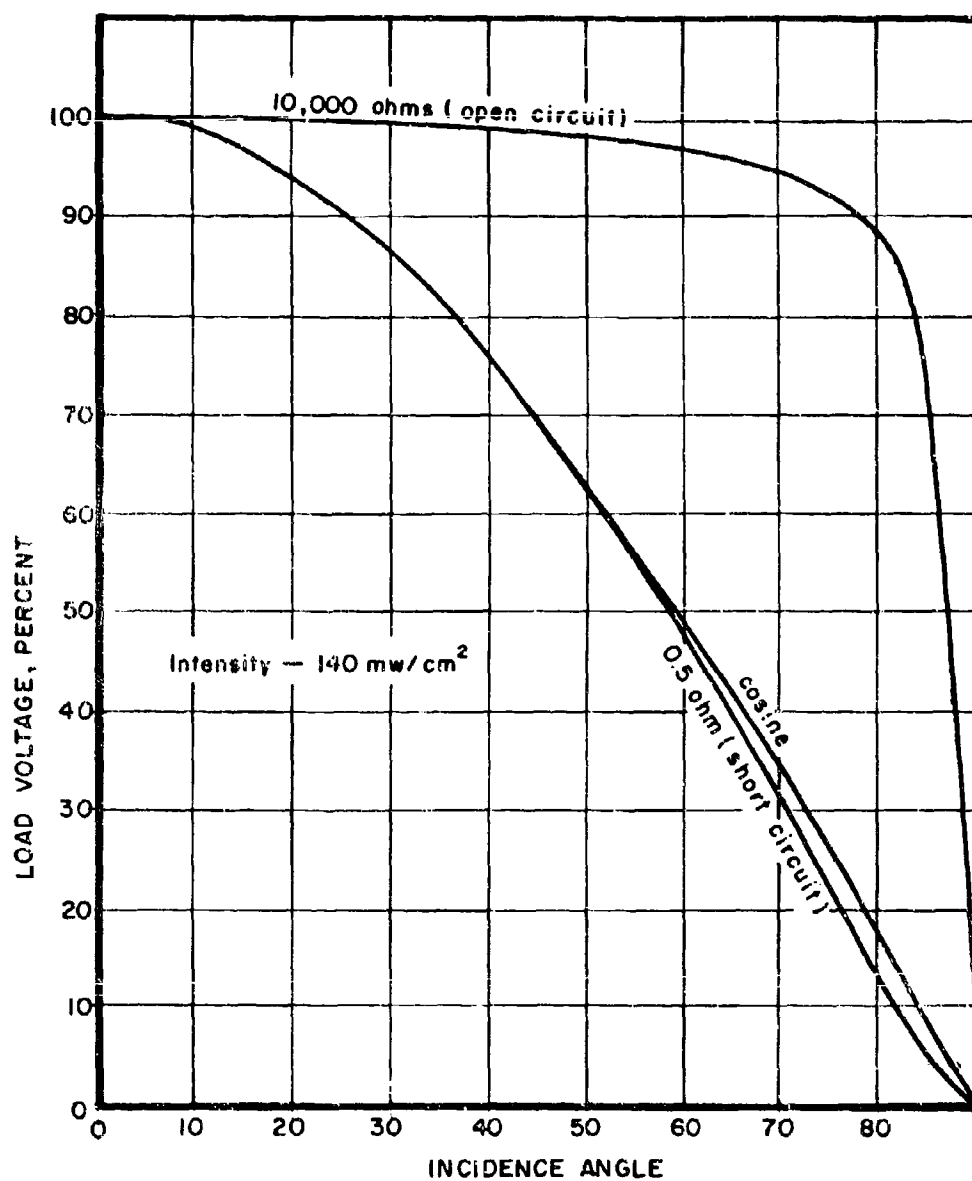
Figure 12. Module WN-1, Angular Response, With X-25 Solar Simulator

31
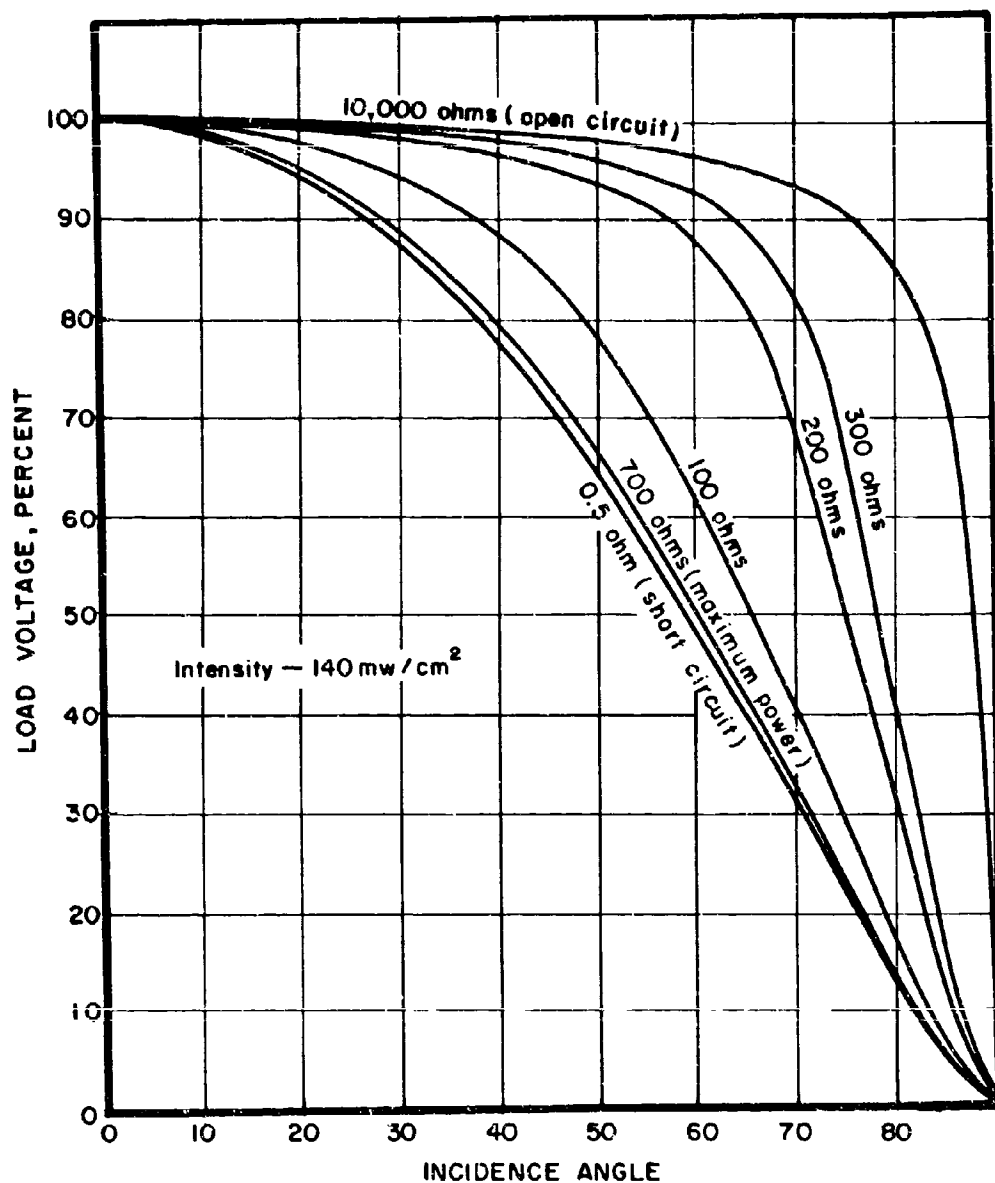
Figure 13.   Module WD-1, Angular Response, With X-25 Solar Simulator
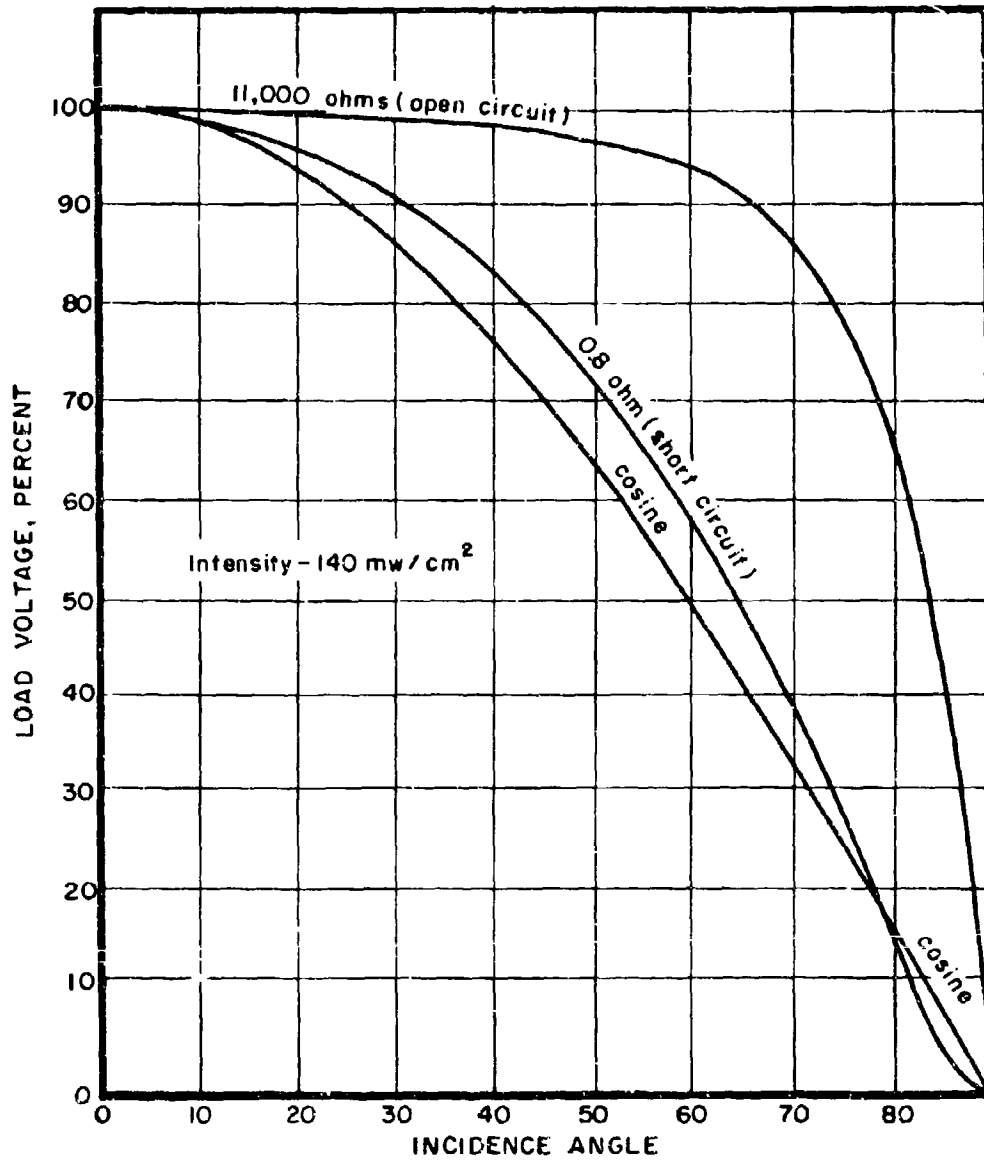
Figure 14.   Module GE-6, Angular Response, With X-25 Solar Simulator
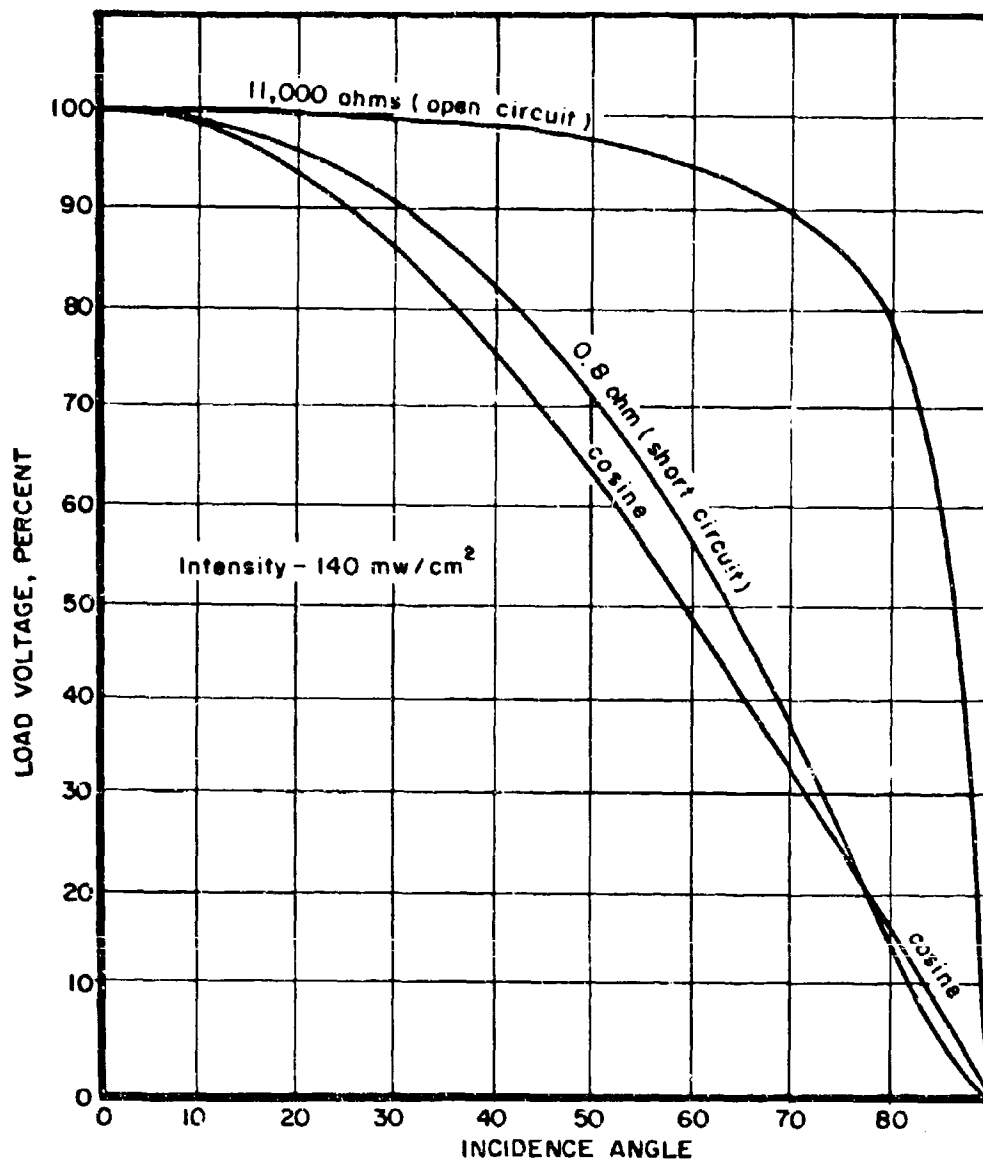
Figure 15. Module AR-7, Angular Response, With X-25 Solar Simulator

34
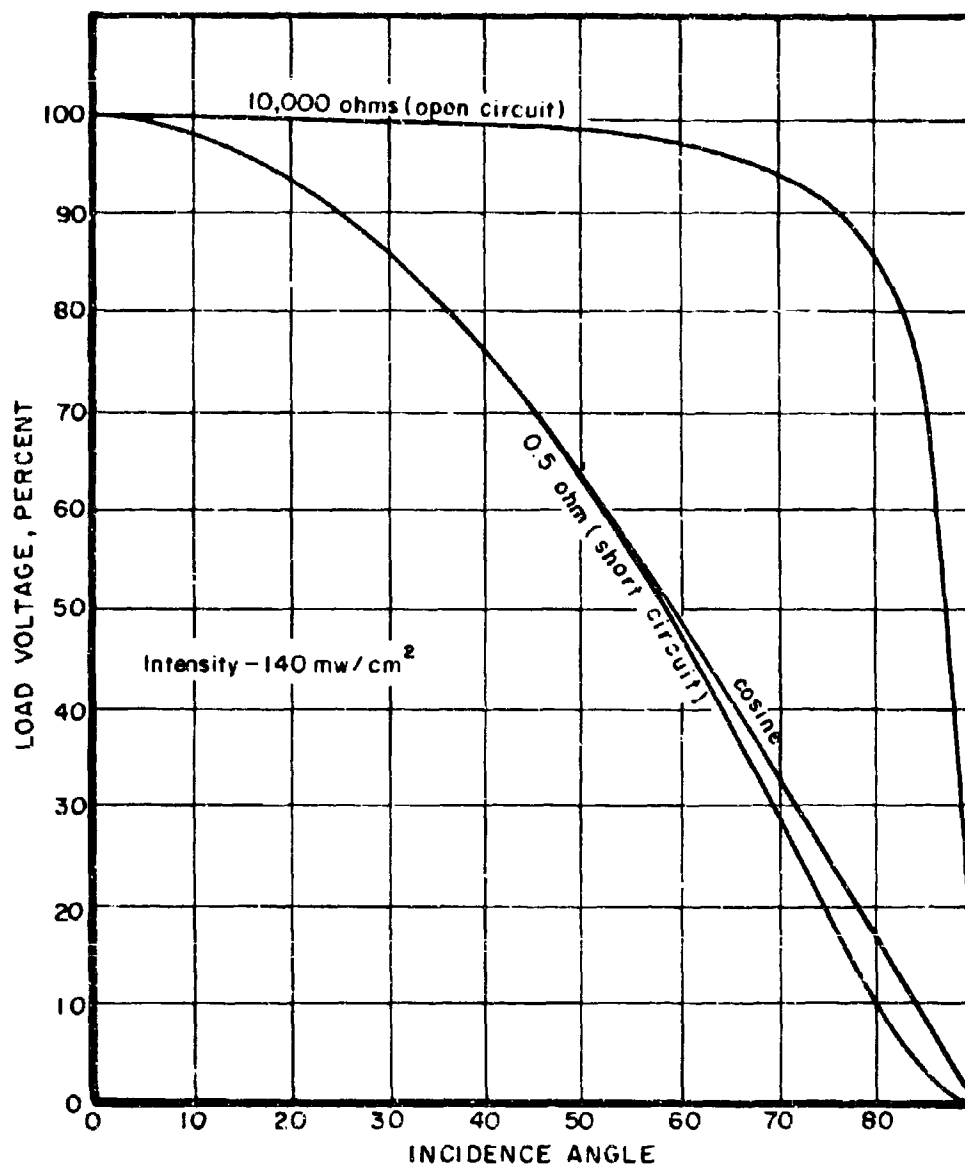
Figure 16.   Module IP-1, Angular Response, With X-25 Solar Simulator
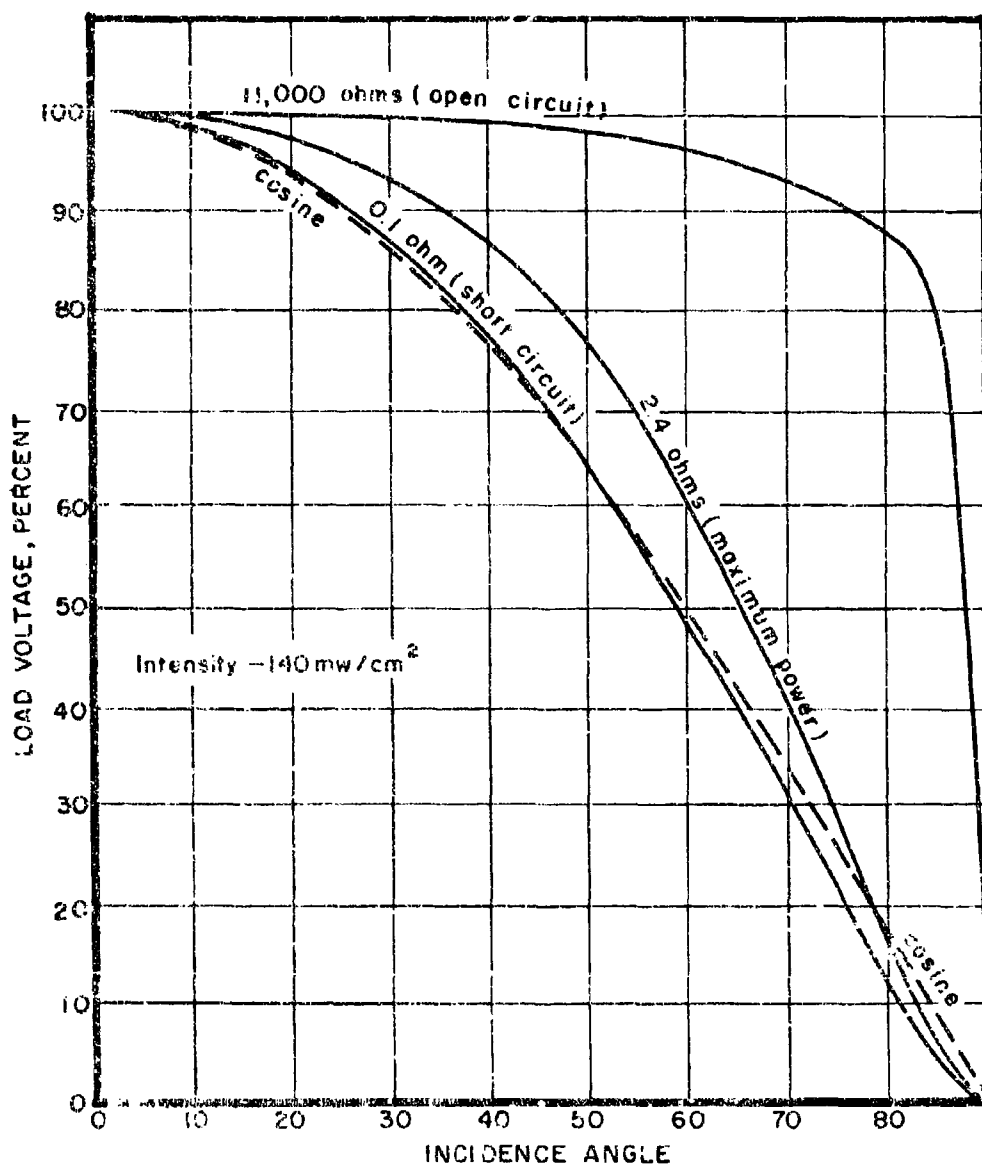
Figure ...   CdTe Cell Nr. L464-8, Angular Response, With X-25
Solar Simulator
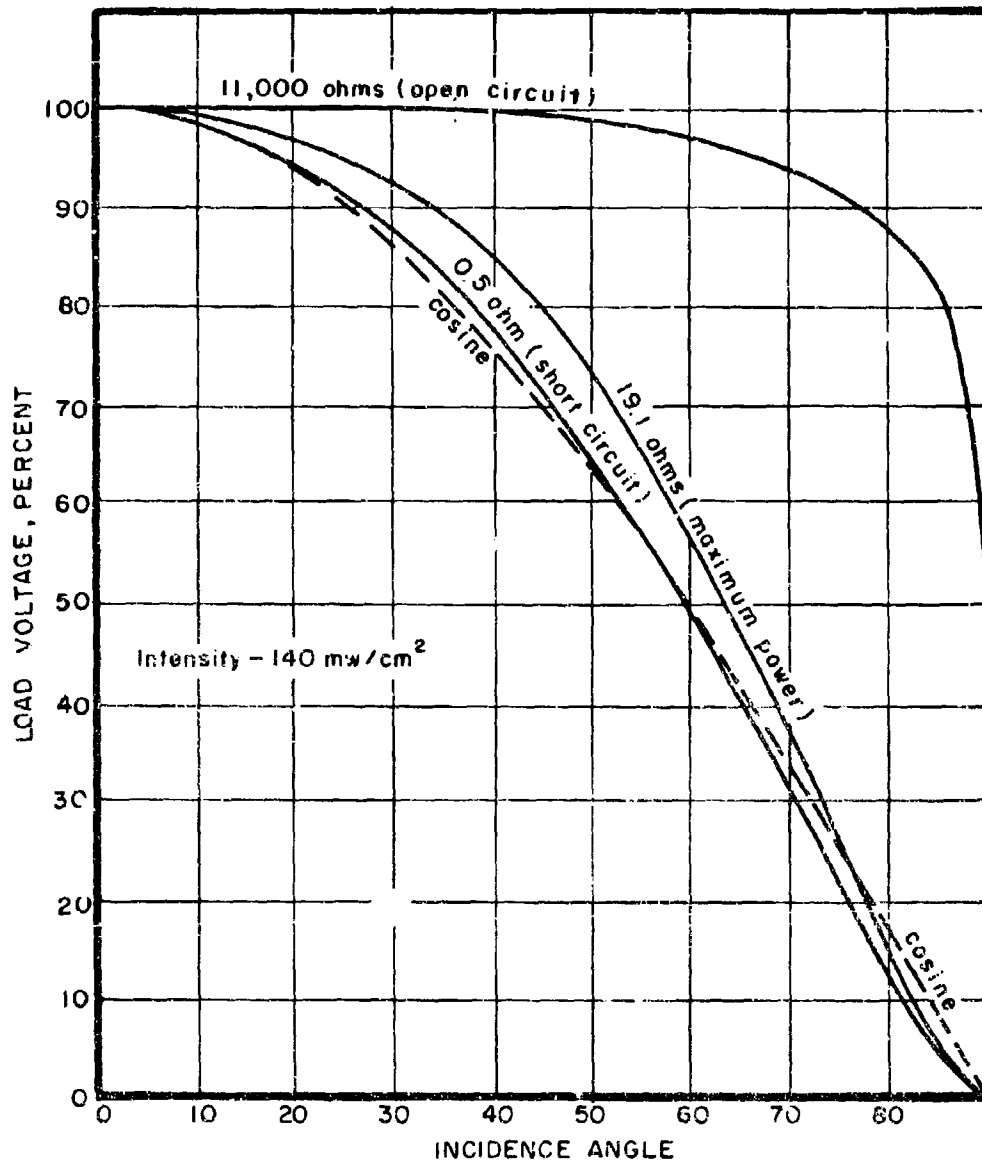
Figure 18. CdS Cell Nr. 8, Angular Response, With X-25 Solar Simulator

37

WN, WD, GE, and IP module output remained stable, but AR module short circuit current increased appreciably during the first few minutes of illumination as shown in Figure 19. This change was temporary and repeatable; initial output was restored after the cell had been covered for several hours. This change was too great and too slow to be directly caused by changes in module surface temperature which were small because the module was mounted upon a large temperature-controlled metal block. Curves similar to Figure 19 for the other modules showed an immediate rise in current to the final value.

3. MODULE PERFORMANCE CHARACTERISTICS

While still mounted and illuminated as described, each module and cell was connected to an automatic electronic load and X-Y plotter. The resulting voltage-current characteristic curves are shown in Figures 20 through 26. Figures 20, 21, and 24 show typical V-I curves for silicon modules in good condition. Figures 22 and 23 show serious deterioration, approximately 50% in short circuit current and 20% in open circuit voltage, of the thin film modules during 2 1/2 years laboratory storage and testing.

4. SPACE ANGULAR RESPONSE DATA ANALYSIS

Data sets were received for about 60 of the 3072 revolutions made by the Flight 2 vehicle. A sample data page is shown in Figure 9. The data set (Revolution 650, -Y arm) covering the greatest range of incidence angles was selected for detailed analysis. Short circuit data at 2° incidence angle intervals, and all open circuit data, were extracted from this data set, and corrected to 100°F and 140 mw/cm^2. All short circuit data exceeding 83 ma for silicon modules and 17 ma for thin film modules had to be discarded because of instrumentation, telemetry circuit saturation. All data obviously affected by shadowing of a portion of a module were also discarded. Corrected short circuit values for each module were then plotted against the laboratory short circuit value for the same incidence angle and module of the same type, as shown in Figures 27 through 31.
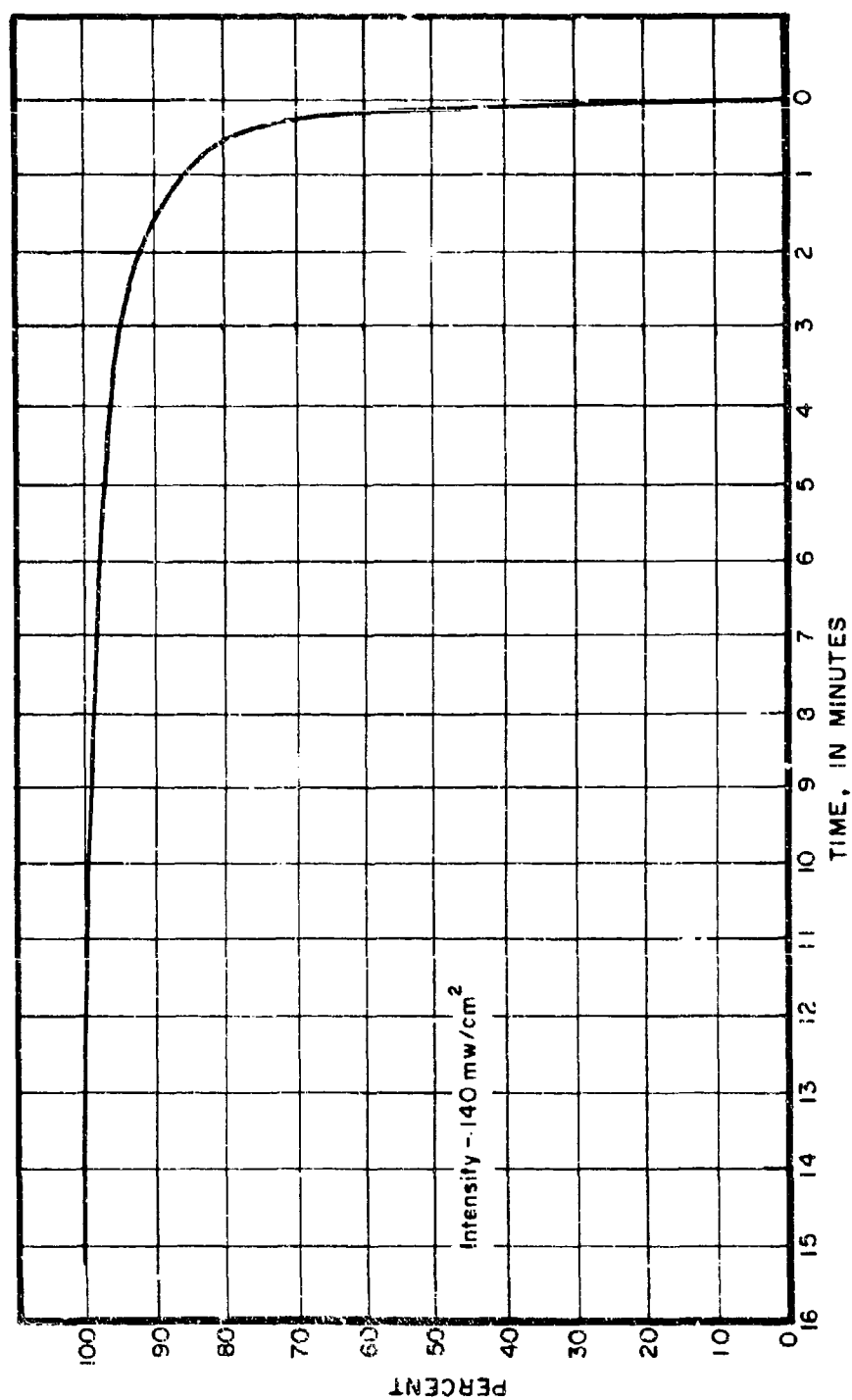
Figure 19.   Short Circuit Current Instability, Module AR-7, With X-25
Solar Simulator

39
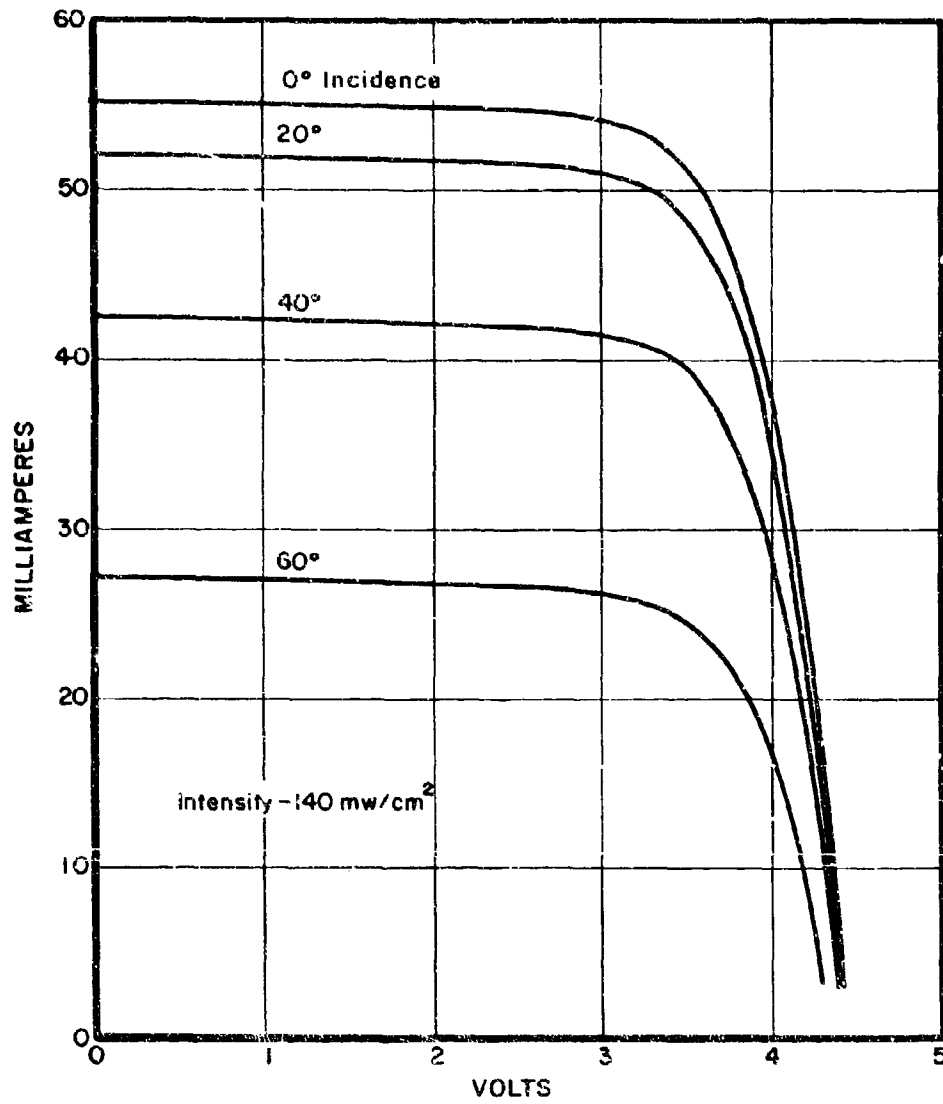
Figure 20.   Module WN-1, V-I Curves, With X-25 Solar Simulator
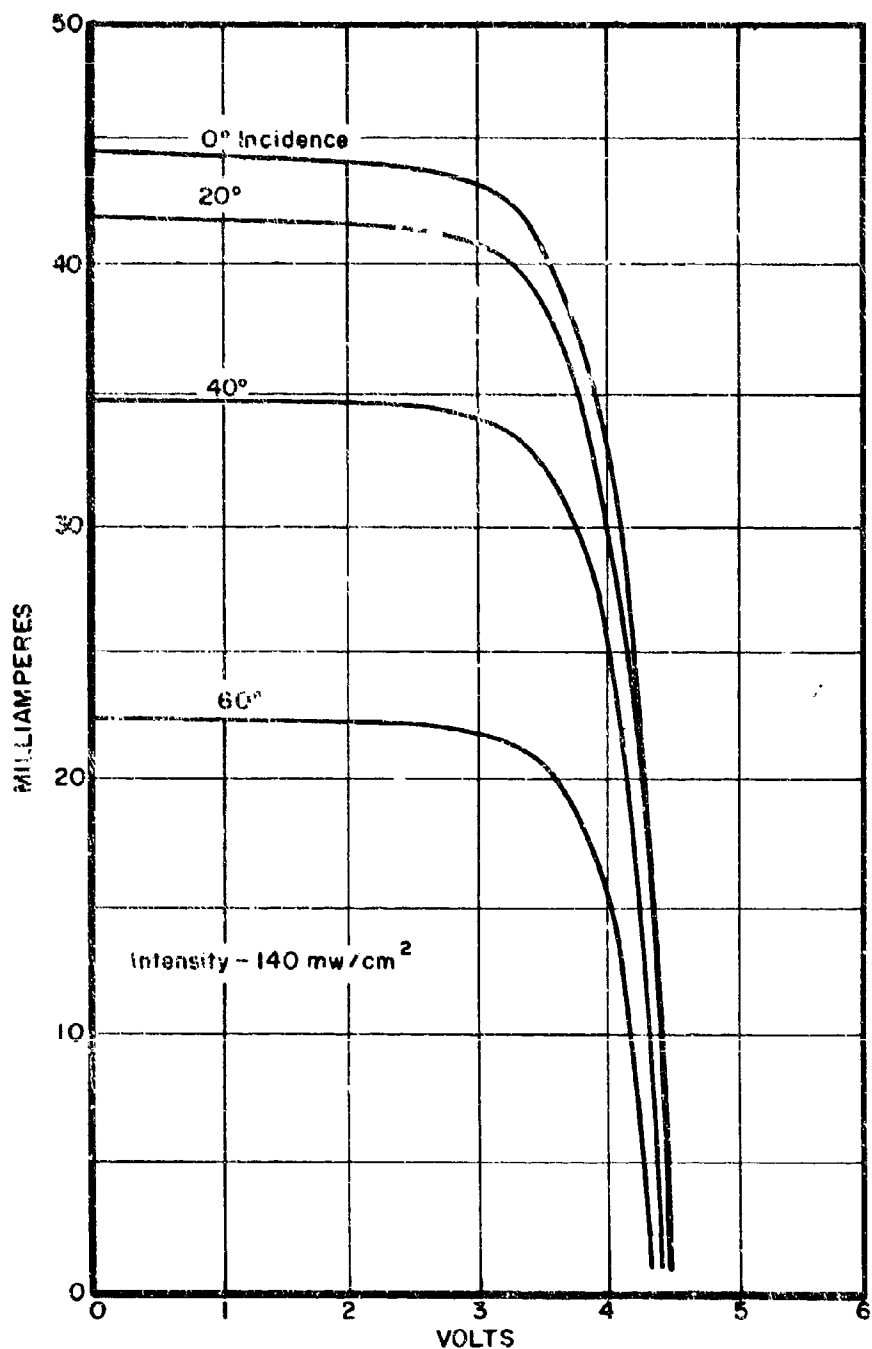
Figure 21.   Module WD-1, V-I Curves, With X-25 Solar Simulator
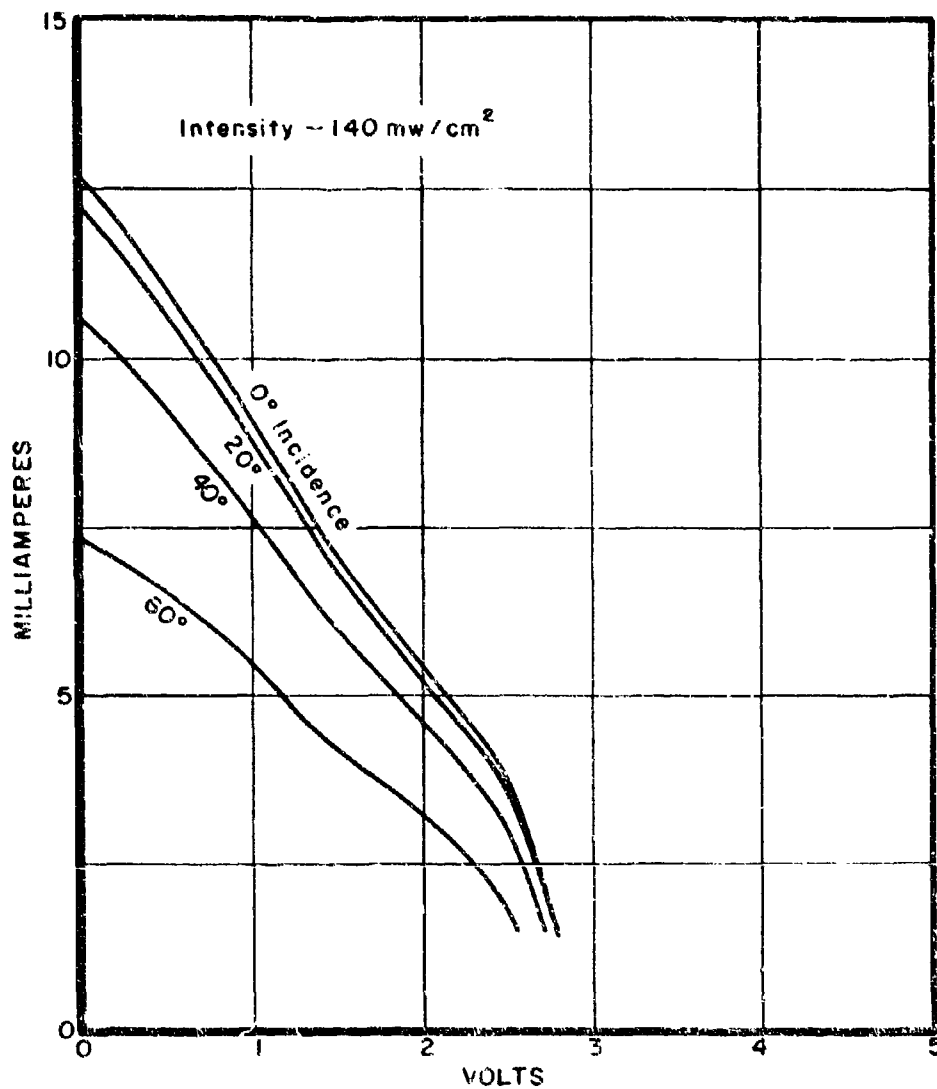
Figure 22.   Module GE-6, V-I Curves, With X-25 Solar Simulator
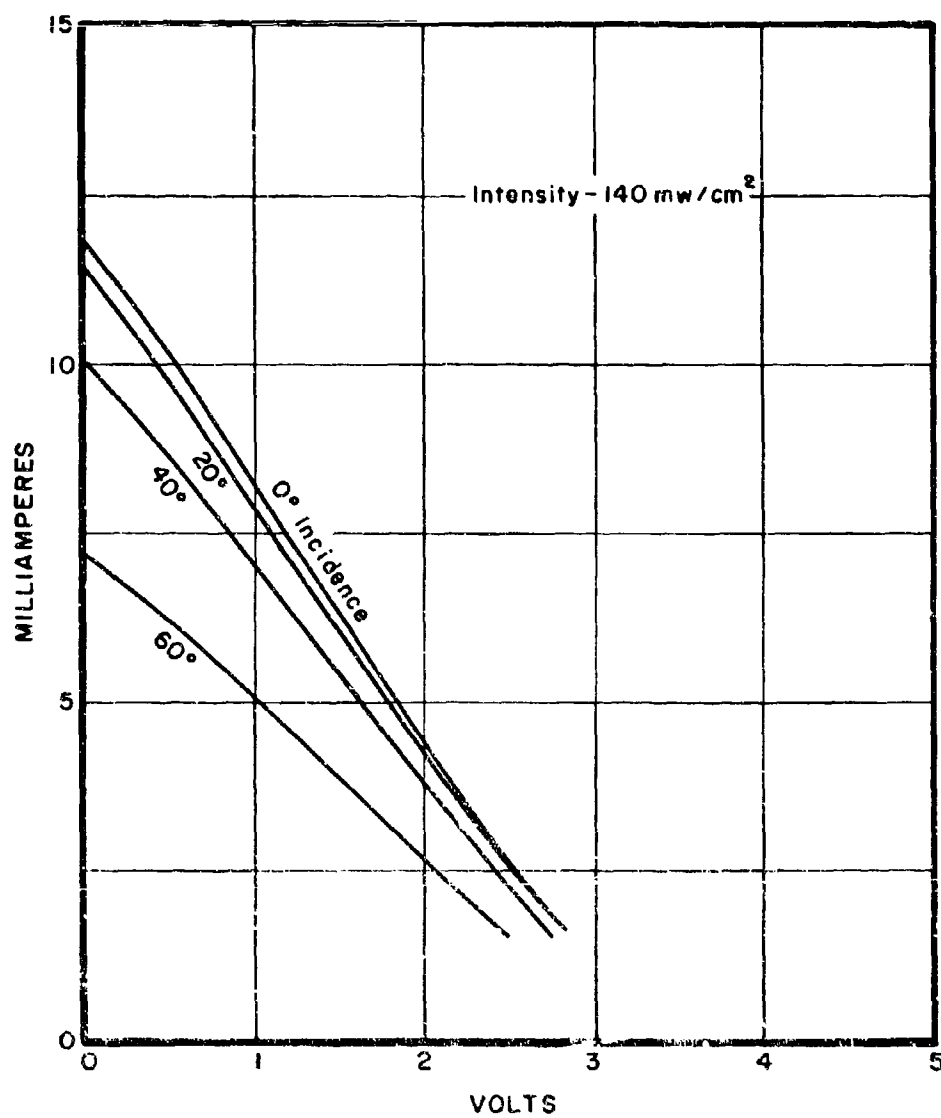
Figure 23.   Module AR-7, V-I Curves, With X-25 Solar Simulator
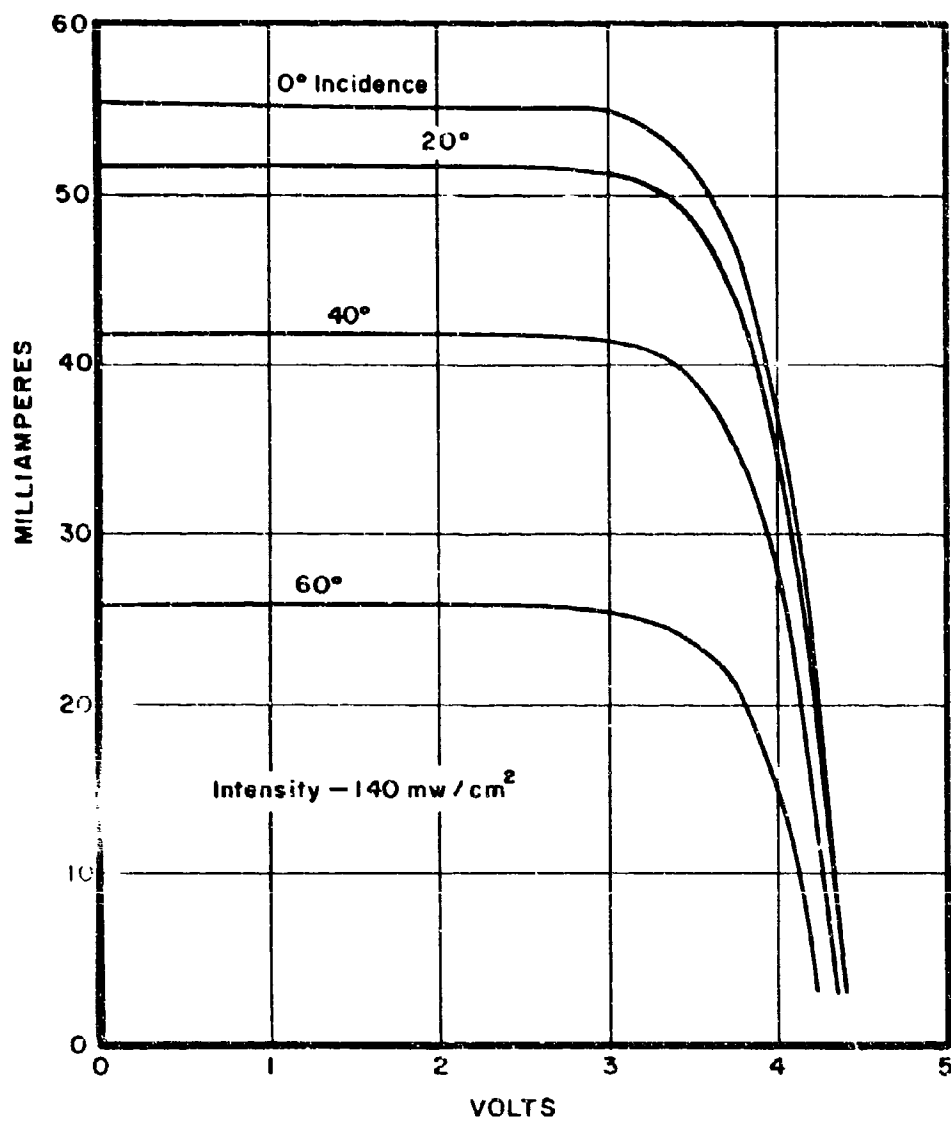
Figure 24.   Module IP-1, V-I Curves, With X-25 Solar Simulator
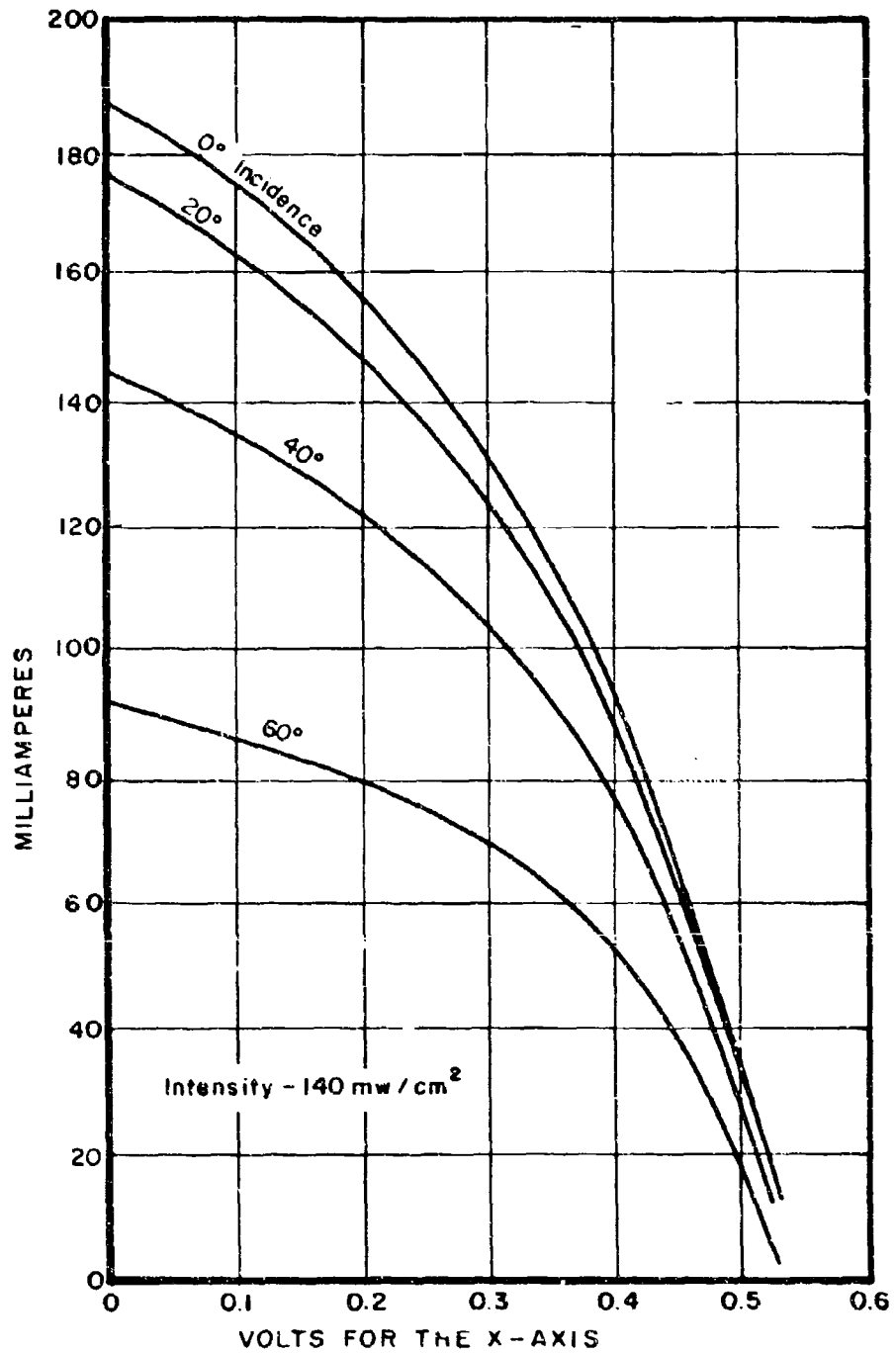
Figure 25.   CdTe Cell Nr. L464 8, V-I Curves, With X-25 Solar Simulator
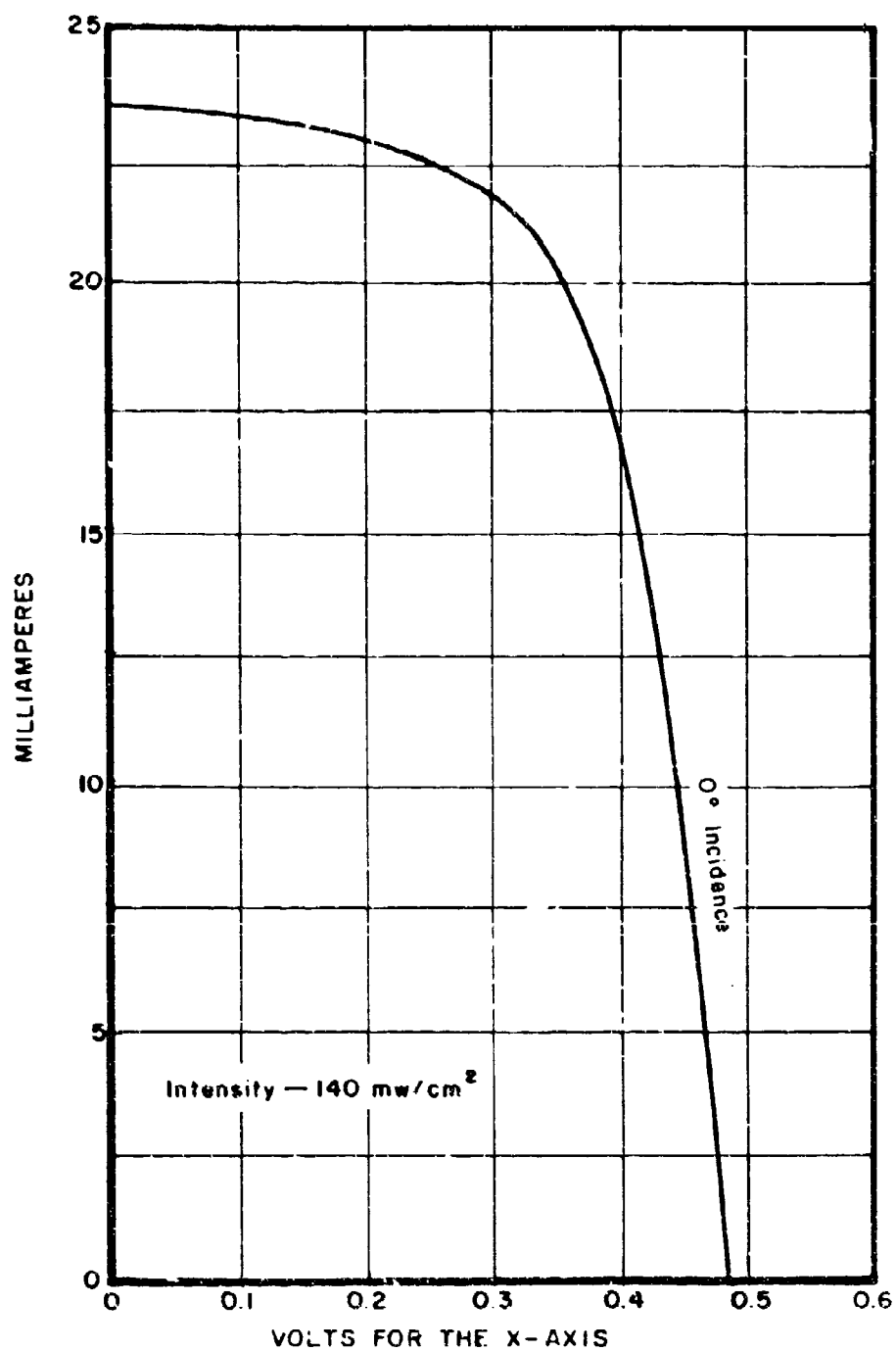
Figure 26.   CdS Cell Nr. 8, V-I Curves, With X-25 Solar Simulator
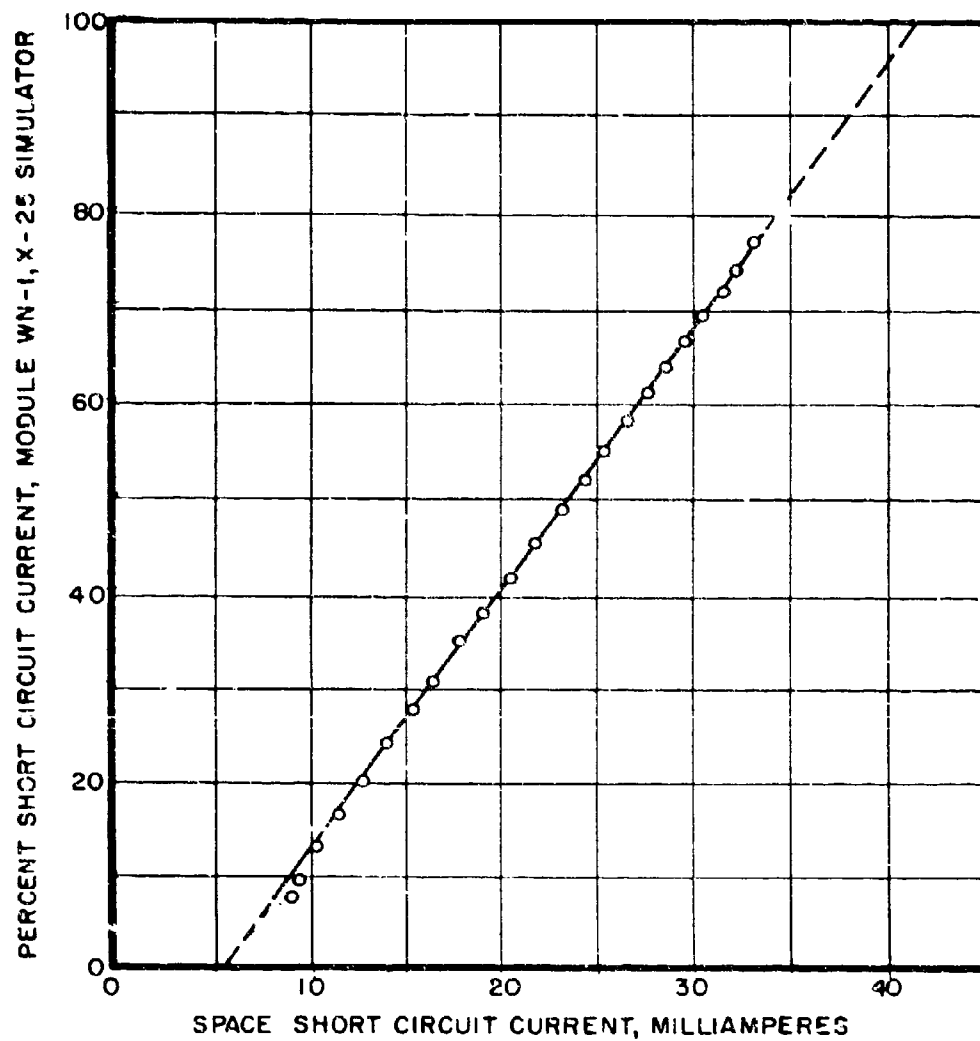
Figure 27.   Module WN-4, Angular Response in Space vs Simulator
Angular Response
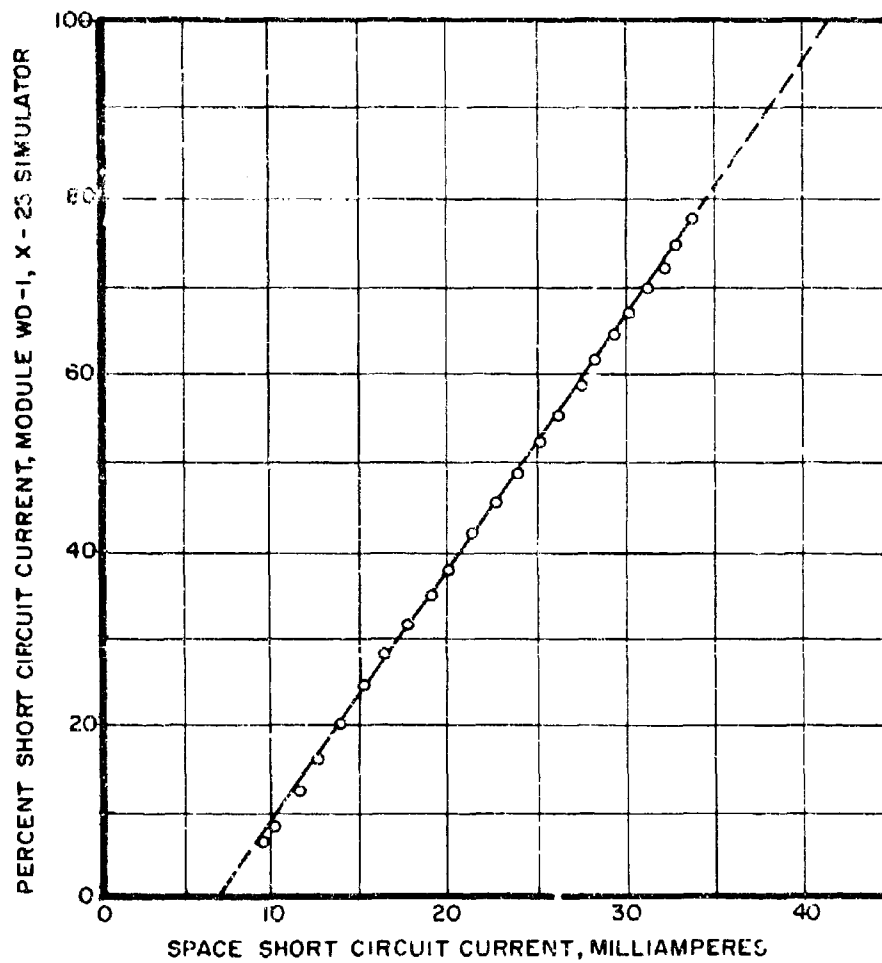
Figure 28.   Module WD-2, Angular Response in Space vs Simulator
Angular Response
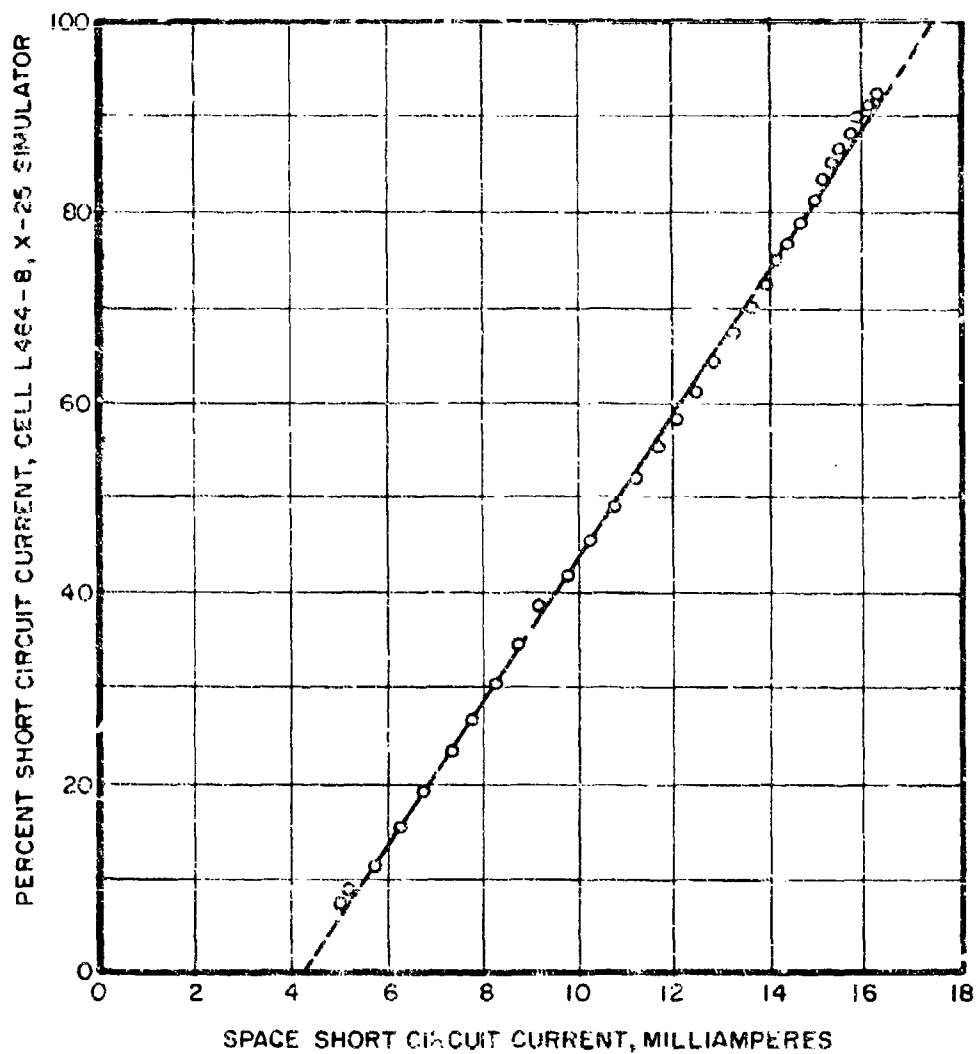
Figure 29. Module GE-3, Angular Response in Space vs Simulator
Angular Response
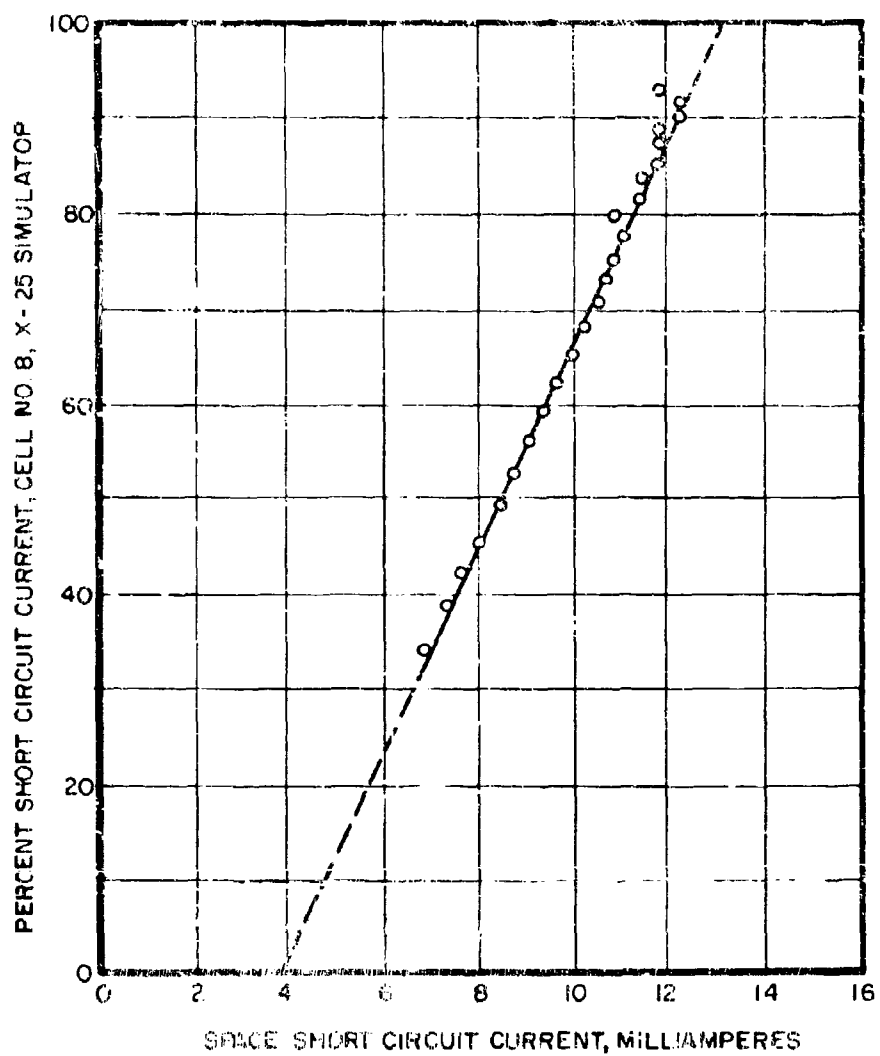
Figure 36. Module AR-16, Angular Response in Space vs Simulator
Angular Response
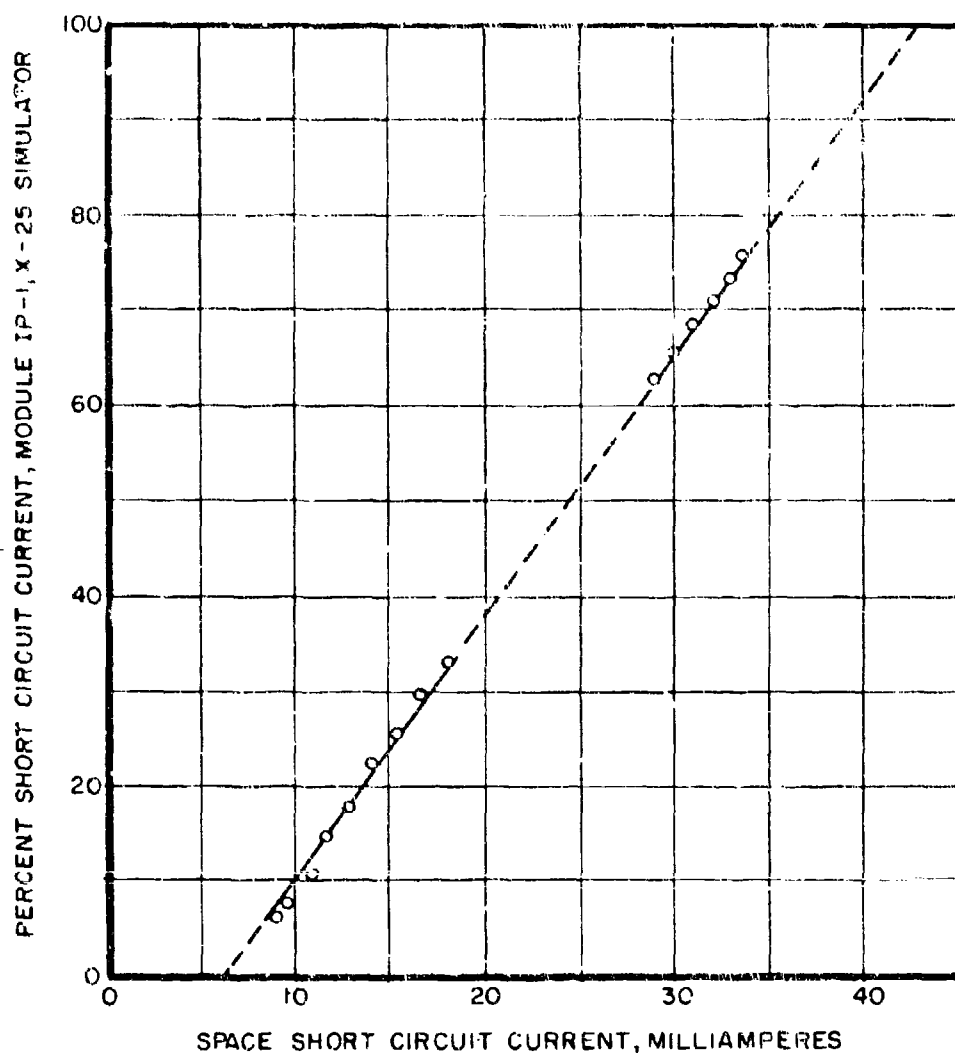
Figure 31.   Module IP-5, Angular Response in Space vs Simulator
Angular Response

The data points in Figures 27 through 31 lie reasonably well on a straight line which does not pass through the origin. This indicates that the space short circuit angular response for each module is similar to the laboratory angular response, except for the effect of reflected radiation from vehicle surfaces and earth's albedo. If it is assumed that this similarity extends over all angles of incidence, short circuit values for 0° and 90° incidence may be determined by straight line extrapolation. Using both corrected data points and extrapolated points, Figures 32 through 36 were plotted to show space angular response for each module. These curves indicate that the reflected illumination, as determined by short circuit current extrapolation to 90° incidence, is between 13 and 29% of the total illumination as determined by short circuit current extrapolation to 0° incidence.

Lines similar to Figure 28 were plotted for the WD modules on both arms of the Flight 2 vehicle for all available data sets. Results were similar in all cases, except for considerable variation (0 to 21% of total illumination) in the magnitude of reflection effects. The results obtained for module WD-4 after 358 days in orbit (revolution 3072, +Y arm) are typical, and are presented in Figures 37 and 38.

5. LABORATORY ANGULAR RESPONSE RESULTS

When accurately tested with an X-25 solar simulator at 140 mw/cm^2, the angular response curves for all modules in good condition, and the cadmium telluride and cadmium sulfide individual cells, were basically similar, and had the following characteristics in common (See Figures 12, 13, 16, 17, and 18):

(a) The short circuit is proportional to the cosine of the angle of incidence from 0° to 50° incidence. From 50° to 90° incidence, the short circuit current is slightly less than proportional to the cosine, probably due to specular reflection losses from the cover. (Silicon cells had 6 mil glass covers, CdS cells were encapsulated with 1 mil Kapton, and CdTe cells were sprayed with a 0.5 mil Krylon overlay.)
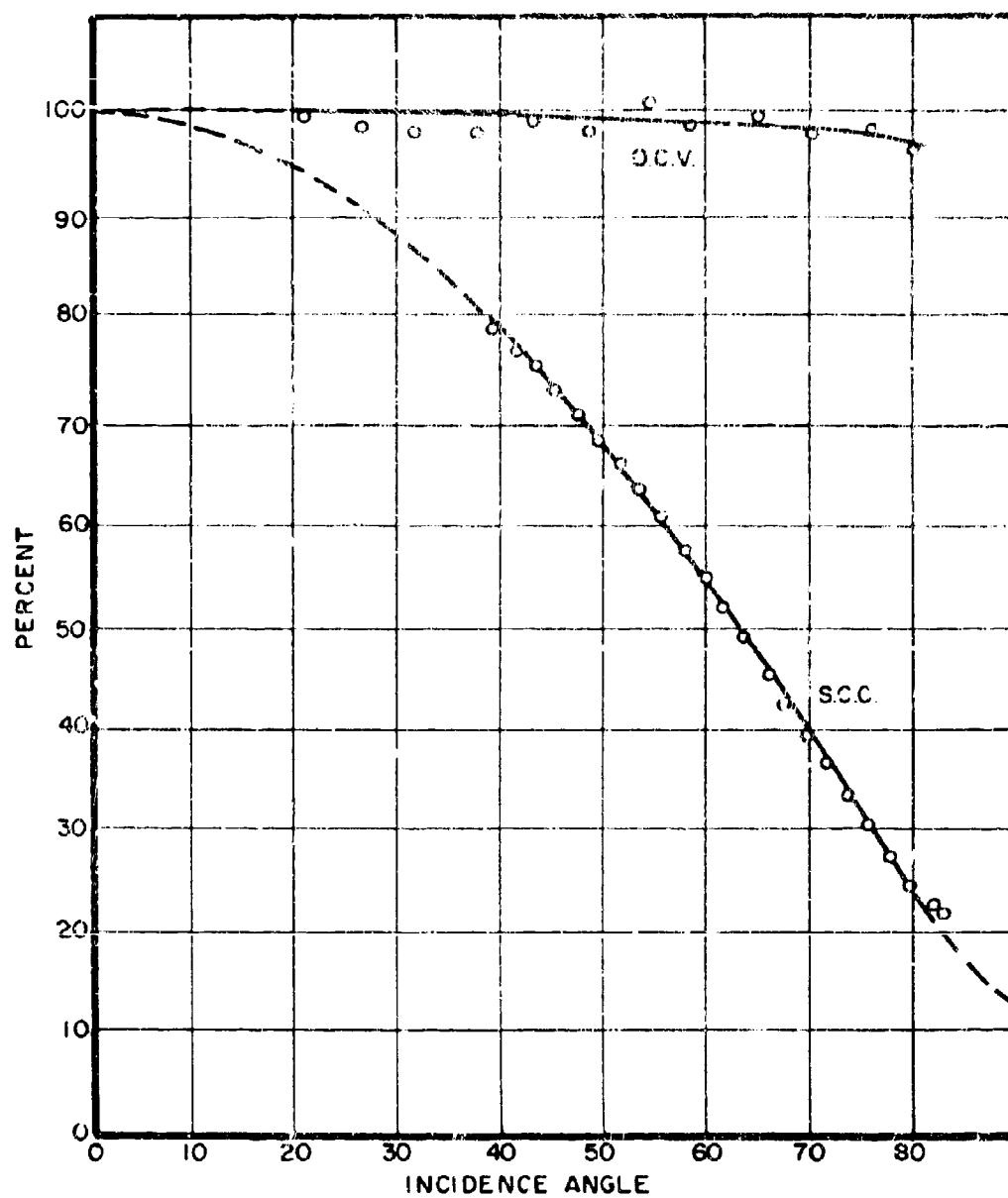
Figure 32.   Module WN-4, Angular Response in Space (75.6 Days)
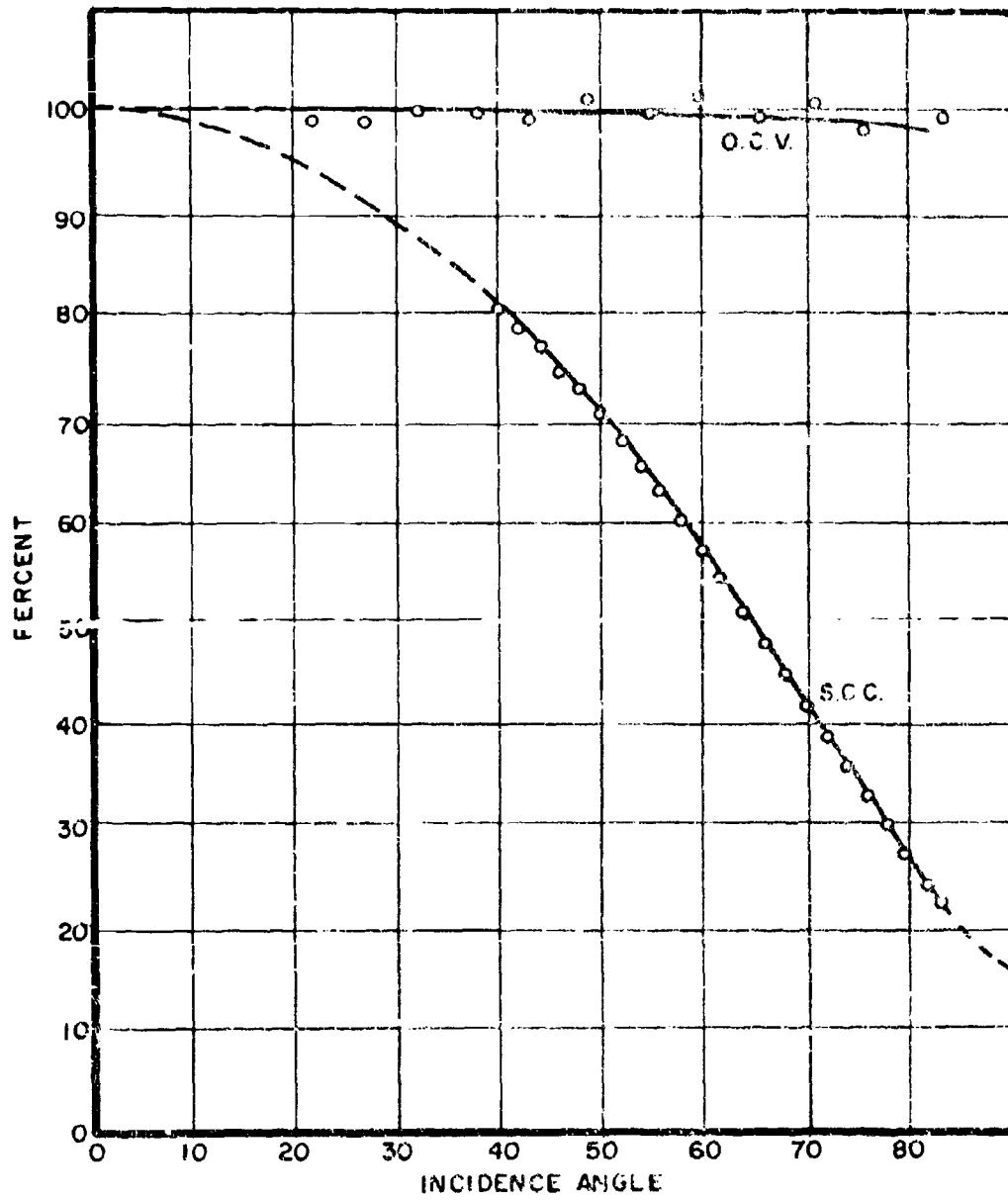
Figure 33.   Module WD-2, Angular Response in Space (75.6 Days)
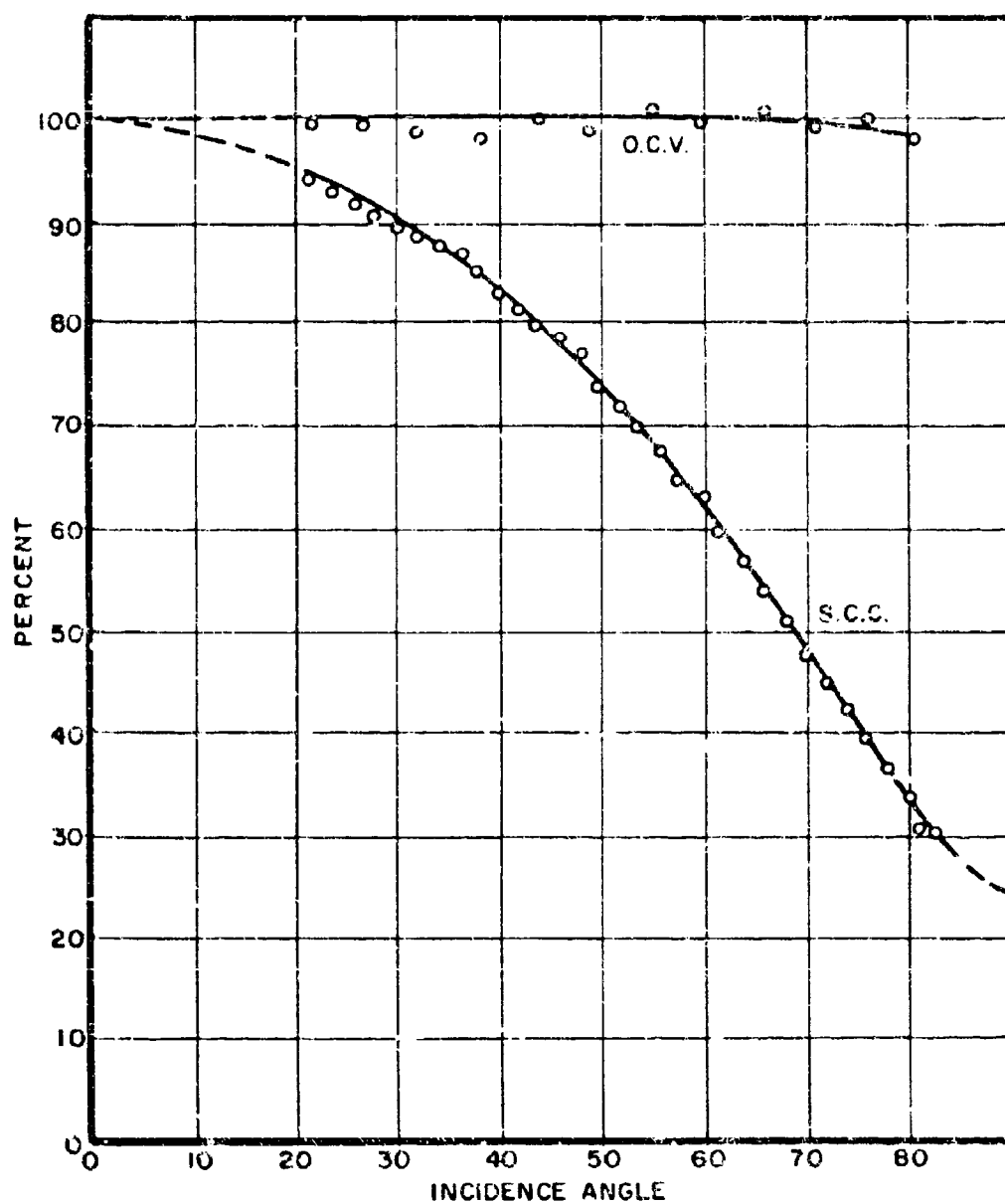
Figure 34. Module GE-3, Angular Response in Space (75.6 Days)
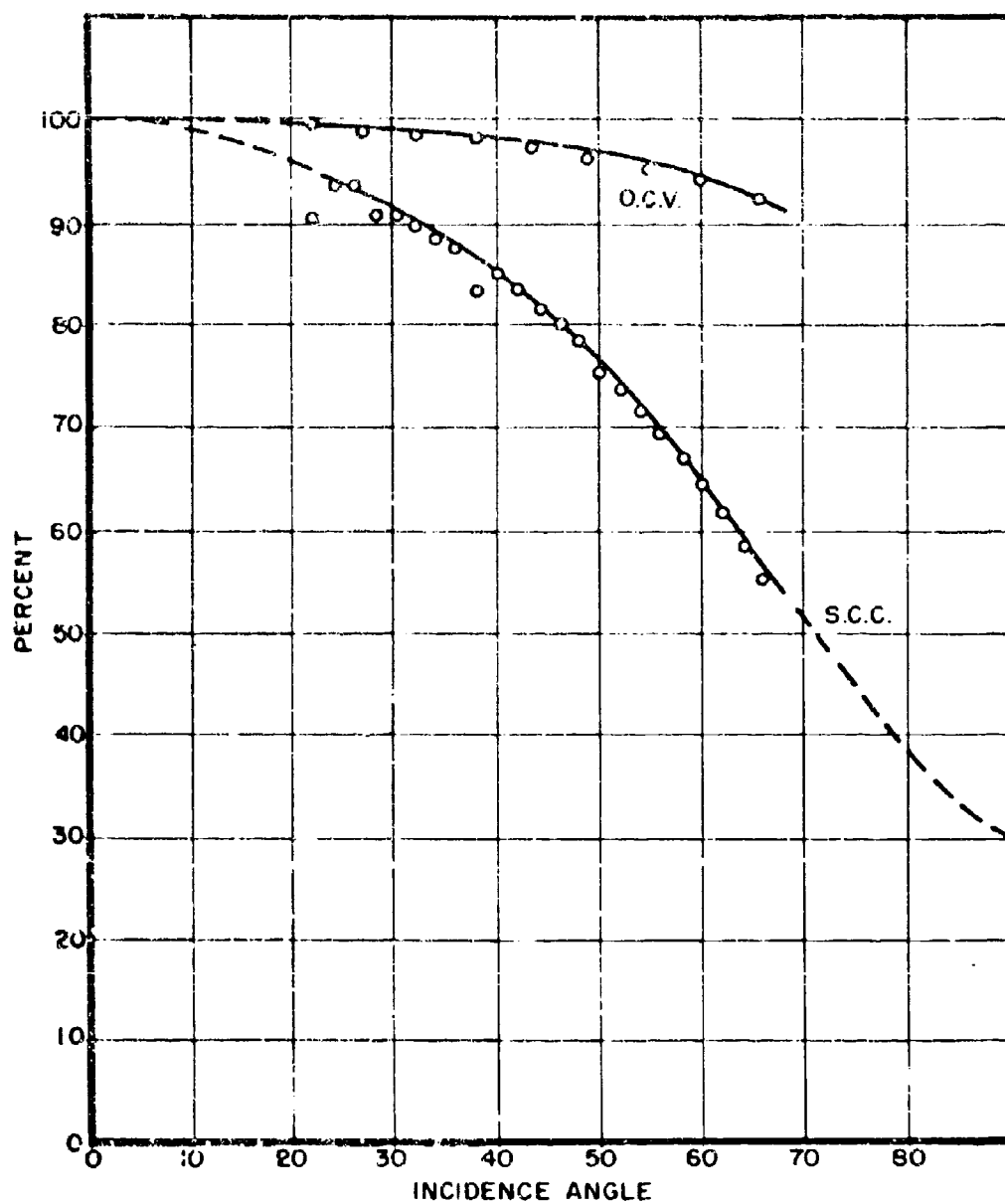
Figure 35.   Module AR-10, Angular Response in Space (75.6 Days)
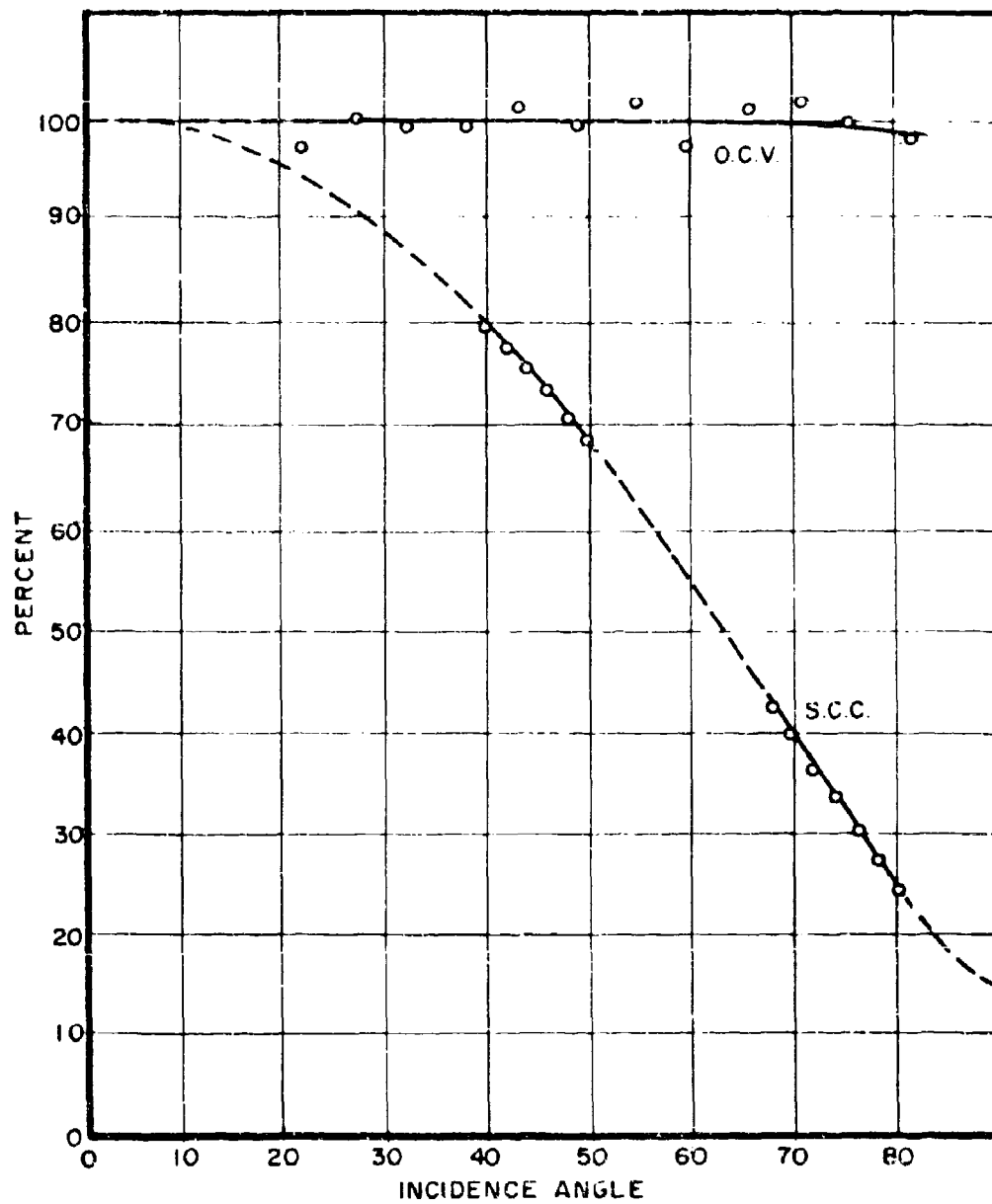
Figure 36.   Module IP-5, Angular Response in Space (75.6 Days)
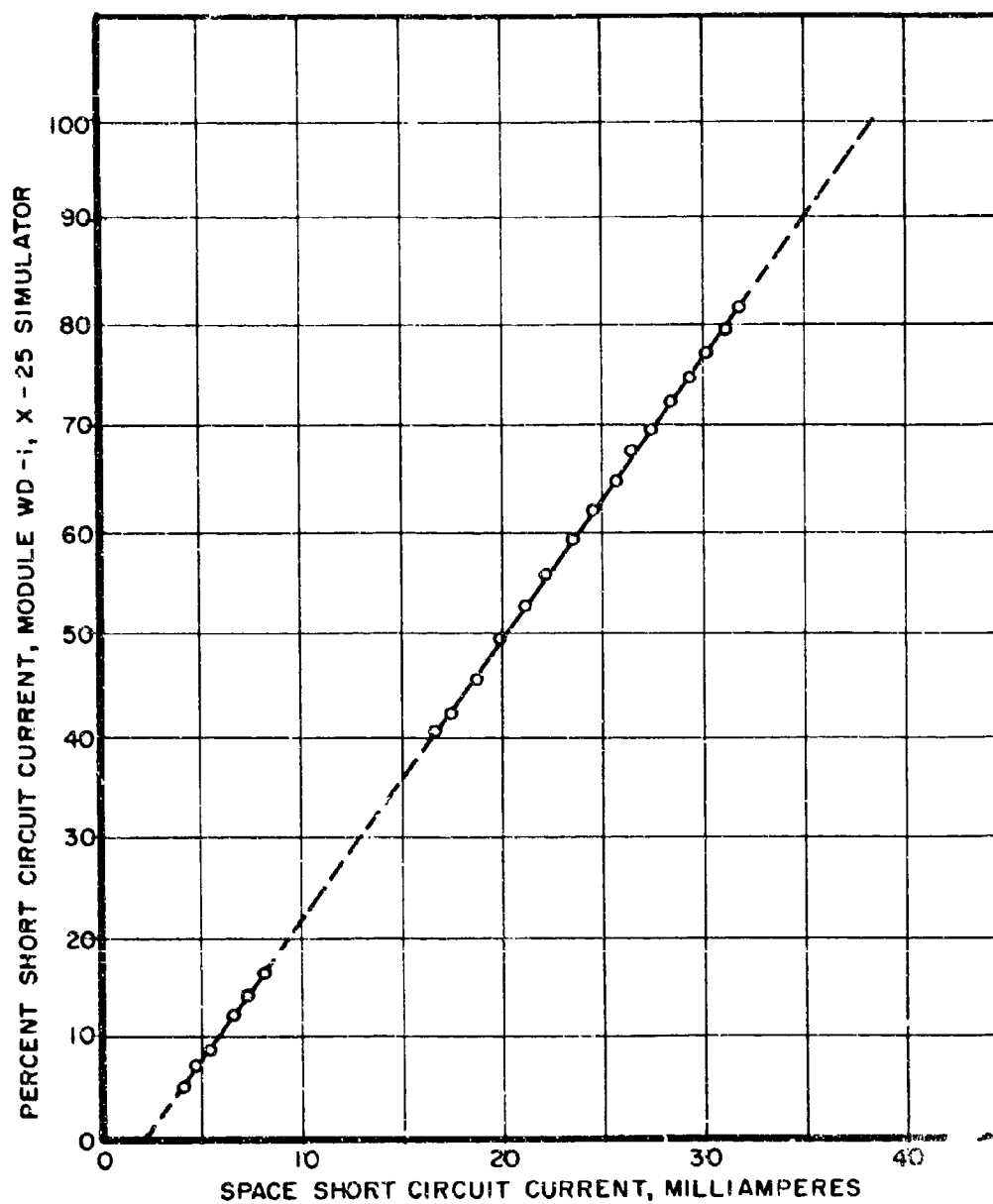
Figure 37.   Module WD-4, Space vs Simulator Angular Response
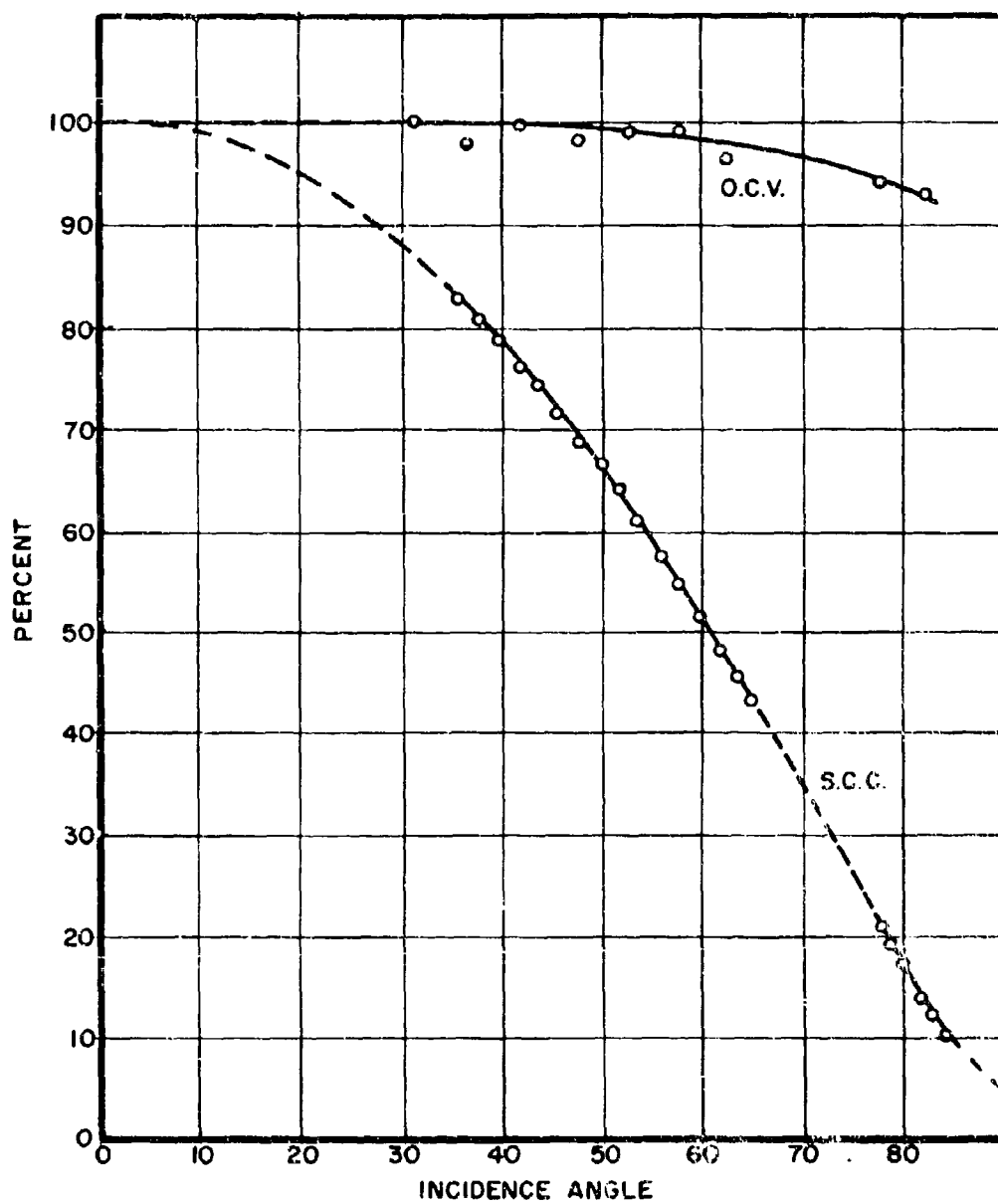
Figure 38.   Module WD-4, Angular Response in Space (358 Days)

(b) The open circuit voltage is relatively unaffected by incidence angle
from 0° to 50° incidence. At 50° incidence the open circuit voltage
reduction is only about 2%, and is about 6% at 70° incidence.

(c) As might be expected, the angular response curves for maximum power
and partial (high resistance loads) lie between the short circuit and
open circuit curves. For a good silicon module, Figure 13, the maximum
power curve closely resembles and is from 0 to 5% higher than the
short circuit curve.

One CdTe and one CdS module, both of which had substantially increased
internal series resistance due to degradation in storage, had short circuit
response curves appreciably higher than the cosine curve, from 0° to 75°
incidence, Figures 14 and 15. These curves are similar in shape to those
for loaded thin film cells in good condition, Figures 17 and 18.

CdS module short circuit current varied appreciable with time, Figure 19,
and with recent exposure history. This variation is slower in time and greater
in magnitude than any variation which could be attributed directly to temperature
changes within the thin film cell.

Voltage-current characteristics for 0°, 20°, 40°, and 60° angles of incidence
are shown in Figures 20 through 26.

6. SPACE ANGULAR RESPONSE RESULTS

Partial angular response data were obtained for 60 of the 3072 revolutions
made by the Flight 2 vehicle. Unfortunately, no short circuit current data
could be obtained at incidence angles less than 40° for silicon modules, and
22° for thin-film modules, because the instrumentation/telemetry circuits
saturated. Furthermore, no direct measurements were made of reflections
from vehicle surfaces or the earth's albedo. The following conclusions are
derived from analysis and extrapolation of the best available data, Figures 27
through 38.

(a) Both short circuit current and open circuit voltage angular response in space appear to be similar to laboratory angular response, except for the effect of reflected energy from vehicle surfaces and the earth's albedo.

(b) On different revolutions, the reflected energy appeared to vary from 0 to 30% of the total energy, as estimated by extrapolation of the short circuit angular response data.

(c) No information was obtained as to how the reflected energy incident upon the modules varied during any one data run; the longest of which was 38 minutes.

(d) Prolonged exposure to the space environment (75.6 days for Figures 27 through 36, and 358 days for Figures 37 and 38) produced no apparent changes in the shape of the angular response curve. Some degradation in total output of each module occurred and is discussed in Section V of this report.

SECTION IV

ENVIRONMENT AT ORBIT ALTITUDE

1. ELECTRON AND PROTON FLUXES

While solar array temperature excursions ranged from -170° to +150°F in hard vacuum during shadow/sunlight transits, the principal item of interest from a solar cell damage standpoint was the energetic charged particle environment due to electrons and protons trapped in the earth's magnetic field. An attempt was therefore made to estimate the total integrated electron and proton fluxes from published models of the Van Allen radiation belt and to correlate these fluxes with damage observed in solar cells by accelerator produced 1 Mev electron flux in the laboratory. The region of interest was the inner zone trapped radiation environment at an altitude of 2000 nautical miles (1.58 earth radii). From Reference 1 (page 51) the following values for omnidirectional proton exposure rate in a 2000 nautical mile, 90 degree inclination orbit were obtained:

Proton Energy	Omnidirectional Exposure Rate ($P/cm^2 \cdot Day$)
E > 4 Mev	8.22×10^9
E > 6 Mev	3.28×10^9
E > 8 Mev	1.32×10^9
E > 10 Mev	5.3×10^8

From Reference 2 (page 61) the following value was obtained for omnidirectional electron exposure rate in this orbit:

Electron Energy	Omnidirectional Exposure Rate ($e/cm^2 \cdot Day$)
E > .5 Mev	4.22×10^{11}

Ignoring the effects of energetic particles produced by solar flare occurrences, the worst case conditions correspond to a proton exposure rate of 8.22×10^9 $P/cm^2 \cdot Day$ (E > 4 Mev) and an electron exposure rate of 4.22×10^{11} $e/cm^2 \cdot Day$ (E > .5 Mev).

2. EQUIVALENT 1 MEV ELECTRON FLUX

From Rosenwelg's data, Figure 39, (Reference 3), the conversion factor from omnidirectional fission electrons to equivalent normal incident 1 Mev electrons is .90 for a shield thickness of .04 grams/cm^2 (6 mil glass).

Therefore:

$$\Phi_e = (.90) \ (4.22 \times 10^{11}) = 3.8 \times 10^{11} \ \frac{e}{cm^2 \cdot day}$$

(e = 1 Mev)

Damage produced by energetic protons can also be estimated by relating the proton exposure rate for the various energy ranges to equivalent 1 Mev electron flux. Figure 40 shows the omnidirectional proton exposure rate (Φ_p) > E at orbit altitude plotted as a function of proton energy from 4 to 10 Mev. It can be seen from this curve that the proton exposure rate decreases significantly with increasing proton energy and that the majority of solar cell damage is produced by the lower energy protons due to their higher number. It should be noted that a 6 mil (.04 gm/cm^2) shield will absorb all protons with energies less than 4.5 Mev.

An equivalent 1 Mev unidirectional, normally incident electron flux for each midpoint in the energy ranges of interest can then be established for each omnidirectional proton/cm^2 from Figure 41, (Reference 3), with the following results:

Proton Energy Range (Mev)	Omnidirectional Exposure Rate (P/$cm^2 \cdot$ day)	Equivalent 1 Mev Electron Flux per proton/$cm^2 \cdot$ day (From Figure 41)	Equivalent 1 Mev Electron Flux e/$cm^2 \cdot$ day
4.5 - 6	3.2 x 10^9	3.2 x 10^3	10.2 x 10^{12}
6 - 8	1.96 x 10^9	2.9 x 10^3	5.7 x 10^{12}
8 - 10	7.87 x 10^8	2.6 x 10^3	2.1 x 10^{12}
> 10	5.3 x 10^8	2.3 x 10^3	1.2 x 10^{12}
		TOTAL	1.92 x 10^{13}

The total equivalent 1 Mev electron flux is obtained by summation of the flux equivalences for each proton energy range midpoint. This summation yields a total 1 Mev electron flux equivalent of
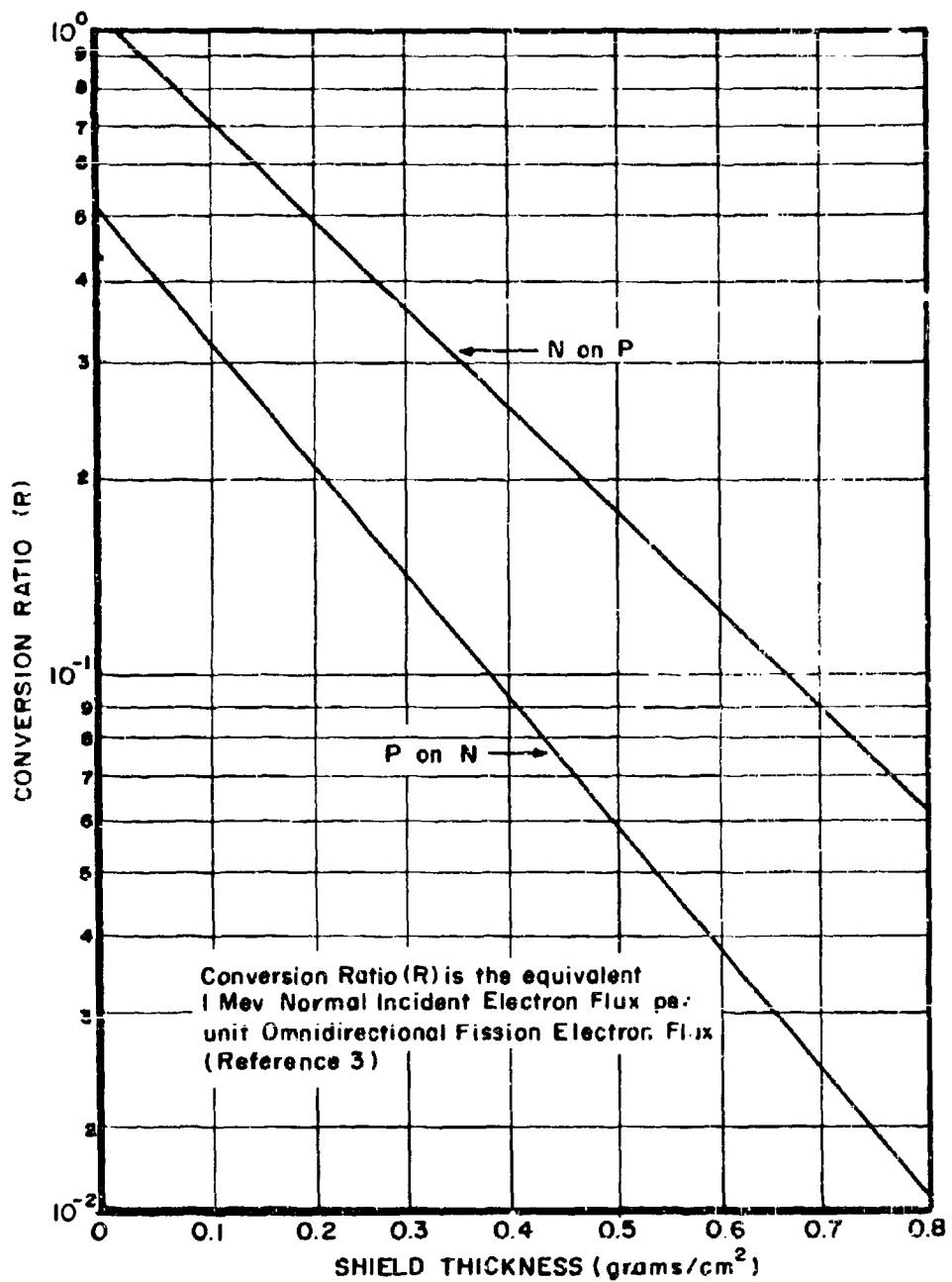
Figure 39. Conversion Ratio From Fission Electrons to 1 Mev
Electrons vs Shield Thickness
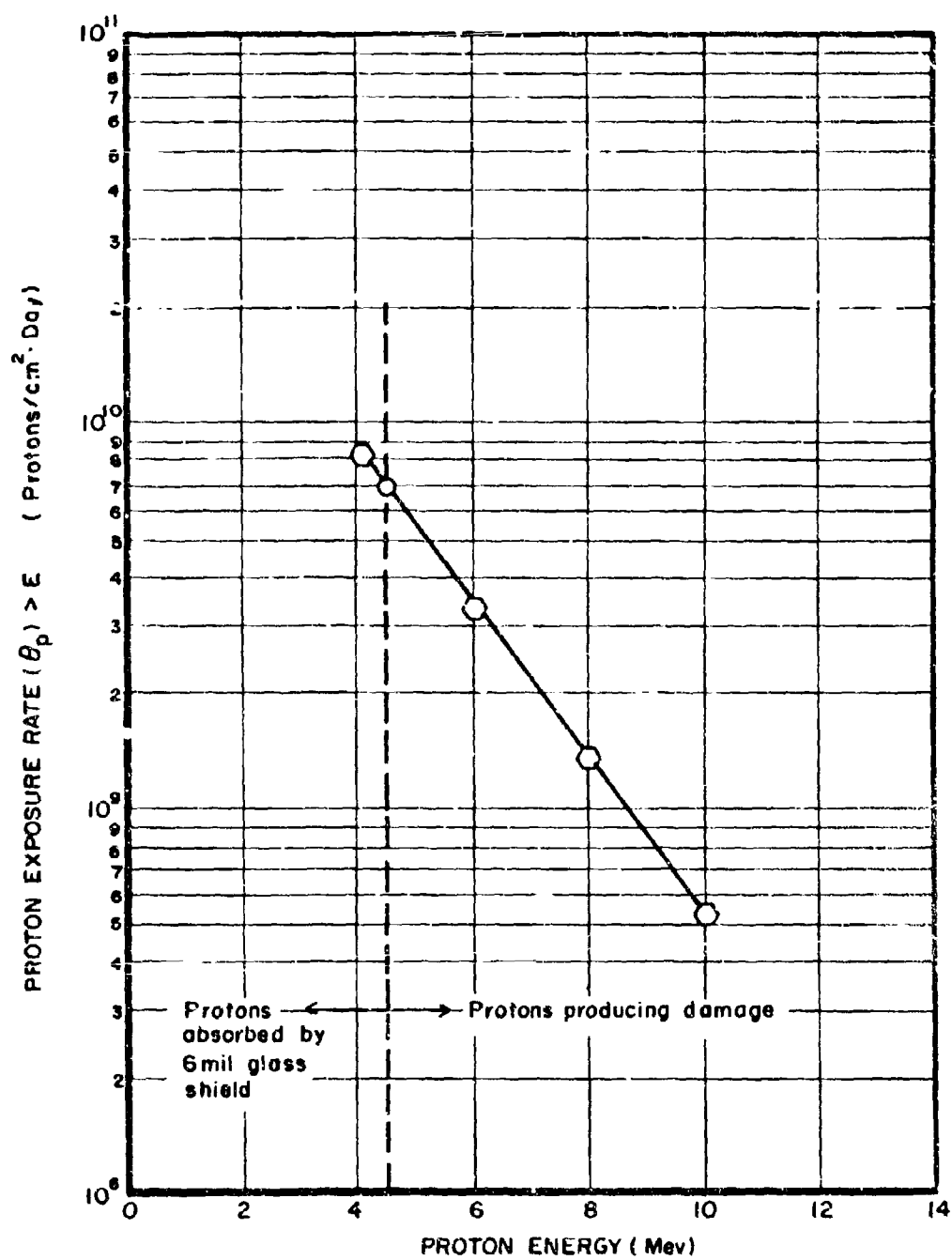
Figure 40.   Omnidirectional Proton Exposure Rate $(\Phi_p) > E$ vs Proton
Energy for 2000 NM Polar Orbit

65
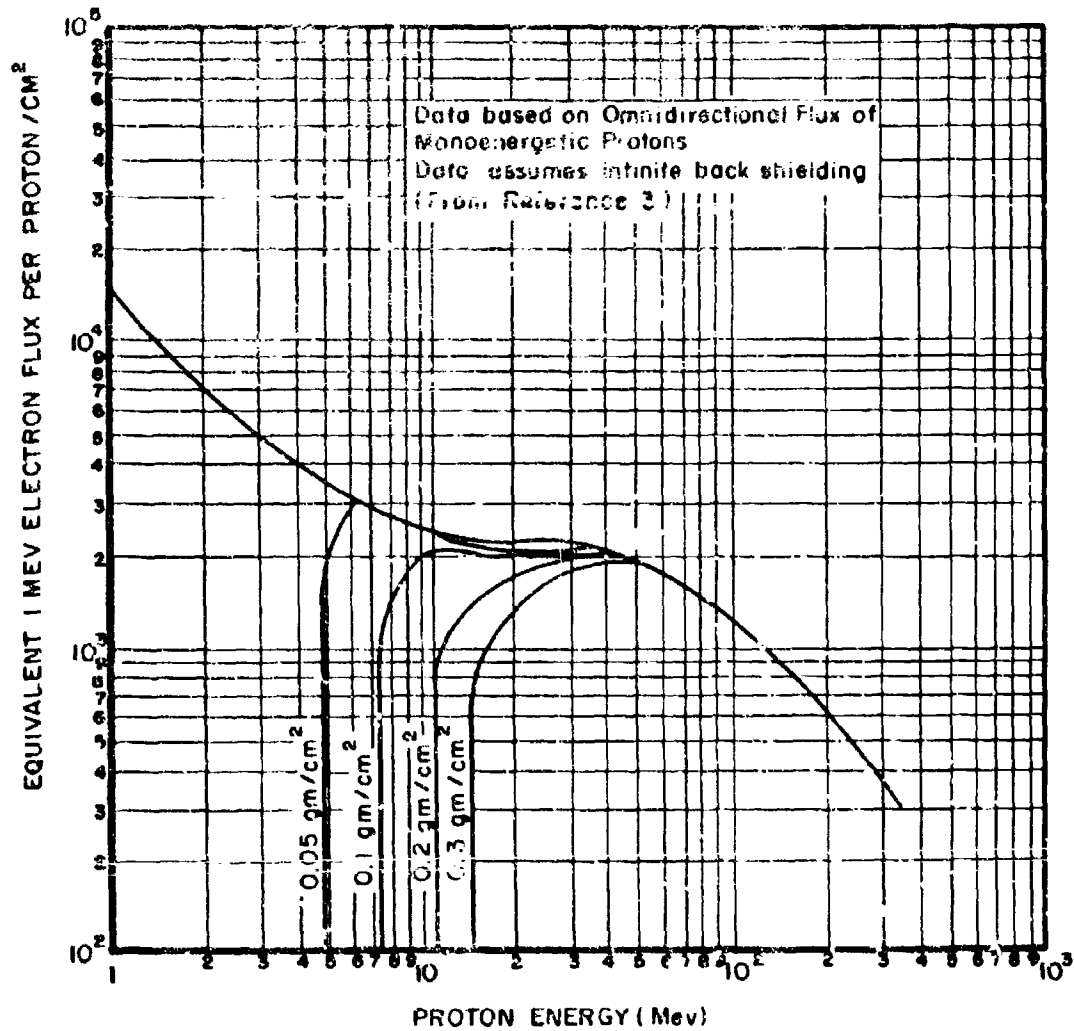
Figure 41.   Equivalent 1 Mev Electron Flux per Proton/cm² vs
Proton Energy for Various Shield Thickness

$$1.92 \times 10^{13} \frac{1 \text{ Mev electrons}}{cm^2 \cdot day}$$

or

$$\Phi_p(1 \text{ Mev electron equivalent}) = 1.92 \times 10^{13} \text{ e/cm}^2 \cdot day$$

The total damage estimated at any given time in this orbit should be based upon a total 1 Mev electron exposure rate of

$$\Phi_e + \Phi_p = (0.038 \times 10^{13}) + (1.92 \times 10^{13})$$
$$\cong 2 \times 10^{13} \frac{1 \text{ Mev electrons}}{cm^2 \cdot day}$$

3. PREDICTED RADIATION DAMAGE

The total equivalent integrated 1 Mev electron fluxes corresponding to time periods throughout the total experiment on-orbit life of 358 days were calculated. The $\frac{I}{I_o}$, $\frac{V}{V_o}$ and $\frac{P}{P_o}$ values were then obtained at the various flux levels from Cherry's and Statler's data on the effects of 1 Mev electrons on silicon solar cells, Reference 4. These estimated damage ratios can be compared with the actual damage observed in the flight experiment for the IP, WN, and WD modules only, since these modules are the only ones containing cells of the same basic types as those included in the Cherry and Statler data. The predicted damage is shown and is compared to the actual flight data in the applicable figures and tables in Section V.

SECTION V

EXPERIMENT RESULTS

1. SHORT CIRCUIT CURRENT AND OPEN CIRCUIT VOLTAGE

The 50° incidence short circuit current and open circuit voltage values for each module after selection. correction, and conversion to percent, as discussed in Section II, were plotted in the following figures:

SCC Figure	OCV Figure	Flight 1 -Y Arm Modules	Flight 2 -Y Arm Modules	Flight 2 +Y Arm Modules
42	47	WN-3	WN-4	WN-5
43	48	WD-5	WD-2	WD-4
44	49	GE-5	GE-3	GE-4
45	50	AR-5	AR-10	AR-8
46	51	IP-2	IP-5	IP-4

The predicted values of short circuit current and open circuit voltage, calculated by the method described in Section IV, are also shown in Figures 42, 43, 46, 47, 48, and 51.

During Flight 2, no data were obtained for the -Y arm panel after 182 days, and no data were obtained for the +Y arm panel during the first 182 days. Both panels were. of course, exposed to the same space environment. Flight 1 data were obtained for the -Y arm panel only, for 127 days. Since Flight 1 and Flight 2 orbits were nearly identical, data from the three panels for each type of module can logically be plotted against time in orbit in the same figure, for direct comparison and analysis.

The degradation values listed in Tables IV through VI, and the following comments, are based upon a careful examination of the results plotted in Figures 42 through 51:

1. The total degradations for the 358-day experiment are listed in Table IV. The open circuit voltage degradations for the three silicon modules are,

for all practical purposes, equivalent, and approximately as expected. The WD module short circuit performance is surprisingly good. The AR modules failed in Flight 1, and appeared to be failing in Flight 2, for reasons other than radiation damage. The GE Modules show excessive current and voltage degradation in Flight 1, and high current degradation in Flight 2, probably for reasons other than radiation damage.

2. Table V shows the initial degradation during the first 20 days in orbit. (Although the test data indicates that the initial degradation occurred in much less than 20 days, the 20 day period was selected in order to obtain a sufficient number of data points to assure a valid average.) It is evident that the initial current degradation for all five types of modules is at least twice as great as expected. The GE and AR degradation is probably due to delamination or other physical deterioration, similar to the degradation of these modules during laboratory storage and testing in the same time period. This rapid initial degradation of the silicon modules may be due to proton damage in edge and/or contact areas of the cells which may not have been completely covered. Of course, some of the apparent initial degradation of all modules might be due to telemetry/instrumentation calibration errors.

3. The approximate annual degradation rates are listed in Table VI, in an effort to isolate long-term radiation damage effects from the excessive initial degradation. These annual rates were determined after the initial 20 days for the test data, and after 160 days for the predicted values. After 160 days the predicted curve essentially becomes a straight line when plotted to the time scale used in Figures 42 through 51. For silicon modules, the actual current degradation is slightly less than expected, and the actual voltage degradation is somewhat greater than expected. The negative current degradation for the WD modules is inexplicable. If the high WD current were due to reflected energy, the WN and IP currents should also have been higher. The cause of the negative voltage degradation for the GE modules is also unknown, but similar behavior has been noticed in long term laboratory vacuum ultra-violet tests.

69
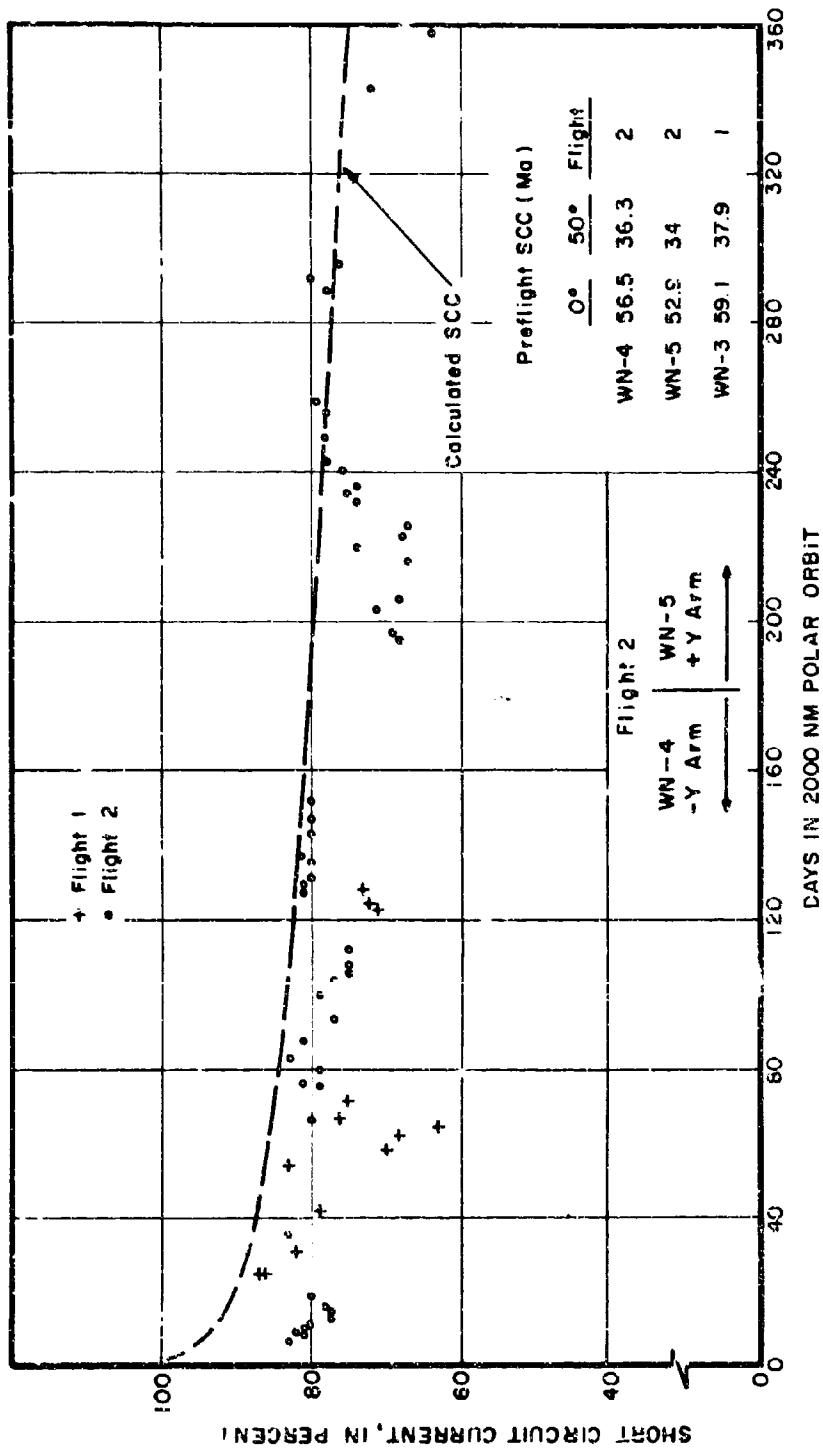
Figure 42. WN Module Short Circuit Current vs Days in Orbit
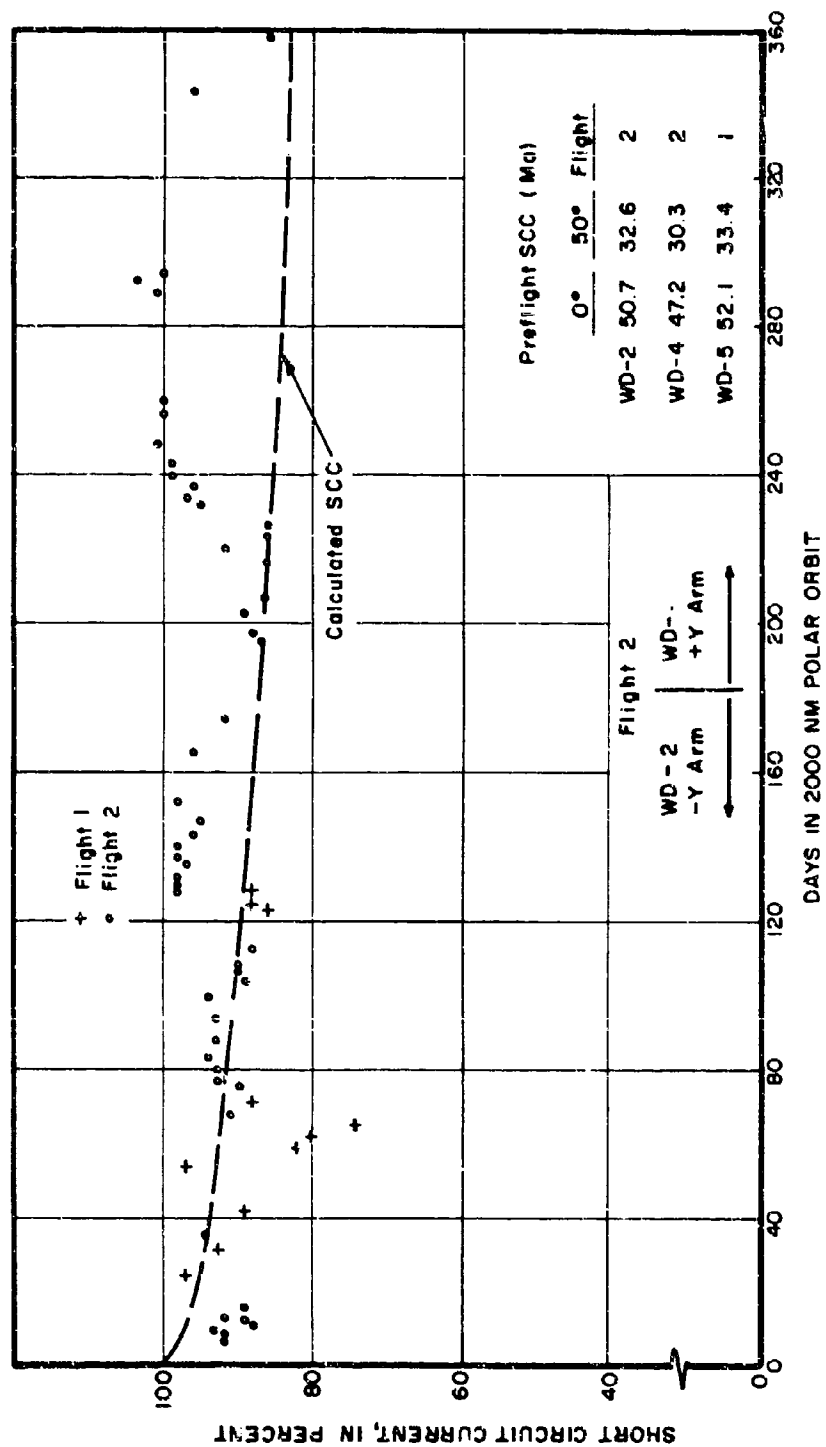
Figure 43. WD Module Short Circuit Current vs Days in Orbit
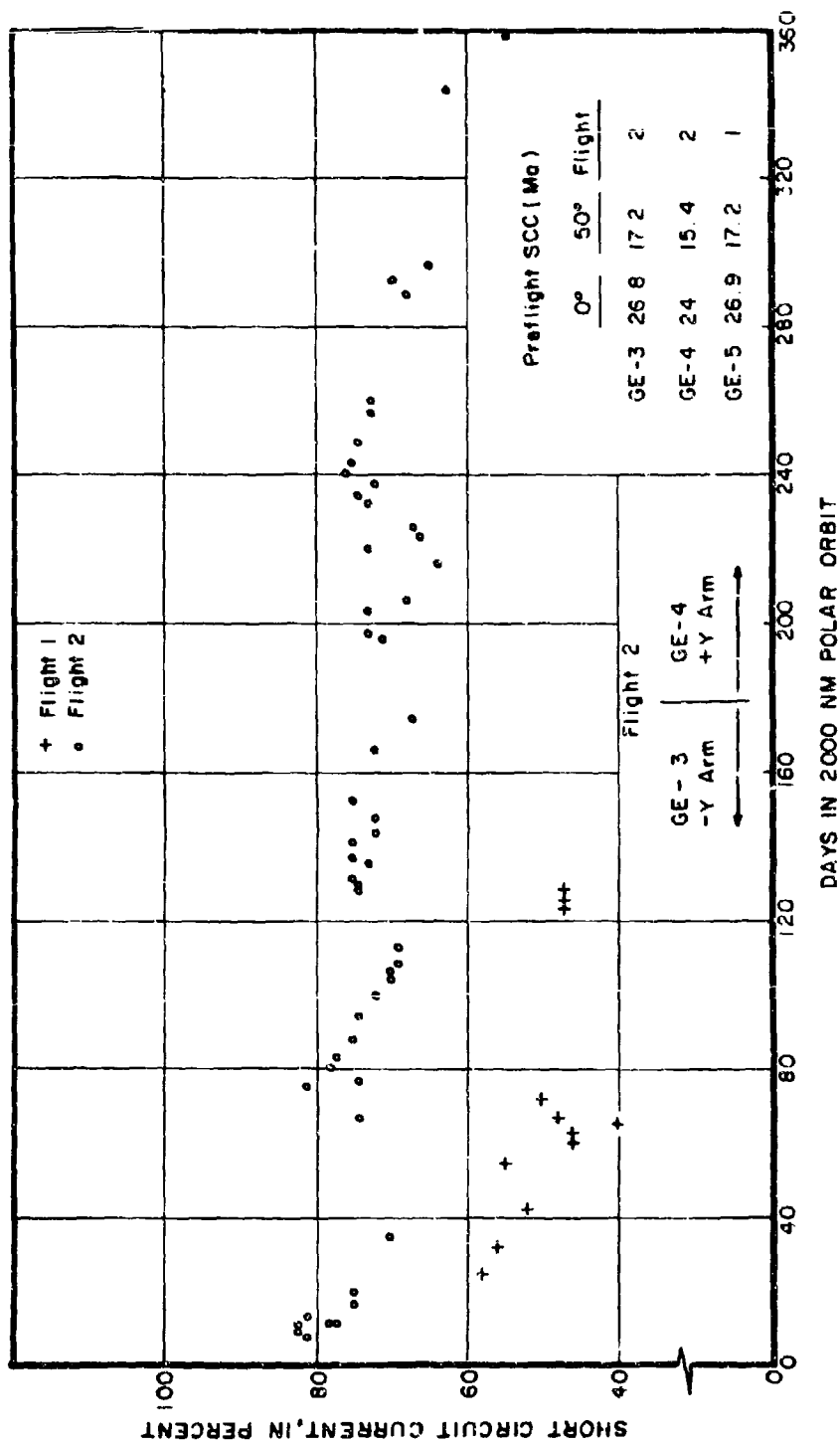
Figure 44. GE Module Short Circuit Current vs Days in Orbit

AFAPL-TR-69-17
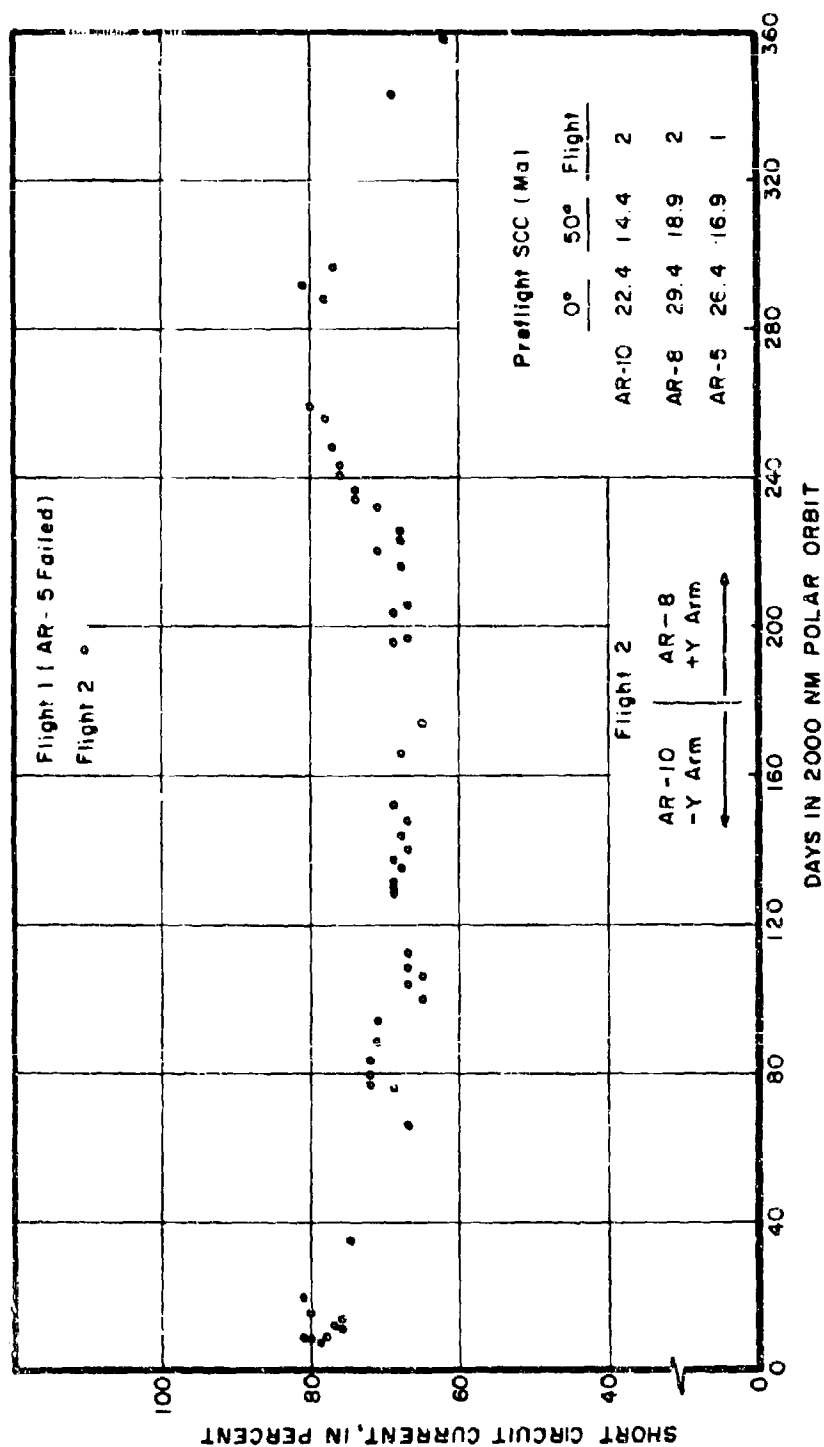
Figure 45.   AR Module Short Circuit Current vs Days in Orbit

73
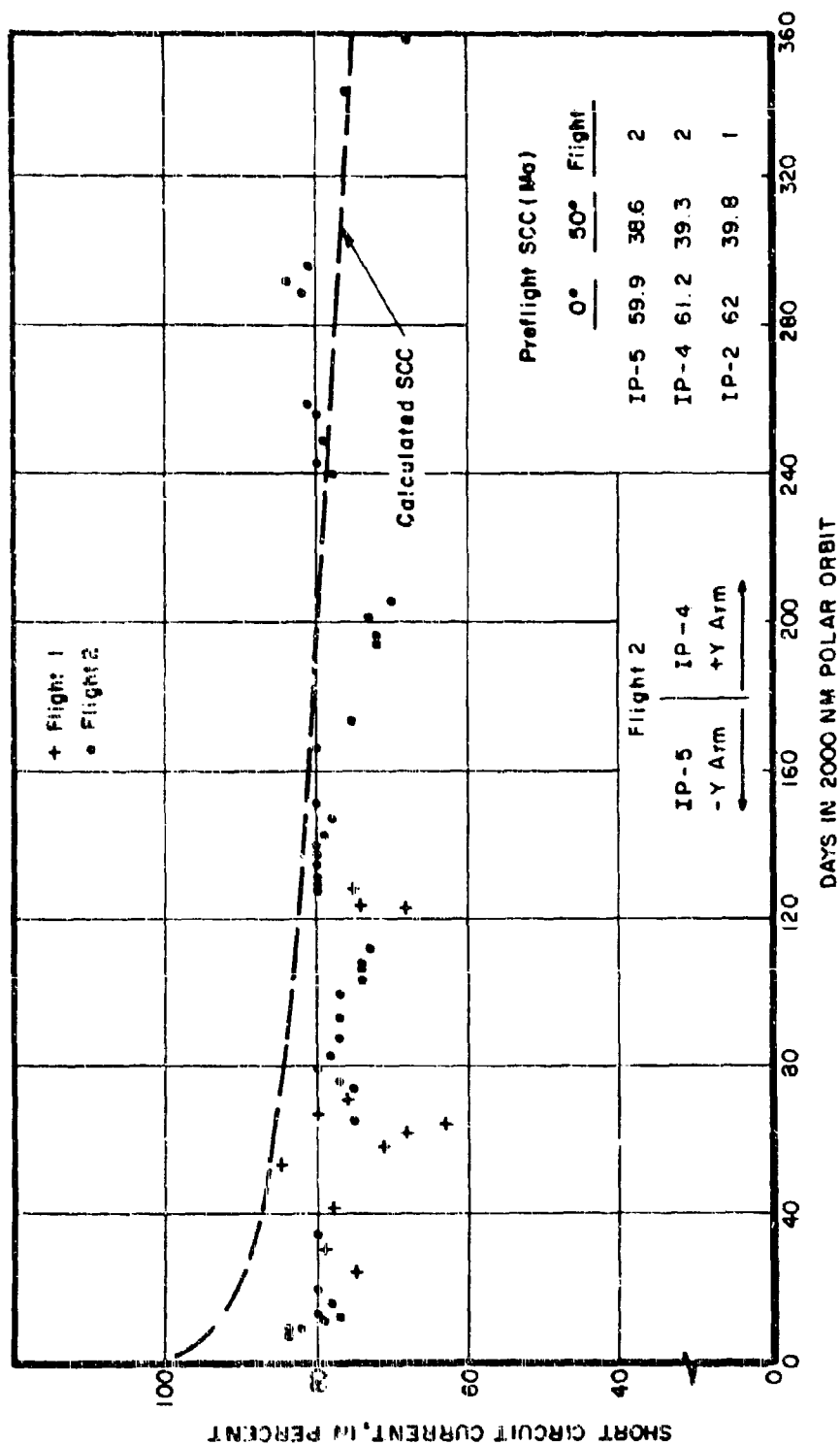
Figure 46.   IP Module Short Circuit Current vs Days in Orbit
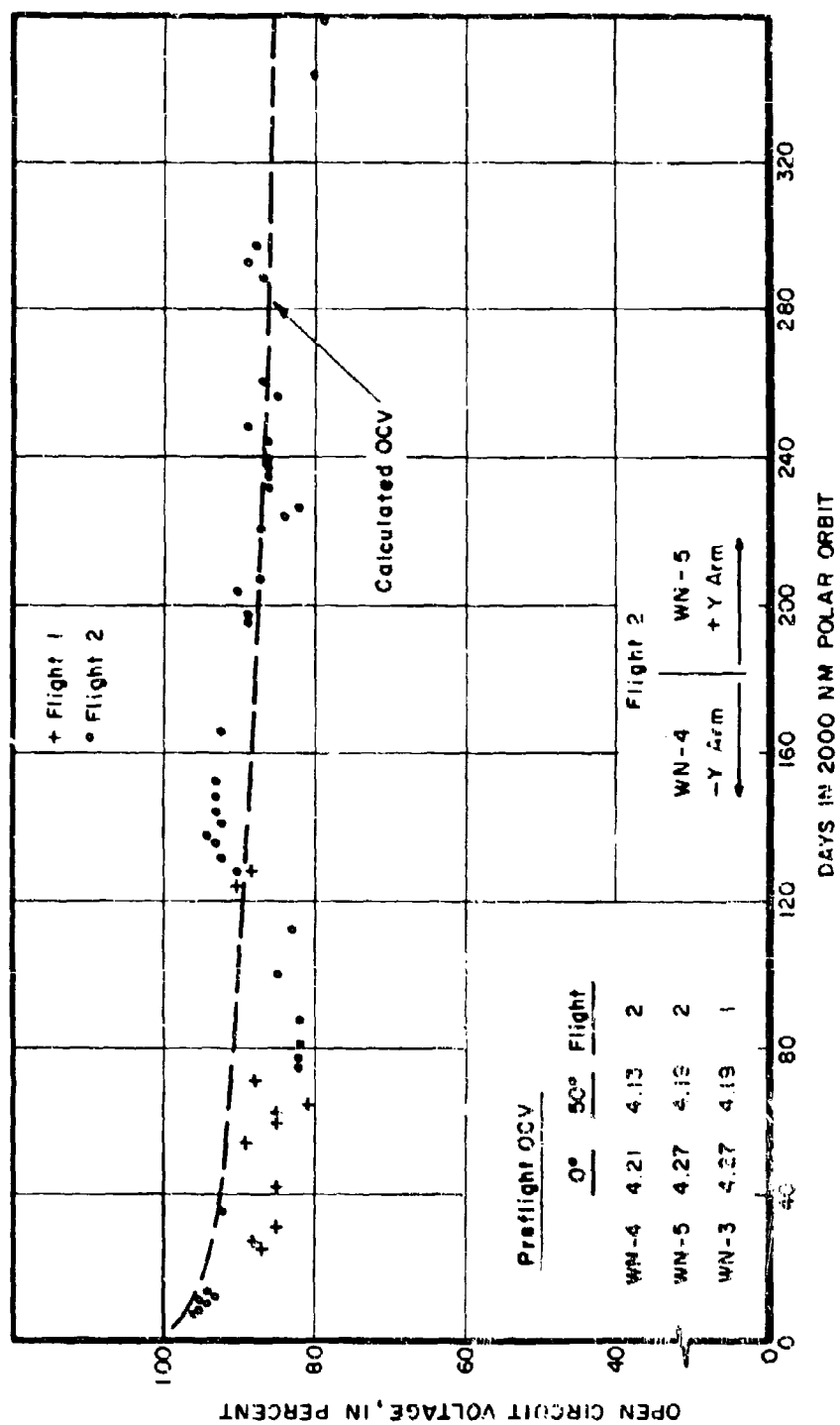
Figure 47. WN Module Open Circuit Voltage vs Days in Orbit

AFAPL-TR-69-17
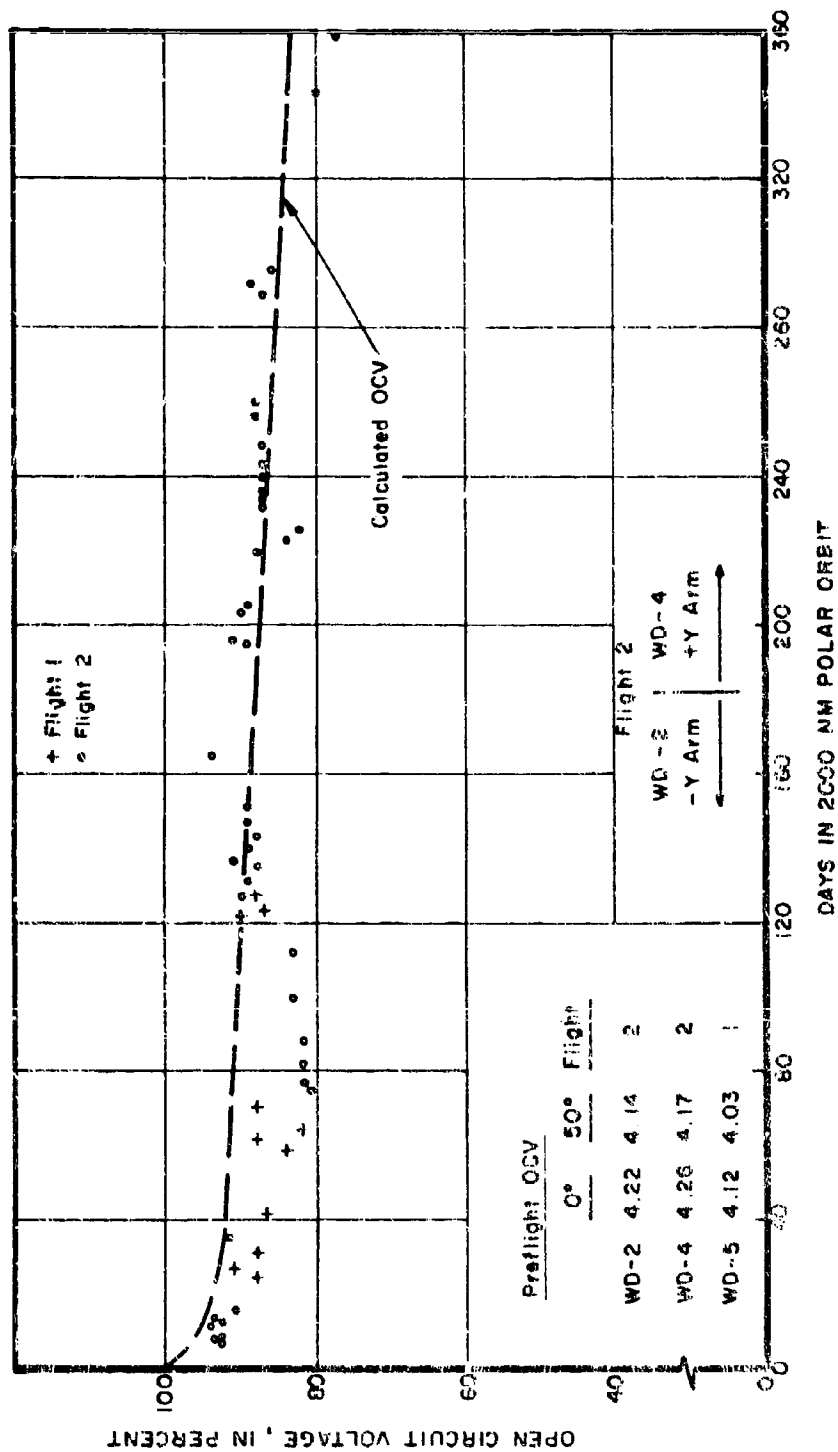
Figure 48. WD Module Open Circuit Voltage vs Days in Orbit

76
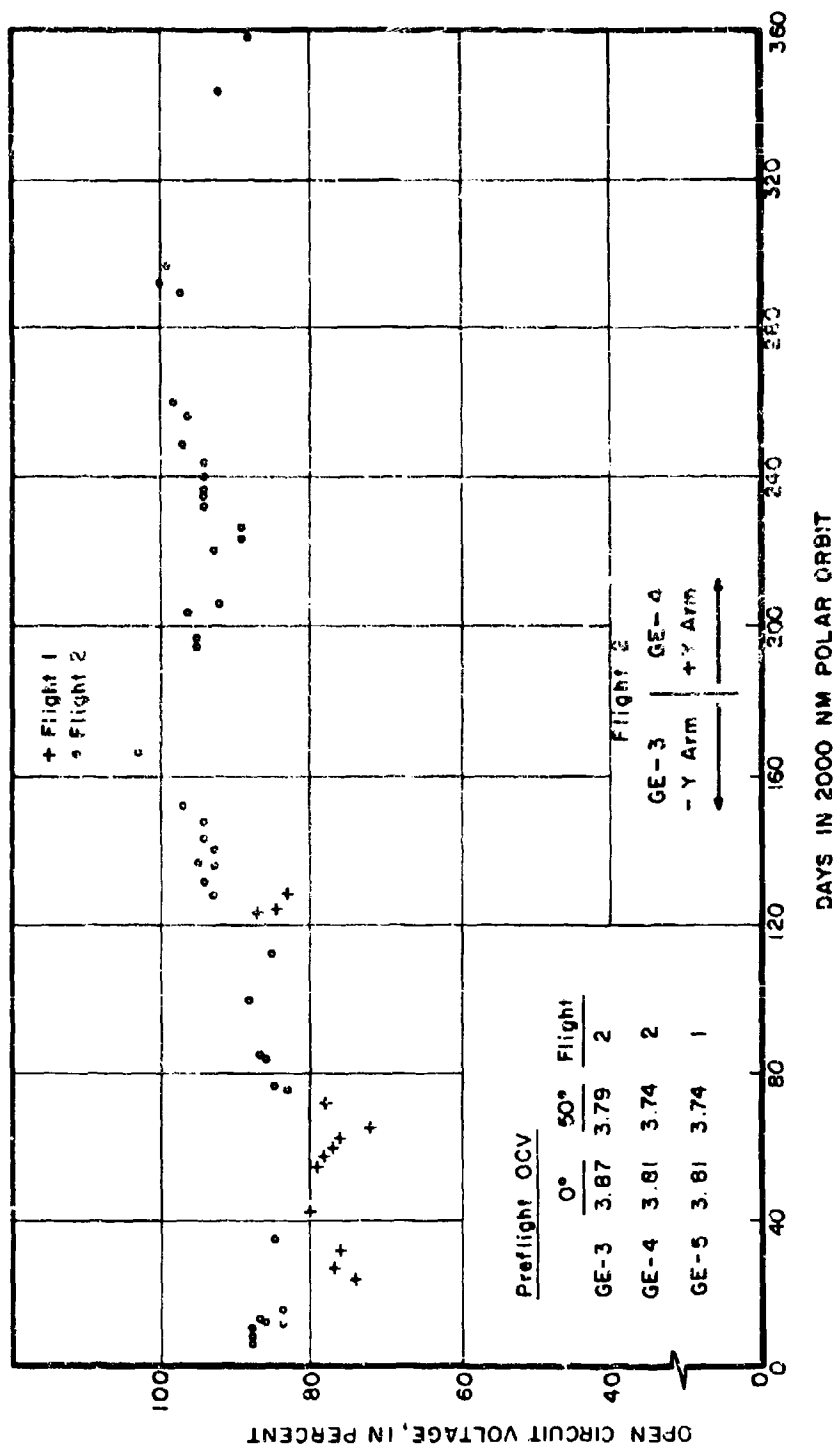
Figure 49. GE Module Open Circuit Voltage vs Days in Orbit
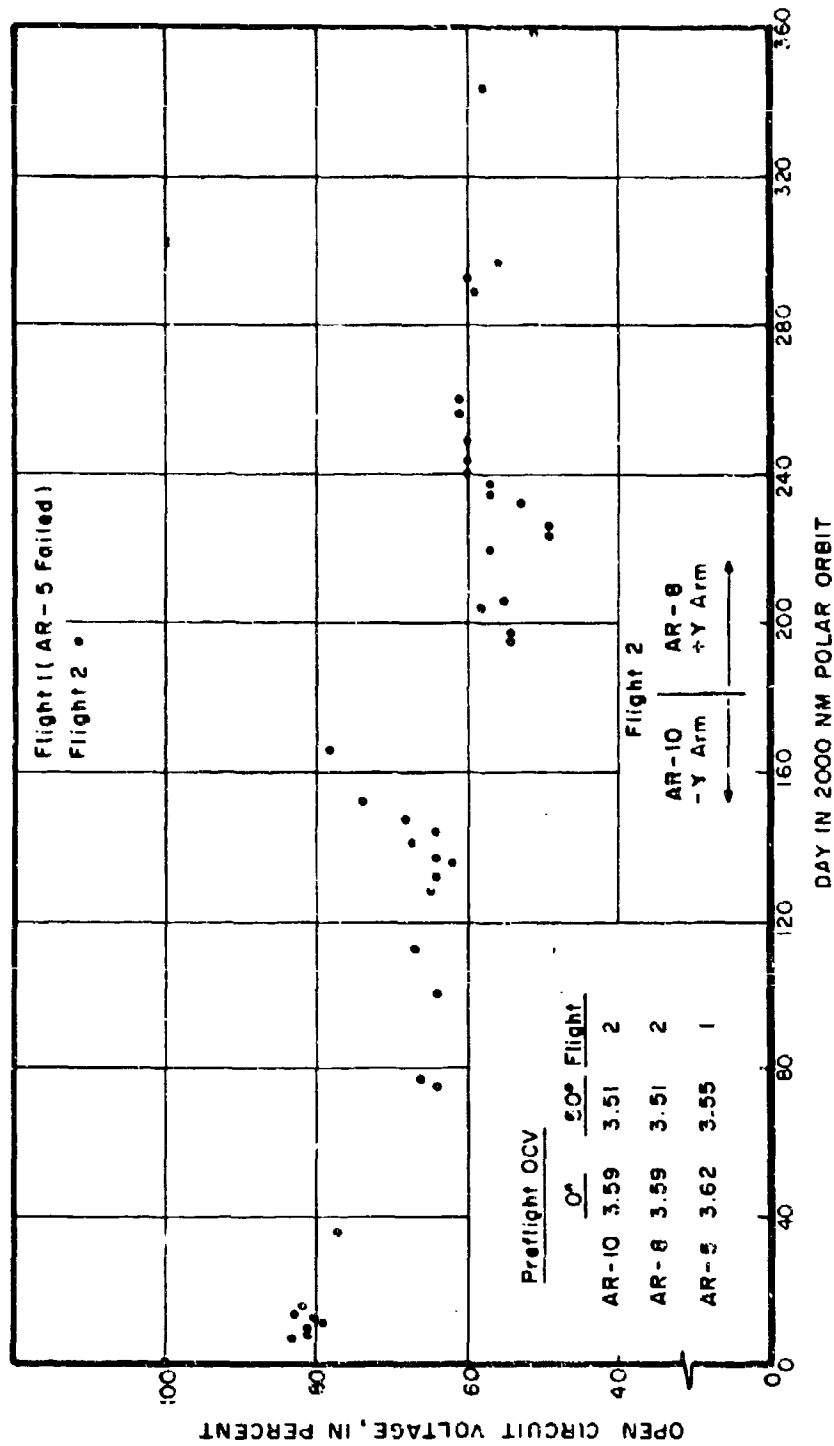
Figure 50.   AR Module Open Circuit Voltage vs Days in Orbit

78
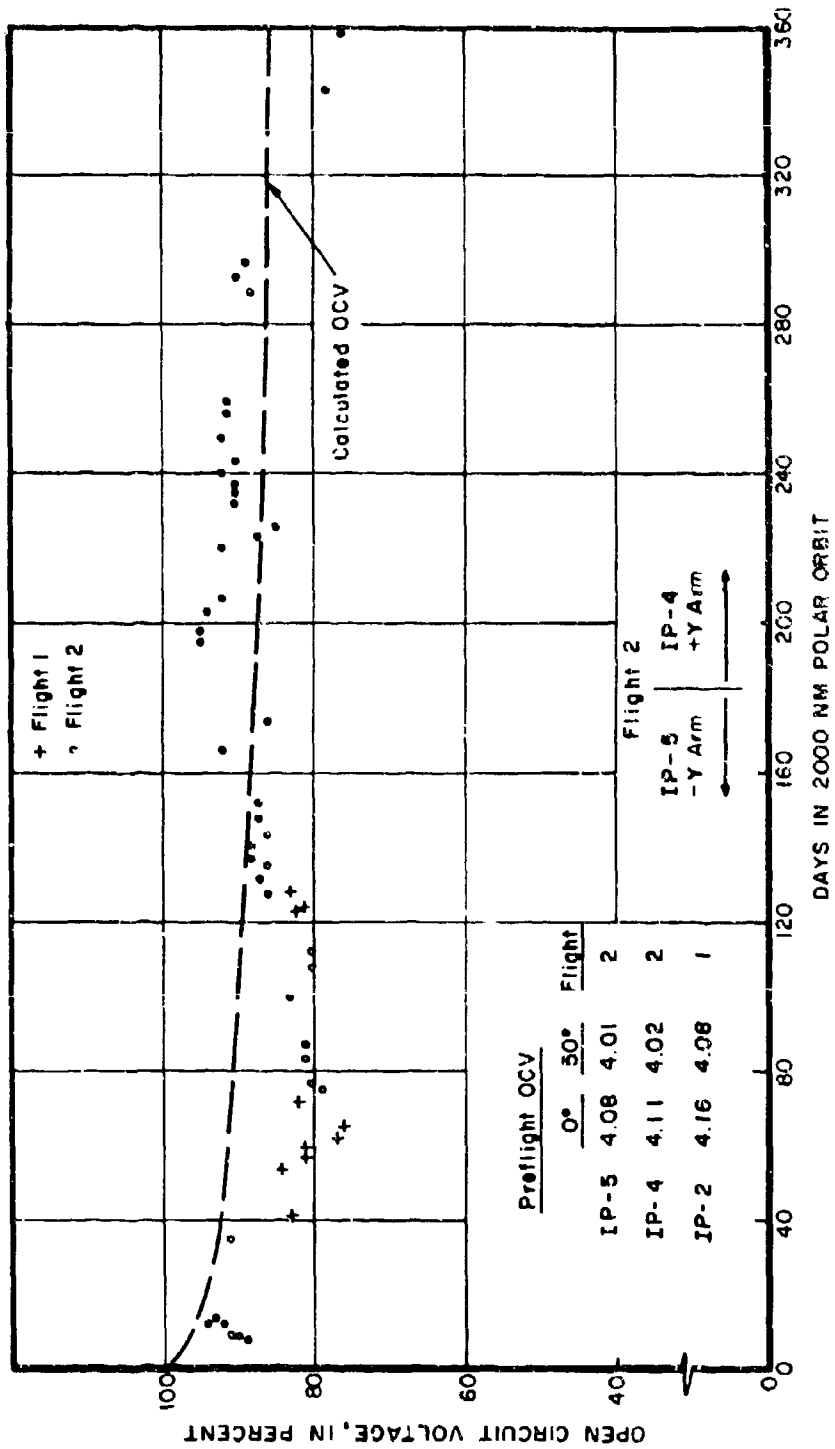
Figure 51. IP Module Open Circuit Voltage vs Days in Orbit

TABLE IV

PERCENT DEGRADATION, AFTER 358 DAYS IN 2000 NM POLAR ORBIT

Module Type	Short Circuit Current		Open Circuit Voltage	
	Predicted*	Test Results**	Predicted*	Test Results**
WN	25	29 ± 7	14	17 ± 4
WD	17	6 ± 8	17	18 ± 4
GE(FTV-2)		36 ± 8		6 ± 6
AR(FTV-2)		29 ± 9		50 ± 6
IP	25	24 ± 8	14	17 ± 7

* Predicted degradation was calculated by method outlined in Section IV

** The band which best contains the valid points in each of Figures 42 through 51 was determined by inspection

TABLE V

PERCENT INITIAL DEGRADATION, AFTER 20 DAYS IN 2000 NM POLAR ORBIT

Module Type	Short Circuit Current		Open Circuit Voltage	
	Predicted	Test Results	Predicted	Test Results
WN	9	20 ± 3	6	6 ± 2
WD	4	10 ± 3	6	7 ± 2
GE(FTV-2)		22 ± 4		14 ± 2
AR(FTV-2)		22 ± 3		19 ± 2
IP	9	20 ± 4	6	8 ± 3

The WD modules clearly provided better overall performance during this experiment than any of the other module types. The WD modules were, therefore, selected as standards for comparison, in an effort to eliminate systematic errors and thereby reduce the data spread. Figures 52 and 53, therefore, show WN, GE, AR and IP currents relative to WD current. Each point plotted was obtained by dividing the uncorrected short circuit current value by the corresponding WD uncorrected value. This procedure should cancel out all errors except random errors, small differences in temperature and temperature correction constants, and possible small differences in reflected energy and/or shadowing effects.

Figures 52 and 53 do, in fact, show greatly reduced data spread, and clearly show the current degradation of all other modules relative to the WD modules. The downward slopes of all lines definitely show that the WD modules have the lowest rate of current degradation.

Figures 54 through 56 show a less successful attempt to treat open circuit voltage data in a manner similar to the above. The voltage data points still show appreciable scatter, probably due to instability of the thin film modules, and the fact that temperature differences have a much greater effect on open circuit voltage than on short c. cult current. These figures do, however, show that:

1.   The three types of silicon modules have only minor differences in voltage degradation rate.

2.   The AR modules degraded rapidly.

3.   The GE modules had a negative open circuit voltage degradation rate – a characteristic which has also been observed in laboratory vacuum ultra-violet tests.

2.   ERROR ANALYSIS

The major types and sources of error in the short circuit current and open circuit voltage space data are:

1.   Telemetry/instrumentation calibration and processing errors.

Figure 52.   WN and GE Module Short Circuit Current, Relative
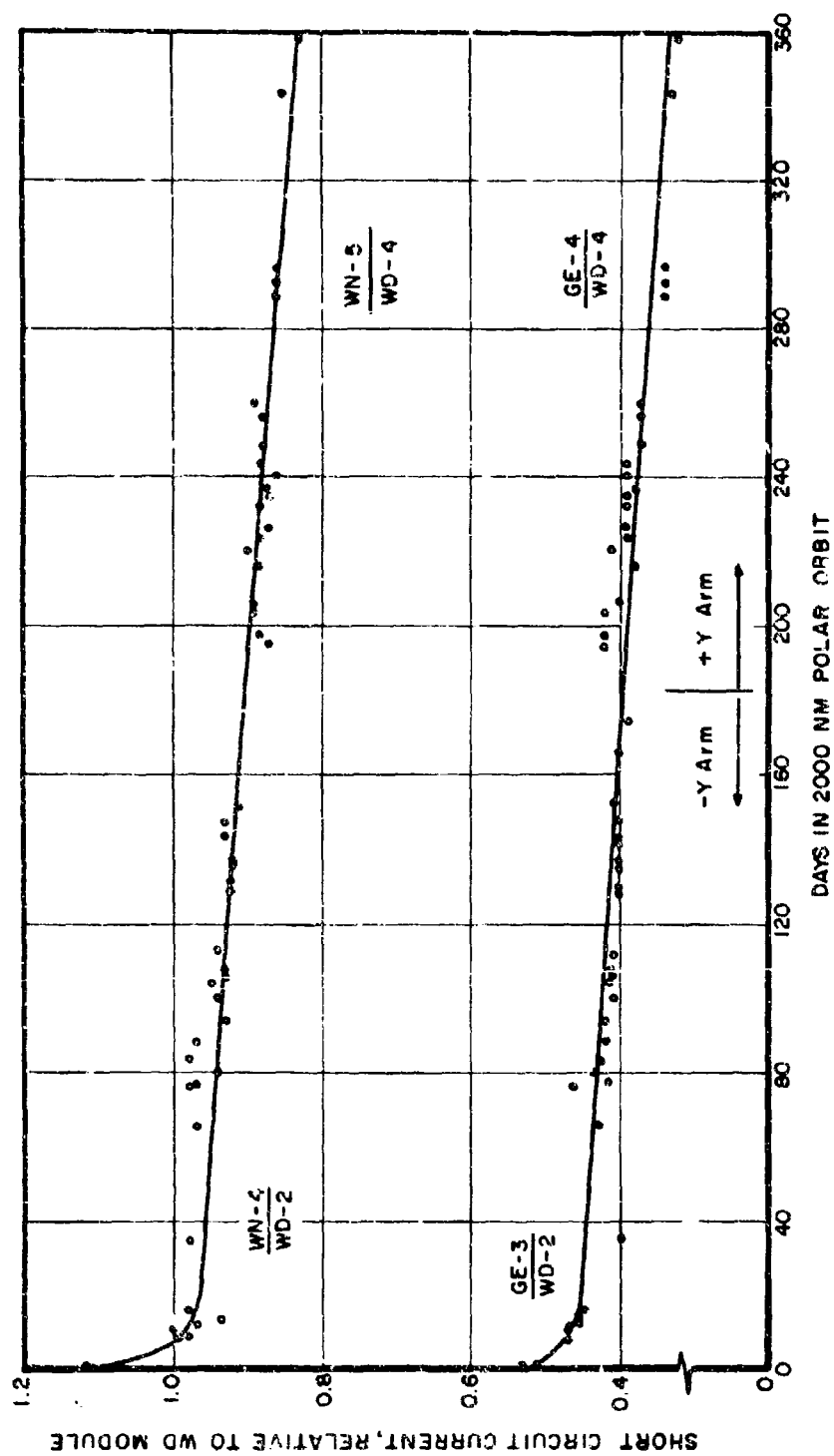to WD Module, Flight 2
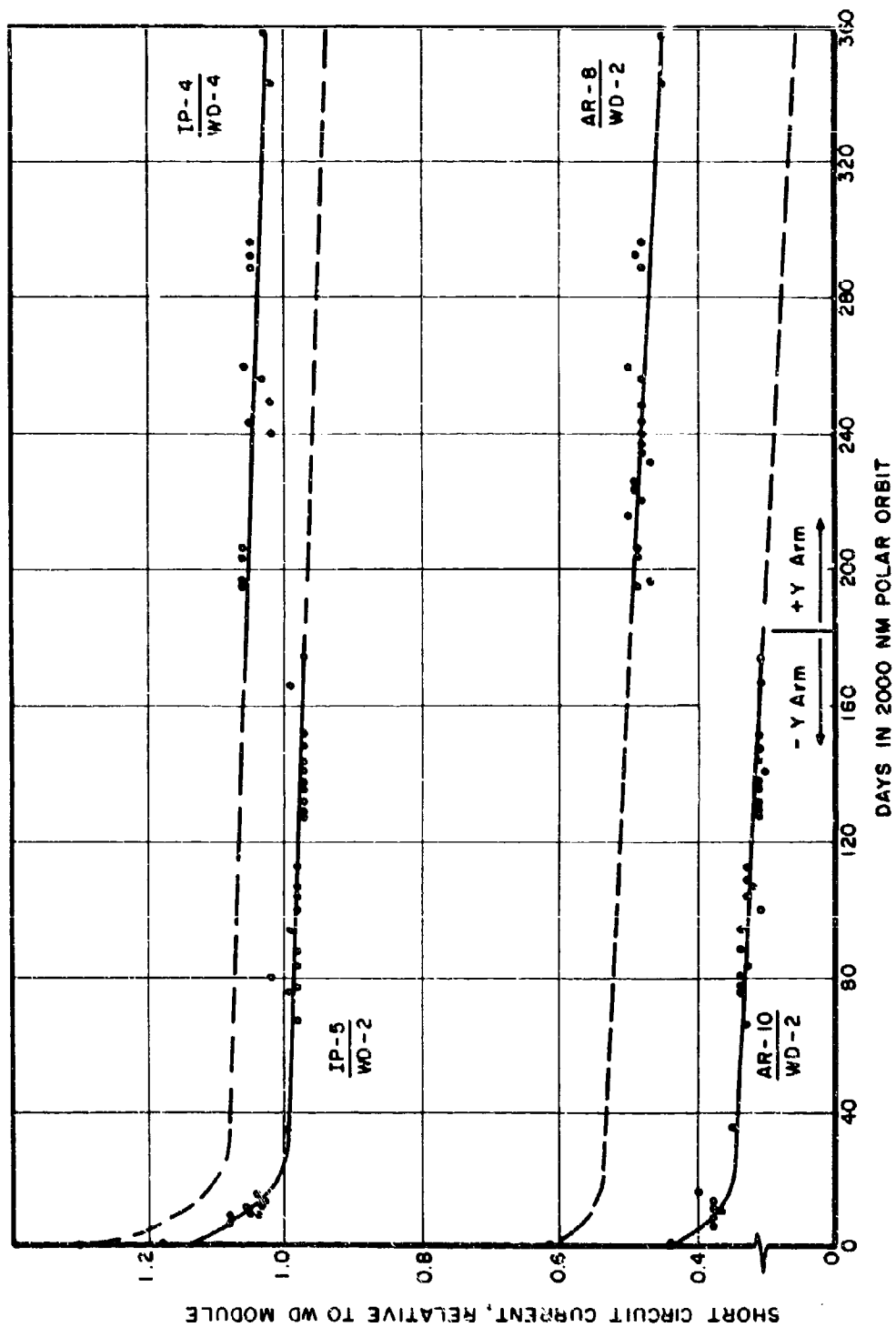
Figure 53.   IP and AR Module Short Circuit Current, Relative to WD Module, Flight 2

83
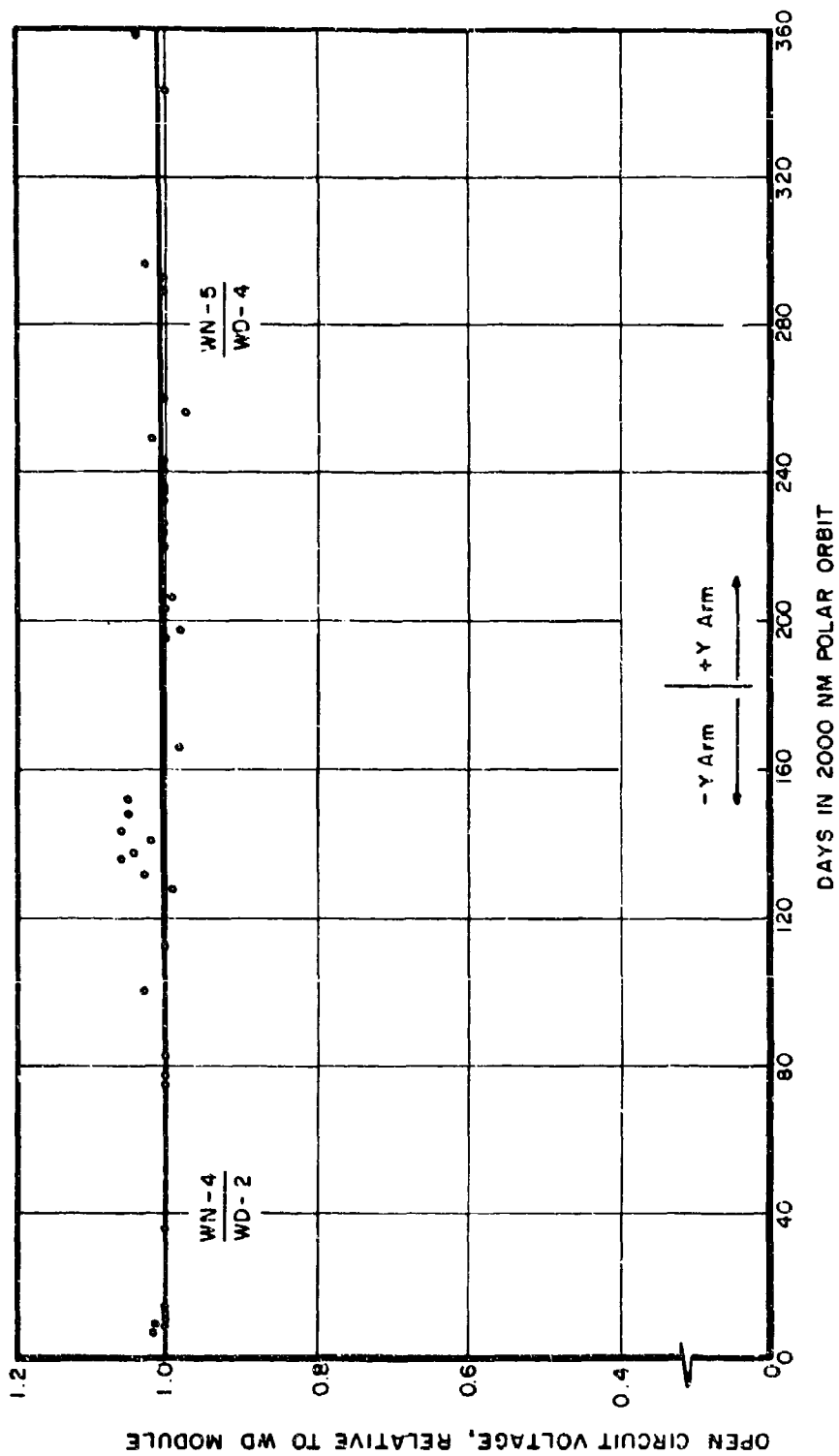
Figure 54. WN Module Open Circuit Voltage, Relative to WD Module, Flight 2

84
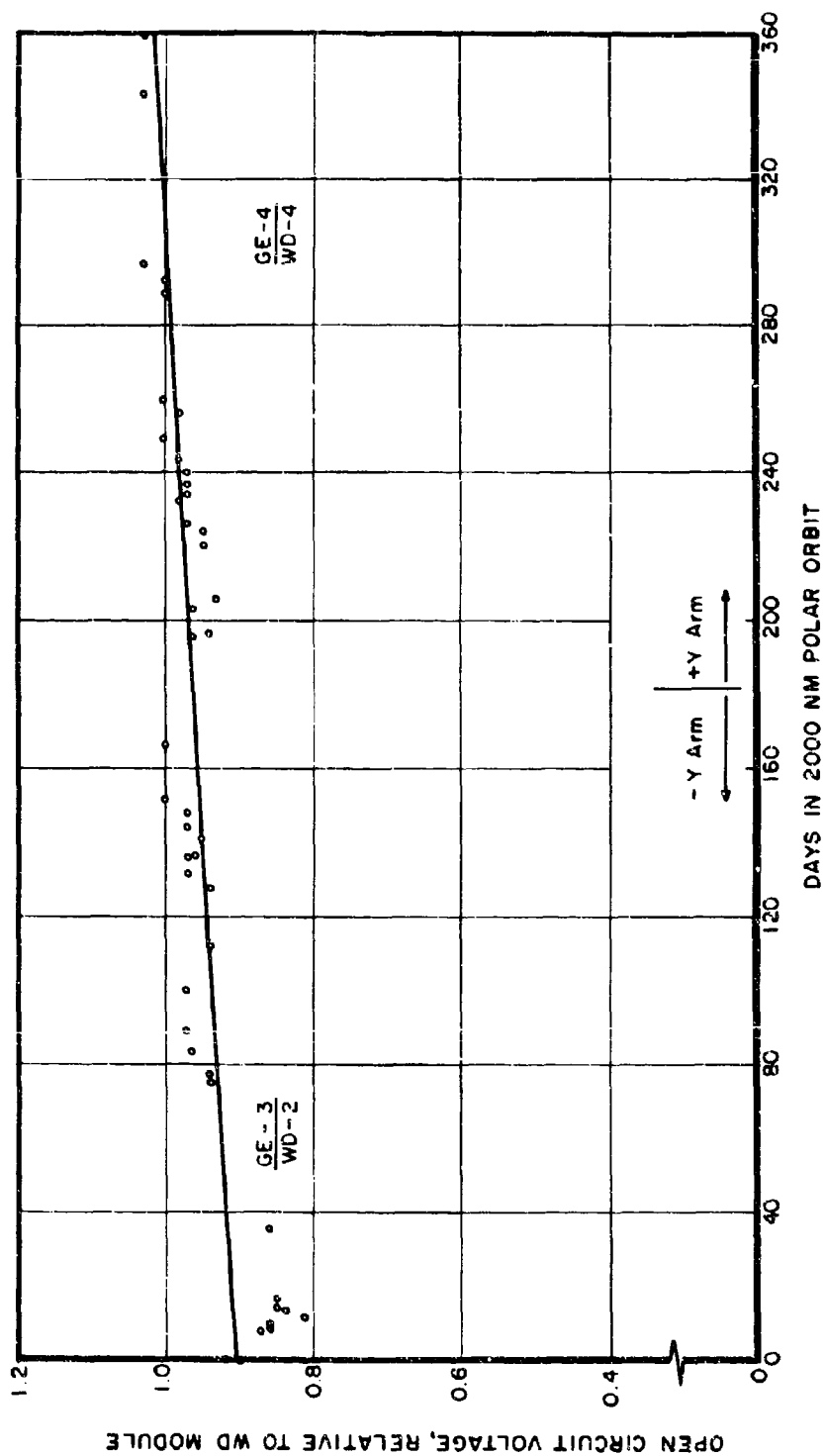
Figure 55. GE Module Open Circuit Voltage, Relative to WD Module, Flight 2

85
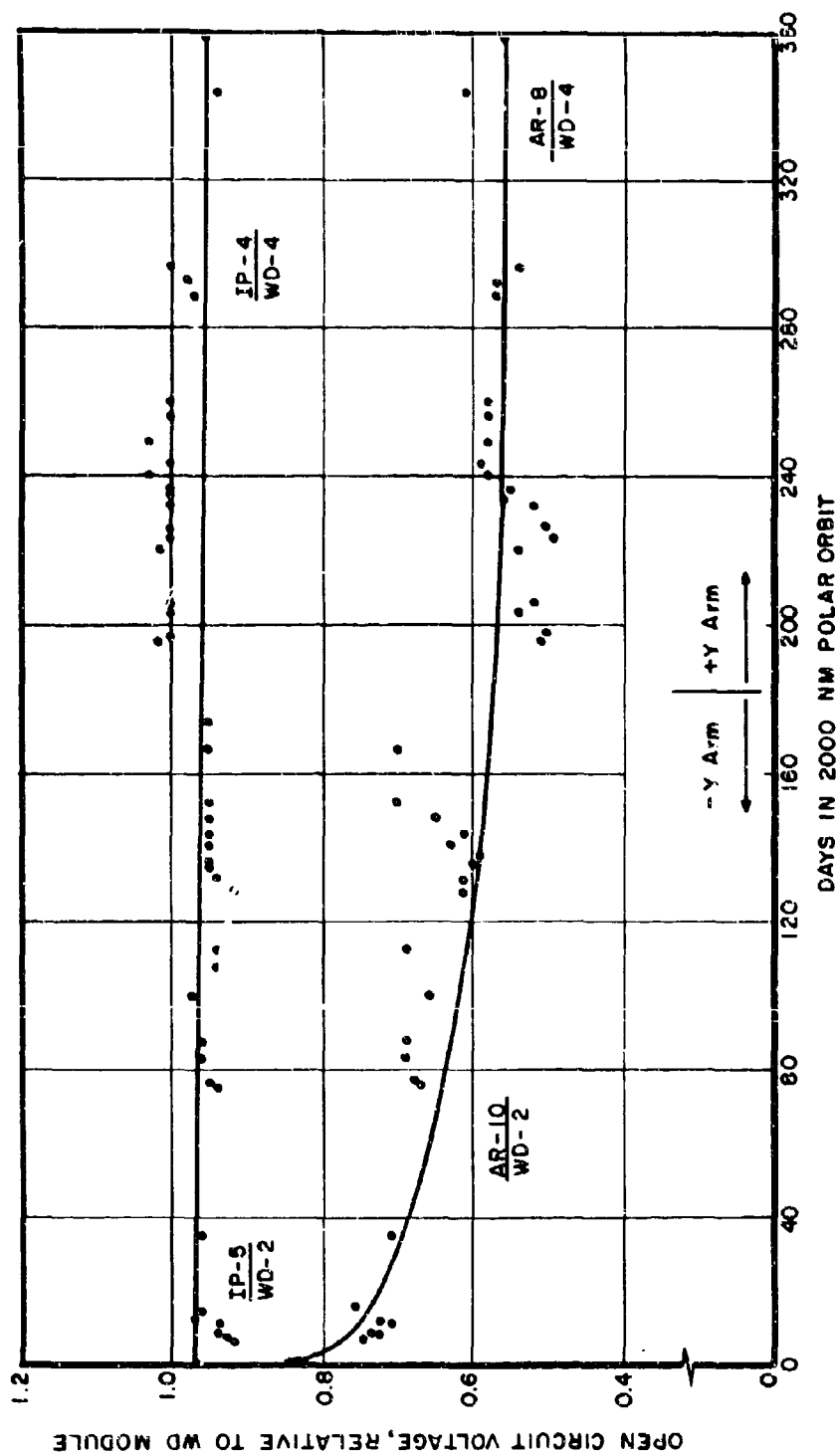
Figure 56. AR and IP Module Open Circuit Voltage, Relative to WD Module, Flight 2

2. Temperature differences (only WD module temperature was recorded).

3. Random errors.

4. Effect of reflected energy.

5. Effect of shadows.

6. Incidence angle measurement errors.

The effect of the above errors, especially 5 and 6, was minimized by the selection of data at 50° ±5° incidence angles, and the discarding of all data apparently affected by shadows, as discussed in Section II. The first type of error listed above is the only one that would equally affect both open circuit voltage and short circuit current.

3. POWER OUTPUT

Although no power measurements were made, the degradation in maximum power output can be estimated by assuming that the shape of the V-I curve did not change during the space experiment. This assumption is essentially valid for silicon cells (Statler's 1 Mev electron damage data on silicon solar cells show only a 2% reduction in fill factor.) Furthermore, the space angular response data of Section III also indicates no change for the silicon cells. This assumption is not necessarily valid for the GE and AR modules, but is used for comparison purposes. These modules showed substantial deterioration of V-I curve shape during laboratory testing and storage.

The data shown in Table VII for the GE and AR modules should, therefore, be regarded as the best case; the actual power output degradation would be somewhat greater.

The relative power output may, therefore, be calculated using the following equation, by assuming that the fill factor, F, does not change:

$$\frac{P}{P_0} = \frac{F(VI)}{F(V_0 I_0)}$$

Table VII presents power output degradation results which were calculated by this method, using data from Tables IV through VI. It is again evident that:

1. The WD modules incurred the least degradation.

2. The initial degradation of all modules was greater than expected.

3. The total (358-day) degradation of the WD modules was less than predicted, whereas the degradation of the WN and IP modules was greater than predicted.

TABLE XI

APPROXIMATE ANNUAL DEGRADATION RATE(PERCENT) AFTER
INITIAL DEGRADATION PERIOD (20 DAYS FOR TEST DATA AND
160 DAYS FOR PREDICTED DATA) IN 2000 NM POLAR ORBIT

Module Type	Short Circuit Current		Open Circuit Voltage	
	Predicted	Test Results	Predicted	Test Results
WN	10	9	6	11
WD	8	-4	7	11
GE(FTV-2)		14		-8
AR(FTV-2)		7		31
IP	10	4	6	9

TABLE XII

PERCENT DEGRADATION IN MAXIMUM POWER OUTPUT,
IN 2000 NM POLAR ORBIT

Module Type	Total (358 Days)		Initial 20 Days		Annual Rate	
	Predicted **	Test Results	Predicted **	Test Results	Predicted After 160 Days **	Test Results After 20 Days
WN	38	41 ± 9	14	25 ± 5	12	19
WD	31	23 ± 10	9	16 ± 5	14	7
GE(FTV-2)		*40 ± 11		*33 ± 5		*7
AR(FTV-2)		*64 ± 9		*37 ± 4		*36
IP	38	37 ± 12	14	26 ± 6	12	13

* Best case, actual degradation is probably greater
** All predicted values were calculated from Cherry and Statler's efficiency degradation
data (Table 6, reference 4)

SECTION VI
CONCLUSIONS

Several conclusions can be derived from the data presented in this Technical Report. If the pre-flight electrical performance data, Table 1, is reviewed, it becomes apparent that the sunlight conversion efficiency of thin film module types is approximately 1/3 the efficiency of silicon module types. Thus for a given initial power requirement, a thin film solar array would require 3 times as much area as its silicon solar array counterpart. Also, since both cadmium telluride and cadmium sulfide modules failed to survive qualification tests, it can be concluded that the environmental resistance of thin film cells, in the configuration described, is inferior to that of silicon solar cells.

The results of laboratory angular response tests show that the short circuit current is proportional to the cosine of the angle of incidence from 0° to 50° incidence, and is slightly less than proportional from 50° to 90° incidence. The open circuit voltage is relatively unaffected by incidence angle from 0° to 50° incidence. At 50° incidence the open circuit voltage reduction is only about 2%, and is about 6% at 70° incidence. As might be expected, the angular response curves for maximum power and partial (high resistance) loads lie between the short circuit and open circuit curves. The maximum power curve closely resembles and is from 0 to 5% higher than the short circuit curve.

Analysis of the space experiment data indicates that both short circuit current and open circuit voltage angular response in space are similar to laboratory angular response, except for the effect of reflected energy from vehicle surfaces and the earth's albedo. This effect varied from 0 to 30% on the short circuit curves, and was negligible on the open circuit curves. Prolonged exposure to the space environment (358 days) produced no apparent changes in the shape of the angular response curve.

The analysis of the radiation environment at orbit altitude of 2000 nautical miles shows that protons in the 4.5 to 10 Mev range are most effective in producing solar cell damage. The total proton–electron environment in this polar orbit corresponds to an equivalent 1 Mev electron flux of 2×10^{13} e/cm^2 per day, or 7.3×10^{15} e/cm^2 per year.

No in-orbit performance advantages of thin film solar cells over silicon solar cells were demonstrated in the space experiment. The cadmium sulfide and cadmium telluride modules suffered severe degradation and/or complete failure due to causes other than radiation damage, since similar behavior was noted in laboratory storage and testing of similar modules during the same time period. *

The in-orbit performance of the drift-field silicon modules was clearly superior to the performance of all other modules. Both predicted and actual results show this superiority. The predicted maximum power degradation for the 358 day orbital test was 31%, whereas actual test results showed 13 to 33% degradation.

The validity of the equivalent 1 Mev electron method, as described in Section IV, for predicting solar cell radiation damage was confirmed. Discrepancies between predicted and actual results were less than the experimental errors encountered. The use of this method is, of course, limited to those solar cells for which laboratory 1 Mev electron test data are available.

In any future solar cell space experiments, it is strongly recommended that suitable shielded, pre-irradiated solar cells be used as standards, and exposed to the same conditions as the test cells. Analysis of test cell performance relative to standard cell performance would eliminate many of the errors encountered in this experiment. Sufficient experimental data should also be obtained to determine the maximum power degradation and the changes, if any, in the voltage-current characteristics of the test cells.

---

*Attention is invited to the fact that the data and conclusions of this report pertain to experimental solar cells which were manufactured in July and August 1965, except for cadmium sulfide modules included in flight 2 which were manufactured in March 1966. All types of cells have been improved since these dates, but a discussion of the specific improvements is outside the scope of this report.

REFERENCES

1.   King, J. H., NASA Report SP-3024, <u>Models of the Trapped Radiation Environment, Volume IV: Low Energy Protons,</u> 1967.

2.   Vette, Lucero, Wright, NASA Report SP-3024, <u>Models of the Trapped Radiation Environment, Volume II: Inner and Outer Zone Electrons,</u> 1966.

3.   Rosenweig, W., "Radiation Damage Studies," <u>IEEE Photovoltaic Specialists Conference Proceedings;</u> Washington, D. C., 10 – 11 April, 1963.

4.   Cherry and Statler, GSFS Report Nr. X-716-68-204, <u>Photovoltaic Properties of U. S. and European Silicon Cells Under 1 Mev Elec ron Radiation,</u> April, 1968.

UNCLASSIFIED
Security Classification

DOCUMENT CONTROL DATA - R & D
(Security classification of title, body of abstract and indexing annotation must be entered when the overall report is classified)

1 ORIGINATING ACTIVITY (Corporate author)	2a. REPORT SECURITY CLASSIFICATION
Air Force Aero Propulsion Laboratory Wright-Patterson Air Force Base, Ohio 45433	UNCLASSIFIED
	2b. GROUP

3 REPORT TITLE

RADIATION DEGRADATION AND ANGULAR RESPONSE OF EXPERIMENTAL SOLAR CELLS IN A 2000 NAUTICAL MILE POLAR ORBIT

4 DESCRIPTIVE NOTES (Type of report and inclusive dates)

Final Report   June 1965 to February 1969

5 AUTHOR(S) (First name, middle initial, last name)

Glenn M. Kevern
Lowell D. Massie

6 REPORT DATE	7a. TOTAL NO. OF PAGES	7b. NO. OF REFS
June 1969	105	4
8a. CONTRACT OR GRANT NO.	9a. ORIGINATOR'S REPORT NUMBER(S)
b. PROJECT NO. 3145	AFAPL-TR-69-17
c. Task No. 314519	9b. OTHER REPORT NO(S) (Any other numbers that may be assigned this report)
d.	

10 DISTRIBUTION STATEMENT

This document is subject to special export controls and each transmittal to foreign governments or foreign nationals may be made only with prior approval of the Air Force Aero Propulsion Laboratory, APIP-2, Wright-Patterson Air Force Base, Ohio 45433.

11 SUPPLEMENTARY NOTES	12 SPONSORING MILITARY ACTIVITY
	Air Force Aero Propulsion Laboratory Wright-Patterson Air Force Base, Ohio

13 ABSTRACT

This report describes an experimental effort to determine solar cell degradation and angular response in a 2000 NM polar orbit. Solar cell experiments including five different types of solar cells were devised for each of two Air Force orbiting vehicles. The cell types were dendritic silicon, dendritic silicon drift field, cadmium telluride thin film, cadmium sulfide thin film, and ion implanted silicon. The cells were tested in a module configuration consisting of eight, 1 x 2 centimeter cells of each type in electrical series.

The short circuit current and open circuit voltage parameters were monitored over a one year period. The measured degradation was compared with predicted degradation based upon the Van Allen inner belt proton/electron model and results of accelerator produced 1 Mev electron radiation. The total proton/electron environment in the 2000 NM polar orbit corresponded to an equivalent 1 Mev electron fluence of 7.3×10^{15} e/cm^2 per year which produced a predicted power degradation of 38 percent in non-drift field silicon cell types and 31 percent in silicon drift field types. Measured quantities were found to substantiate the validity of the 1 Mev electron method for predicting silicon solar cell damage. Thin film solar cells (in the configuration described in the report) failed in earth orbit for reasons other than radiation damage. Thermal effects and mechanical delamination are believed to be the most likely reasons for their failure.

DD FORM 1473

UNCLASSIFIED
Security Classification

14 KEY WORDS	LINK A		LINK B		LINK C	
	ROLE	WT	ROLE	WT	ROLE	WT
Solar Cells						
Radiation Degradation						
Angular Response						
Thin Film/Silicon						
Flight Experiment						

DD Form 1473 (Cont'd)

The angular response of solar cells in space agreed with angular response measurements taken in the laboratory except for effects of stray radiation from earthshine and vehicle reflections. Angular response was also determined to be independent of radiation damage level.

(This abstract is subject to special export controls and each transmittal to foreign governments or foreign nationals may be made only with prior approval of the Air Force Aero Propulsion Laboratory, APIP-2, Wright-Patterson Air Force Base, Ohio 45433.)